AD_____

Award Number: W81XWH-04-1-0596

TITLE: Novel Micro/Nano Approaches for Glucose Measurement Using pH-Sensitive Hydrogels

PRINCIPAL INVESTIGATOR: Michael J. McShane, Ph.D.
Haifeng Ji

CONTRACTING ORGANIZATION: Louisiana Tech University
Ruston, LA 71272

REPORT DATE: June 2005

TYPE OF REPORT: Annual

PREPARED FOR: U.S. Army Medical Research and Materiel Command
Fort Detrick, Maryland 21702-5012

REPORT DOCUMENTATION PAGE

Form Approved
OMB No. 0704-0188

1. REPORT DATE *(DD-MM-YYYY)*	2. REPORT TYPE	3. DATES COVERED *(From - To)*
01-06-2005	Annual	1 Jun 2004 - 31 May 2005

4. TITLE AND SUBTITLE

Novel Micro/Nano Approaches for Glucose Measurement Using pH-Sensitive Hydrogels

5a. CONTRACT NUMBER

5b. GRANT NUMBER
W81XWH-04-1-0596

5c. PROGRAM ELEMENT NUMBER

6. AUTHOR(S)

Michael J. McShane, Ph.D.
Haifeng Ji

5d. PROJECT NUMBER

5e. TASK NUMBER

5f. WORK UNIT NUMBER

7. PERFORMING ORGANIZATION NAME(S) AND ADDRESS(ES)

Louisiana Tech University
Ruston, LA 71272

8. PERFORMING ORGANIZATION REPORT NUMBER

9. SPONSORING / MONITORING AGENCY NAME(S) AND ADDRESS(ES)
U.S. Army Medical Research and Materiel Command
Fort Detrick, Maryland 21702-5012

10. SPONSOR/MONITOR'S ACRONYM(S)

11. SPONSOR/MONITOR'S REPORT NUMBER(S)

12. DISTRIBUTION / AVAILABILITY STATEMENT
Approved for Public Release; Distribution Unlimited

13. SUPPLEMENTARY NOTES

14. ABSTRACT – SEE ATTACHED PAGE

15. SUBJECT TERMS
Hydrogels; biosensors; glucose monitoring; MEMS; microcantilevers; Resonance energy transfer

16. SECURITY CLASSIFICATION OF:			17. LIMITATION OF ABSTRACT	18. NUMBER OF PAGES	19a. NAME OF RESPONSIBLE PERSON
a. REPORT	b. ABSTRACT	c. THIS PAGE			19b. TELEPHONE NUMBER *(include area code)*
U	U	U	UU	75	

Abstract

This project aims to couple environmentally-sensitive hydrogel materials with immobilized enzymes and two novel readout techniques to develop general platforms for biosensing. The need for improved testing methods for diabetics as well as the potential for use of glucose level as a general marker of metabolic status is the primary motivation for this work. This project is focusing on the use of sensitive transduction schemes that allows reliable detection of small physical/mechanical changes in gel size or water content, specifically: microelectromechanical systems (MEMS) and fluorescence resonance energy transfer (RET) optical systems. At the completion of one project year, successful demonstrations of glucose sensing have been accomplished in both areas, and interesting discoveries of hydrogel structure and properties have been uncovered using the novel measurement approaches. While the project is ahead of schedule according to the expected milestones for demonstrating sensing capabilities, optimization of sensitivity, range, and stability are key goals for the second project year. The project has generated three manuscripts to be submitted for peer review and four conference reports, with similar products expected for the second year.

Table of Contents

INTRODUCTION:

Glucose sensors have been of tremendous interest, and the subject of many research and development projects, due to the need for improved testing methods for diabetics as well as the potential for use of glucose level as a general marker of metabolic status. Despite the effort devoted to this type of work, there is still a need for more reliable methods for glucose monitoring, as well as measurement of other medically-relevant species. "Smart gels", pH-sensitive hydrogels, are a class of materials that exhibit changing structural and hydration properties in response to the pH of the solvent, and in this project these have been made to respond specifically to species other than H^+ by inclusion of active components (enzymes) for catalyzing reactions leading to pH changes in proportion to substrate concentration. This project has focused on establishing stable, efficient enzyme immobilization techniques for different smart gels, and developing suitable readout technology is required to measure gel swelling. The latter task requires a sensitive transduction scheme that allows reliable detection of small physical/mechanical changes in gel size or water content, and we have specifically pursued two technologies to accomplish this: microelectromechanical systems (MEMS) and fluorescence resonance energy transfer (RET) optical systems. The studies will develop novel integrated sensing materials and readout techniques for chemical measurement systems, specifically glucose sensors, which will test new concepts toward developing useful glucose monitoring devices, and will also produce novel sensor instrumentation schemes that are general in applicability and easily modified for other species.

BODY:

The following description of experimental work, interpretation results, explanation of accomplishments and plans for future efforts is organized according to the original statement of work, with tasks and subtasks stated at the beginning of the corresponding discussion. All tasks completed are discussed, including those initially planned for Months 13-24; tasks not fully completed are included and reasons for incomplete status are noted in the text. Two separate gel systems (chitosan, a natural biopolymer, and polyacrylamide, a synthetic polymer) are being studied in parallel, and generally the results for the two systems are discussed individually.

Task 1. To identify a procedure for efficient and stable immobilization of glucose oxidase enzyme into pH-sensitive hydrogel. (Months 1-6):

a. Develop a pH-sensitive hydrogel with GOx immobilized by specific biomolecular recognition-based (biotin-avidin) self assembly, and assess loading efficiency, enzyme activity, and stability. (Months 1-3)

pH-Sensitive Hydrogel Systems: 1) Chitosan

Overview/Objectives

Among the commercially available polymers for intelligent hydrogels, chitosan is currently receiving a great deal of interest for its interesting intrinsic properties. These include biocompatibility, biodegradability under certain conditions, wound-healing promotion and anti-bacterial properties.[1,2] Chitosan is a copolymer of β-(1→4)-linked-2-acetamido-2-deoxy-D-glucopyranose and 2-amino-2-deoxy-D-glucopyranose. This polycationic biopolymer is

generally obtained by alkaline deacetylation from chitin, which is the main component of the exoskeleton of crustaceans, such as shrimp and crawfish. Due to the presence of ionizable amino groups, chitosan is a cationic polyelectrolyte with a pKa value of 6.5, and one of a few naturally-occurring materials that can form a hydrogel by complexation with anionic polyelectrolytes. For example, gelatin (type B) with an isoelectric point (pI) value around 5.0 can form polyelectrolyte complexes (PEC) with chitosan. Gelatin is the partially denatured product of collagen, and gelatins of different pI can be prepared with proper preconditioning of the gelatin stock.[3] To improve the mechanical properties of the PEC hydrogels, crosslinking is performed. However, because some crosslinkers used to perform covalent crosslinking (e.g. glutaraldehyde) may induce toxicity if found in trace quantity before administration, ionically crosslinked chitosan hydrogels are generally thought to be preferred, as they are well-tolerated biologically and their potential medical and pharmaceutical applications are numerous since typical ionic crosslinkers (multivalent ions) are often biocompatible.[32]

Chitosan was evaluated as a candidate smart gel for the proposed sensor technologies. The first objective in this assessment was to quantitatively determine the response of chitosan/gelatin hydrogel slabs to pH. This information was necessary to determine the expected response of the material to the byproducts of the GOx-glucose-oxygen interaction.

Methods

Chitosan/gelatin hydrogel samples were made with a 1:1 ratio of 2% weight chitosan solution and 2% weight gelatin solution following a similar protocol to that used for a chitosan hydrogel that was previously shown to have a pH-sensitive response.[4,5,6,7] The hydrogel was formed with 2% weight chitosan dissolved in 1% weight acetic acid solution and 2% weight gelatin was included for stability. Gelatin forms a solid at low temperatures, and stabilizes the pre-hydrogel material prior to crosslinking. The solutions were mixed at a 1:1 ratio and stirred for 2 hours to make a pre-gel solution. The well-mixed pre-hydrogel solution was poured into a custom circular mold made from silicone rubber, and left to solidify in the refrigerator at 3°C for 4 hours. The solidified pre-hydrogel was then immersed in a 2% weight sodium tripolyphosphate (TPP) solution at 3°C overnight. The TPP forms an ionic crosslink among the enzyme and polymer molecules in the pre-hydrogel solution, which results in the formation of a hydrogel. The crosslinked, solidified hydrogel was removed from the refrigerator, washed in DI water for 15 minutes, and placed in an oven at 40°C for drying.

Separate hydrogels were crosslinked with 2 or 3.5% weight TPP solutions, and dried according to the same protocol. The increased concentration of TPP was used to provide a higher crosslinking density in the material, which was expected to result in a stronger hydrogel. The samples were rehydrated and preconditioned in pH 7.0 PBS for 24 hours, and then moved into a PBS solution in the range of pH 4-8. Each sample was weighed periodically over the next 48 hours, in accordance with the described time-course swelling glucose sensitivity measurements. Weight measurements according to the standard techniques reported in the literature.[8,9] These experiments were used to determine steady-state swelling characteristics of the gels due to the environmental pH, using the following equation to normalize to initial (pH 7.0) gel weight:

$$\Delta W\ (\%) = \frac{(W_{pH} - W_{pH7.0})}{W_{pH7.0}}$$

Results

This experiment was performed three times, and each time the hydrogels exposed to pH of approximately 6 showed a lower overall percent change in weight than hydrogels exposed to

pH 8. It was also observed that the standard deviation of the percent weight change increased with decreasing pH (Figure 1); this can be attributed to the difficulties in handling more swollen hydrogels, which become flimsy and mechanically unstable as the water content increases. Also, the increase in standard deviation and decrease in average percent change in the hydrogel samples versus the decrease in pH could be due to loss of some of the hydrogel matrix components during swelling interactions.

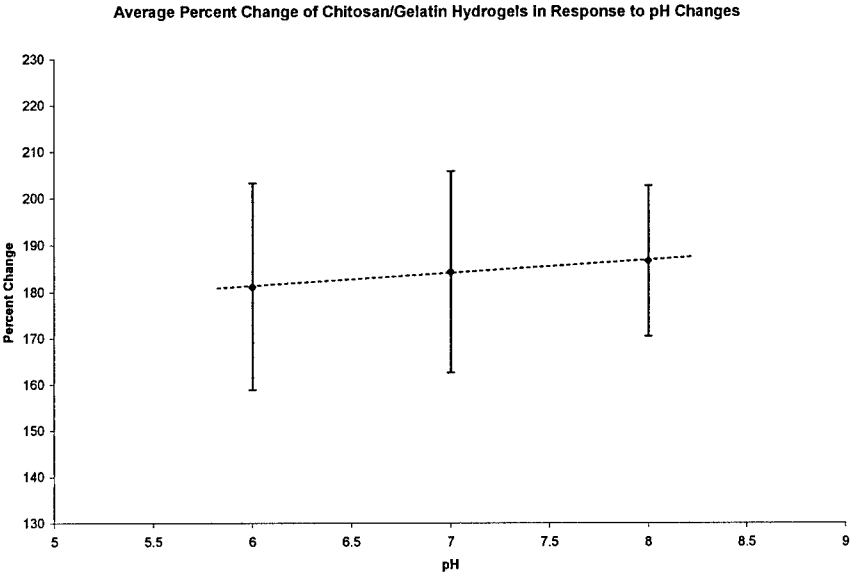

Figure 1: Results from the First Chitosan/Gelatin Hydrogel Glucose-Sensitivity Experiment

The plot of the experimental data seems to show a slight linear trend of increasing weight with an increase in pH; however, the large standard deviations present in the data make this small change insignificant. The large variability indicates the difficulty in the measurement of swelling, due to the inexact removal of water and the sensitivity of the gels to handling.

Conclusions

The results of swelling tests highlight the difficulty of obtaining reliable, consistent measurements of swelling using typical methods, and further support the importance of our project in developing sensitive systems to transduce swelling behavior. The method of swelling measurement by weight analysis was carefully reviewed, as well as the method of exposure of the sample to various solutions. In order to weigh the hydrogel samples, excess solution must first be removed from the surface to avoid inconsistencies in weight resulting from excess solution on the hydrogel surface. This is typically performed by absorption of water with paper,[10] but we have found this to be messy and inconsistent, as the hydrogels often adhere to the tissue paper, resulting in tearing or breaking of the hydrogel sample. Drying with nitrogen (N_2) was attempted, but this method seemed to result in the removal of water from the hydrogel matrix due to evaporation, and when removing surface fluid, the force of the N_2 jet on the hydrogel caused sample breakage. Also, all of the hydrogels made in the previously mentioned results were cut from molds, which increased the amount of dissolution, thus skewing results further. This could be attributed to a low crosslinking density at the boundaries of the cut hydrogel samples. It is apparent that the hydrogels respond to environmental conditions, and better

methods of swelling measurement are needed to fully characterize the transient and steady-state response of the material. The chitosan system, while known to exhibit pH-dependent swelling behavior, is difficult to use in large-dimension formats. As discussed and proven later, this does not preclude use of chitosan for microscale systems, so these negative findings were not discouraging.

pH-Sensitive Gel Systems: 2) Polyacrylamide(PAM)/Polyacrylic Acid (PAA) Hydrogels

Overview/Objectives

The large-scale (dimensions great than a few millimeters) chitosan/gelatin hydrogels proved to be difficult to process and handle. PAM and PAA hydrogels were investigated as a robust, pH-sensitive alternative. This material combination has shown a repeatable response to temperature and pH, and has been used in many applications requiring environmentally-sensitive polymers.[10-12] For this work, the PAM/PAA gels were subjected to the same testing of chitosan gels to determine the relative strength/ease of handling, response to pH, and the effect of fluorescent labeling.

Methods

PAA/PAM hydrogels were made according to a protocol outlined in several papers.[10-13] All chemicals used in these experiments, including 2-dimethylamino ethyl methacrylate (DMEM), acrylamide (AMD), N,N'-methylenebisacrylamide (bis-AMD), and the UV photo-initiator diethyoxyacetophenone (DEAP), were used as received from Aldrich. High-purity de-ionized water was obtained with a Milli-Q water system from Millipore.

A pre-hydrogel solution containing 2.1mmol (0.15g) of AMD, 0.27 mmol (45mg) of DMEM, 0.072mmol (11mg) of bis-AMD, and 0.072mmol (15mg) of DEAP dissolved in 3 ml of water was prepared. The hydrogel slabs were created by pouring the pre-hydrogel solution into the desired PDMS mold shape (typically, 9mm disc), and exposed to UV light for 10 minutes. After crosslinking with exposure to UV light, the molded PAA/PAM hydrogels were removed from their molds by exposing them to ethanol, which removes any homopolymers that might have been created during crosslinking and dehydrates of the hydrogel, resulting in gel shrinkage and allows for easy sample removal from the mold.

Once detached from the mold, each sample was washed in fresh ethanol and placed in an oven at 40°C for two hours to remove any excess ethanol. The dried disc of PAA/PAM material was then weighed, and placed into a PBS solution with a known pH in the range of pH 5-8. It is important to note that the PAA/PAM hydrogels made in this manner were observed to influence the local pH of the solution in which the material is immersed. It is possible that unreacted acrylic acid monomers were released into the solution, acting as a source of protons and dropping the pH. Following this observation, a flow-through chamber was used to continually replace the PBS solution around the hydrogel slabs and ensure constant external pH values. Swelling measurements were made on gels treated in this manner and compared to the dry weight of the sample material. Similar experiments were performed on the hydrogels following attachment of fluorescent labels, as described in Task 3.

Results

Experiments testing the pH-sensitive swelling response of the PAA/PAM hydrogel slabs prove that there is an increase in swelling with increasing pH (Figure 2). The PAA/PAM

hydrogel slabs better withstood the mechanical stresses during weighing procedures, resulting in smaller amounts of standard deviation and a more repeatable pH-sensitive response. However, it was also observed that the more the PAA/PAM hydrogels swelled, the more delicate they became, resulting in greater difficulty in handling and higher standard deviation in measured swelling values at more alkaline pH.

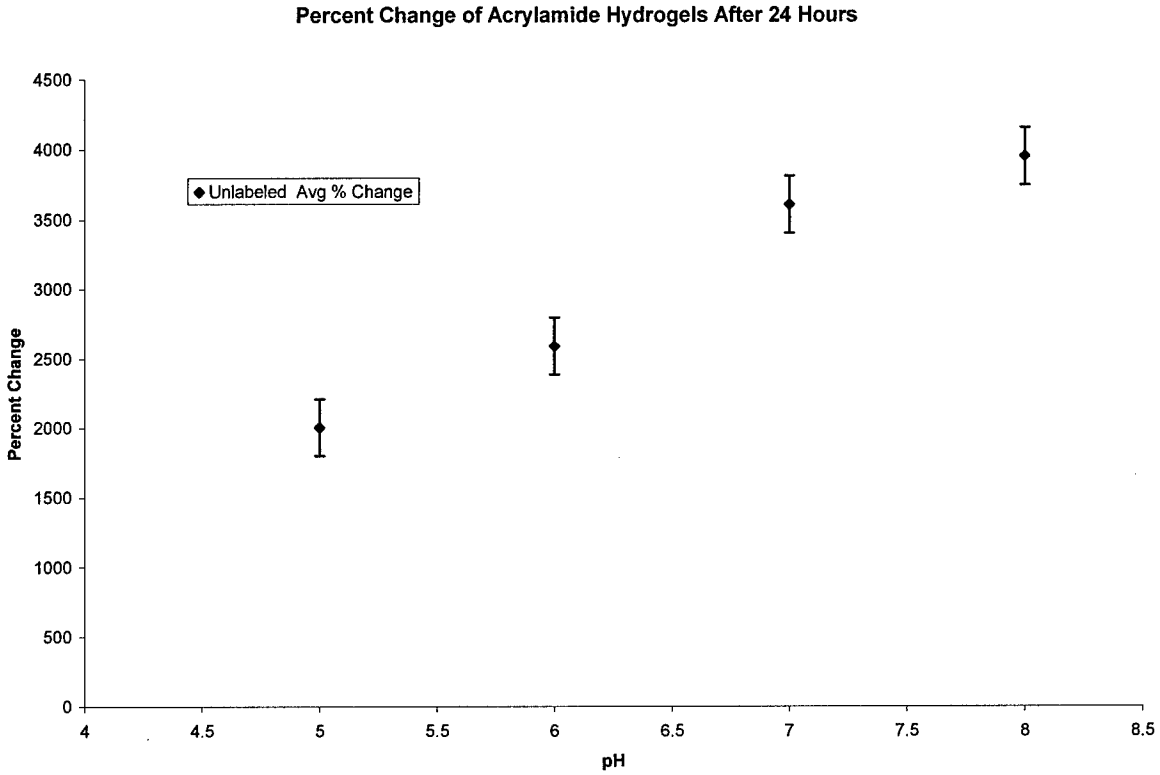

Figure 2: Results from PAA/PAM Hydrogel pH-Sensitivity Test

Conclusions

The results of the pH-sensitivity experiments are promising, and show swelling data similar to that observed by others.[14,15] The results show that there is a larger percent change in weight with increasing pH, and the rate of change of swelling is directly proportional to the pH of the surrounding solution. The results show that the material in pH 8 solutions will swell to a weight that is almost twice that in a pH 5 solution. It was also observed that the strength of the hydrogel materials is inversely proportional to the amount of swelling experienced by the material. This is most likely due to the increased presence of water in the swollen hydrogel matrix, which reduces the number of interactions between hydrogel matrix components. While the data could be improved by more careful control of the fabrication, processing, and measurement protocols, these data were considered sufficient to demonstrate the sensitivity of the gels to pH, and adequate to support further exploration of these gels for smart sensors. In particular, because of the sensitivity of the proposed microcantilever and RET fluorescence readout approaches, it was deemed appropriate to move forward with the production of microscale gel systems based on PAM/PAA.

GOx immobilization

Overview/Objectives

Three main methods of glucose oxidase (GOx) inclusion were compared: 1) direct addition, with only physical interactions entrapping GOx; 2) molecular loading, with electrostatic interactions anchoring GOx; and 3) immobilization with a specific biotin-avidin molecular recognition interaction. The premise for each of these approaches is described here. In the first case, the enzyme is included in the pre-gel solution, and is trapped as the gel is formed by polymerization and crosslinking reactions. For the molecular loading method, a hydrogel is formed in the desired architecture first, then exposed to a concentrated solution of GOx; the GOx molecules diffuse into the hydrogel matrix, and electrostatic interactions occur among the various charges in the hydrogel matrix. The third method relies upon the specific interaction between biotin and avidin; the technique requires the conjugation of biotin to a polymer molecule in the pre-hydrogel solution, as well as attachment of biotin will to GOx, and the biotinylated polymer molecule is then connected to GOx through the addition of avidin (see Figure 3). As an alternative, biotinylated polymer could be used with commercially-available GOx-avidin. The experiments investigating these methods are described below.

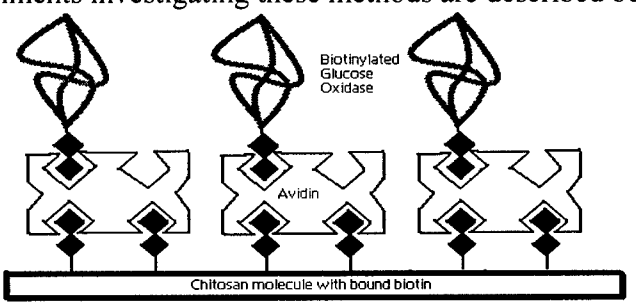

Figure 3: Cartoon Illustrating Chitosan/Biotin/Avidin/GOx Architecture

Approach 1: Direct Addition

Methods

A concentrated solution of GOx was directly added to the pre-hydrogel polymer solution prior to crosslinking. During the crosslinking step, GOx is thought to be involved with the other molecules in the pre-hydrogel solution, and links are formed between all of the polymer and enzyme molecules in the solution. The ionic crosslink is relatively weak, and during swelling interactions, could be easily broken, resulting in lower enzyme stability.

For preliminary direct-addition experiments, chitosan hydrogels were prepared as described above. A "pre-gel addition" method of GOx inclusion was accomplished with a 10mg/mL solution of GOx in DI water. Concentrated GOx (1mL) solution was added to 25mL of 2% weight chitosan solution and stirred for 2 hours, then 25mL of 2% weight gelatin solution was slowly added to the GOx/chitosan solution, and this pre-hydrogel solution was stirred overnight. The well-mixed pre-hydrogel solution was poured into a custom circular mold made from silicone rubber, and left to solidify in the refrigerator at 3°C for 4 hours.

The solidified pre-hydrogel was then ionotropically gelled using TPP, and the crosslinked, solidified hydrogel was removed from the refrigerator, washed in DI water for 15 minutes, and placed in an oven at 40°C for drying. The gels were periodically weighed and allowed to heat until no further weight change observed; depending on the thickness of the hydrogel prior to drying (typically 5-10mm), this process required between 24 and 48 hours. The dried samples

were then gently removed from their molds, and if the molds were too large, samples were cut to the desired size. For preliminary hydrogel slab experiments, hydrogels were made and dried in large molds, and then scored with a scalpel into a 1mm X 1mm square. In later hydrogel slab experiments, the hydrogels were cut to the desired size prior to drying, but this method resulted in more extensive hydrogel dissolution during swelling experiments. In the final set of hydrogel slab experiments, which has become the standard procedure for testing all new hydrogel formulations, 9mm diameter molds were made in poly(dimethylsiloxane) (PDMS) cured around a standard plastic replica mold. This method involves no cutting and has resulted in the least amount of hydrogel dissolution over the course of the swelling experiments.

The chitosan gels prepared with GOx added to the pre-gel mixture were found to be very unstable without additional (covalent) crosslinking. In experiments aimed at assessing the efficiency and stability of the enzyme immobilization, it was observed that the gels were dissolving rapidly (within a day) under standard pH 7 PBS storage conditions; thus, the stability of enzyme in the gels fabricated in this approach was not assessed.

Approach 2: Electrostatic Loading

Overview/Objectives

It was hypothesized that gels formed from cationic chitosan would attract and retain anionic glucose oxidase, similar to what we have observed for anionic alginate gels and cationic macromolecules.[16] This approach to immobilization is expected to extremely efficient and stable as long as the gel is stable.

Methods

In order to observe the process of GOx loading into chitosan gels, chitosan microspheres were prepared (spheres were labeled with TRITC and Alexa Fluor 647™ as an energy-transfer pair, details of labeling and preparation are provided under Task 3), and sequential images were collected using confocal microscopy following the addition of FITC-GOx into the microsphere suspension. All three fluorophores were simultaneously excited and imaged at their respective appropriate excitation/emission wavelengths. The average relative fluorescence intensity of FITC for three regions of interest within the sequence of images (three separate 10μm particles) was calculated and plotted versus time to determine the time-dependent uptake behavior of the gels.

Results

A typical confocal image sequence for the GOx-loading experiments is presented in Figure 4. It can be observed from this time-lapse imaging (each frame=4 seconds) that the localized fluorescence intensity of the green (FITC) channel increases rapidly with time relative to the TRITC (red) channel, indicating an increase in the GOx concentration in the chitosan spheres with time. This is quantitatively confirmed from area-normalized intensity plots (Figure 5), which also prove the consistency of the loading into different spheres; the loading profile and final intensity is similar for three independent measurements within the same experiment. Interestingly, the blue channel intensity (AF 647 emission at approximately 700nm) also increased with time, apparently due to increased energy transfer as GOx levels increased. From these results, it is clear that GOx diffuses rapidly into chitosan microspheres, leading to uniform distribution with high loading efficiency. Furthermore, the stability of this immobilization

appears to be extremely high. While the stability under dynamic conditions of changing glucose/pH has not yet been quantitatively determined, this is the subject of ongoing studies, and preliminary results are promising (described further under Task 3).

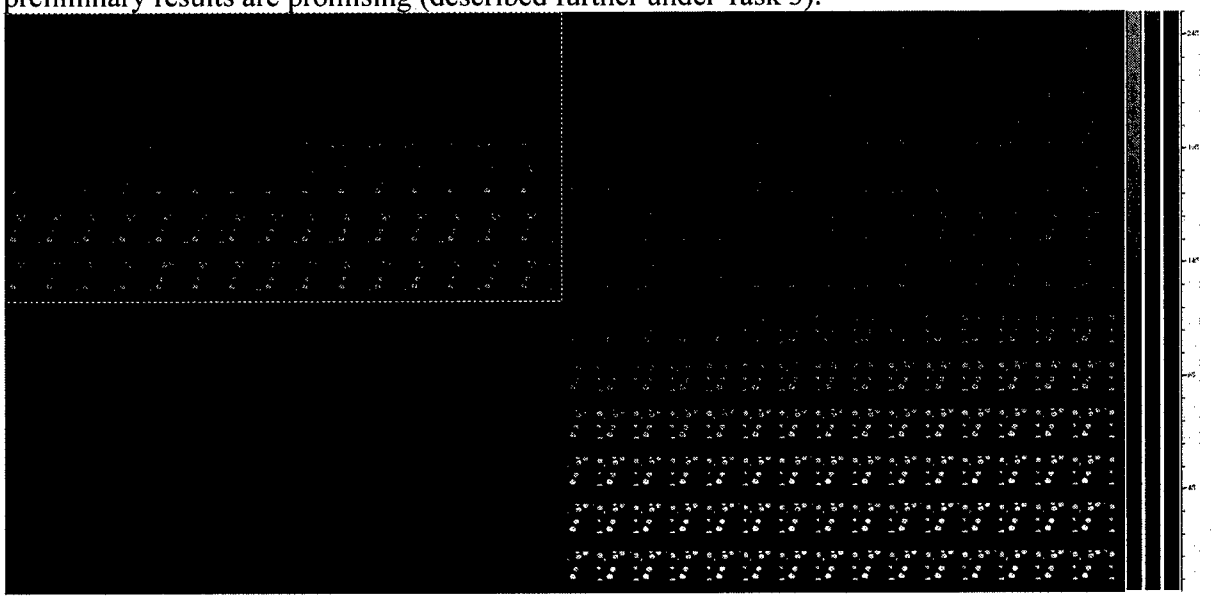

Figure 4: The confocal microscopy sequential images of the TRITC and Alexa Fluor 647™ dual-labeled microspheres solution after addition of FITC-GOx

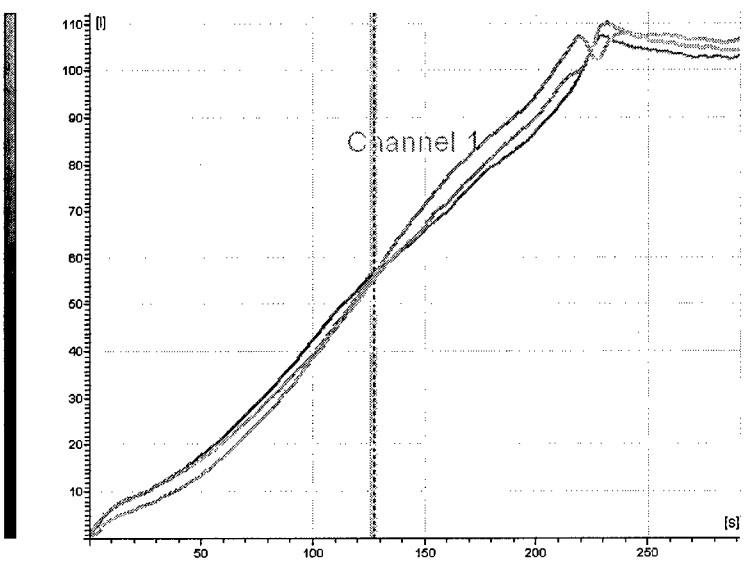

Figure 5: The plot of FITC fluorescent intensity vs. time. (From three microspheres in the picture above)

Approach 3: Biotin-Avidin Interaction

Overview/Objectives

This method requires, as a first step, the conjugation of biotin to one of the polymers in the hydrogel matrix. Chitosan has many available sites for conjugation, due to the large number of amine groups available on the polymer chain. Following attachment of biotin to chitosan

molecules, the introduction of GOx into gels via avidin-biotin interactions was pursued as a stable immobilization method.

Methods

Several methods of biotin introduction were assessed to link biotin to chitosan. N-hydroxysuccinimidobiotin was made synthesized via a reaction of NHS with biotin in dimethyl sulfoxide (DMSO), as described described previously. [17], [18] EZ-Link® N-hydroxysuccinimidobiotin (NHS-biotin) is also available from Pierce Chemicals (www.piercenet.com). Prepared solutions of 2% weight chitosan at pH ~3.0 were used in biotin conjugation reactions. NHS-biotin was dissolved in dimethylformamide (DMF), and slowly added to the 2% weight chitosan solutions in molar ratios of 1:1 and 1:7 (chitosan:biotin), while continually stirring the chitosan solution. The resulting mixture was left to stir overnight, then a small sample of the mixture was dried onto silicon wafers in a vacuum oven. Fourier Transfer Infrared Spectroscopy (FTIR, reflection mode) measurements were performed on the dried samples to determine if conjugation of NHS-biotin to chitosan occurred, as would be indicated by the change in vibrational structure due to the formation of new bonds.

Results

FTIR measurements on low molecular weight chitosan reacted with NHS-biotin in DMF resulted in inconsistent FTIR spectra; some measurements showed a decrease in the amide III (1660 cm^{-1}) peak, and when this measurement was repeated on a different portion of the same material, the measurements showed an amide III peak comparable to that in pure chitosan (Figure 6, Figure 7).

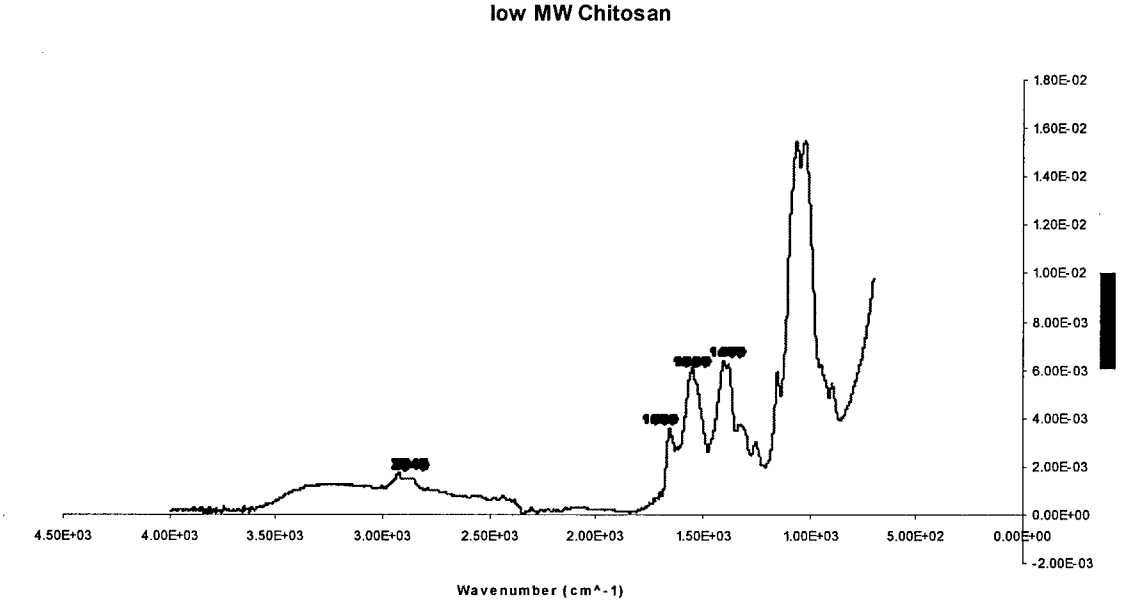

Figure 6: FTIR Spectra of Pure Chitosan

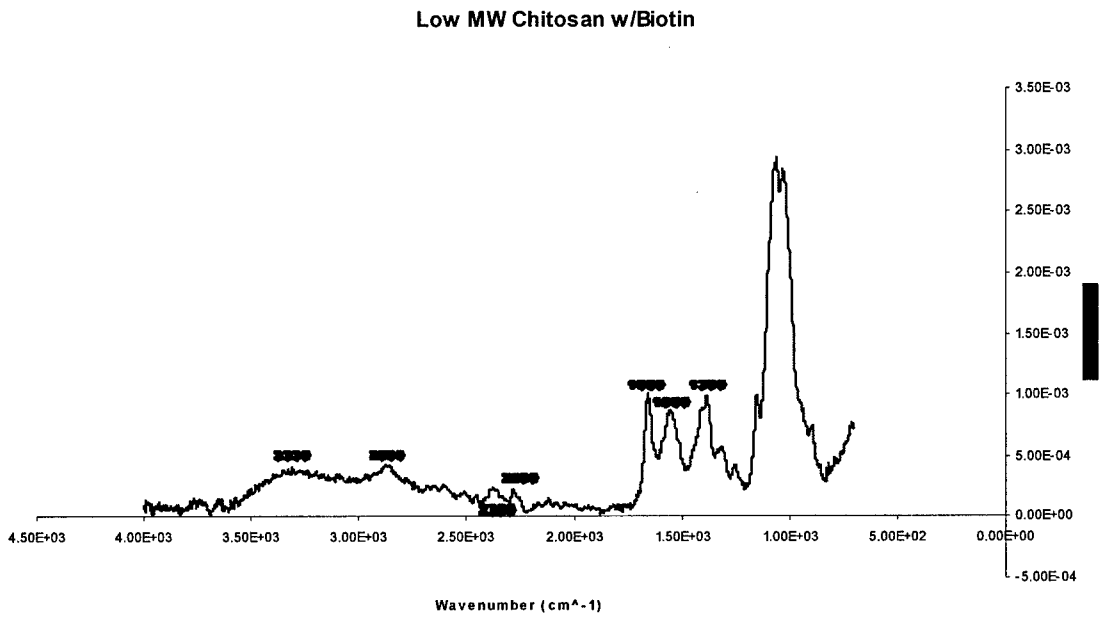

Figure 7: FTIR Spectra of Chitosan Mixed with NHS-Biotin

In addition, when low molecular weight chitosan was exposed to EZ-Link® NHS-biotin dissolved in DMF, the resulting FTIR spectra showed no decrease in the amide III peak. These recently acquired results suggest that biotin has not been successfully bound to chitosan (Figure 8, Figure 9, and Figure 10).

GOx biotinylation was also attempted, but the FTIR spectra from each method attempted showed no significant signs of a bond between GOx and biotin. Nevertheless, this material is also commercially available from Pierce Chemicals, along with GOx conjugated to avidin. Once biotinylation of chitosan is achieved, GOx-avidin will be obtained and used in GOx immobilization. This method should prove more reproducible, and is certainly less complicated than trying to bind biotinylated chitosan and biotinylated GOx through avidin.

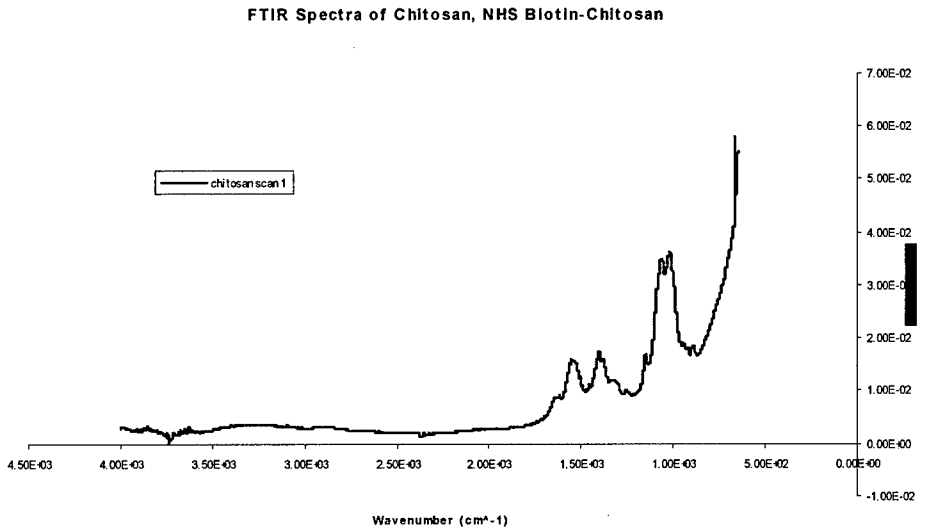

Figure 8: FTIR Spectra of Pure Chitosan

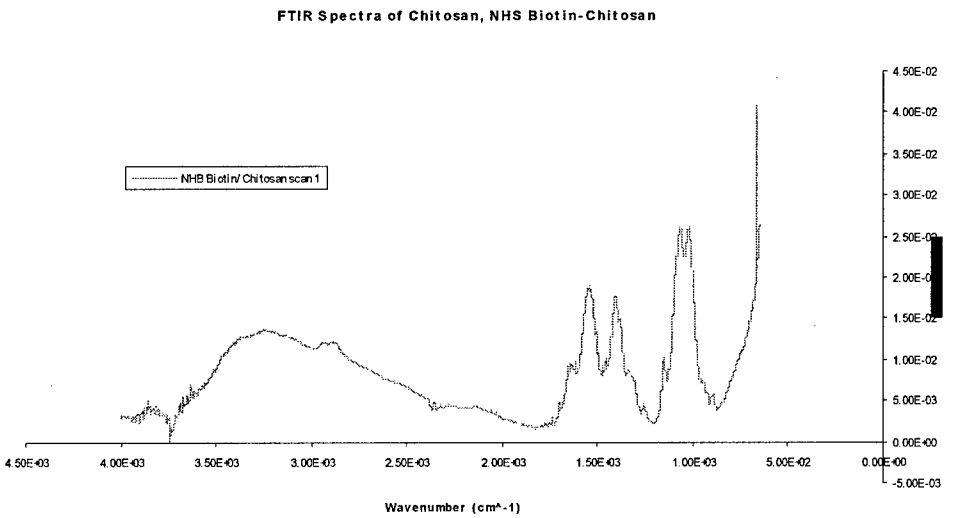

Figure 9: FTIR Spectra of Chitosan Mixed With NHS-Biotin

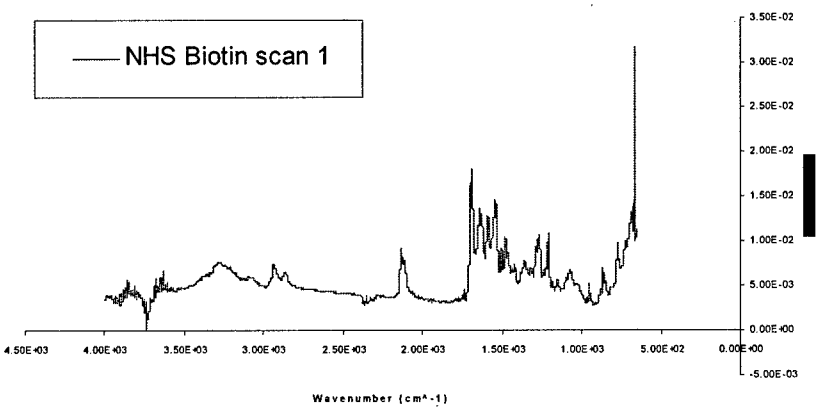

Figure 10: FTIR Spectra of Pure NHS-Biotin

Conclusions

One of the problems with the biotinylation reaction involving chitosan is that the pH of the chitosan solution is too low to allow for efficient conjugation of the NHS-containing material. At more alkaline pH, where the reaction is more favorable, chitosan precipitates out of solution, due to folding of the polymer in response to the decreased concentration of hydrogen ions. An answer to this problem is to use a proton-acceptor to slowly increase the pH of the solution to a higher level, which would result in a more efficient interaction between NHS-biotin and the deprotonated amine group on the chitosan polymer, while keeping chitosan dissolved in the solution. Two potential proton-acceptors that will be used to improve this reaction are triethylamine and triethanolamine. Chitosan solutions will be titrated to a pH of approximately 6 using these solution, and NHS-biotin conjugation will be further attempted.

Higher chitosan:NHS-biotin labeling ratios, between 1:10 and 1:20, will also be used, and the effect of increased labeling will be determined with quartz crystal microbalance (QCM) measurements, as well as FTIR measurements. QCM measurements will involve adsorption of one layer of either biotinylated or unbiotinylated chitosan. The resonant frequency of the chitosan layer adsorbed to the crystal will be recorded, and the coated crystal will be exposed to a concentrated solution of avidin. At acidic pH values, both chitosan and avidin exhibit a positive charge, and unbiotinylated chitosan should not interact with avidin, and should produce only a small change in QCM frequency. However, avidin should interact with the biotinylated chitosan and produce a marked decrease in QCM frequency, indicating biotin/avidin bonding.

The results of some QCM experiments performed with biotinylated chitosan with a 7:1 biotin:chitosan molar ratio and unbiotinylated chitosan can be seen in Figure 11 and Figure 12 below. The data show that there is a decrease in QCM frequency when exposing the biotinylated chitosan to a solution of avidin, whereas there is no decrease in QCM frequency when exposing unbiotinylated chitosan to a solution of avidin. These results indicate that the biotinylated chitosan is capable of absorbing and binding avidin, even though there are positive charges on avidin and chitosan that would usually keep these two materials separated.

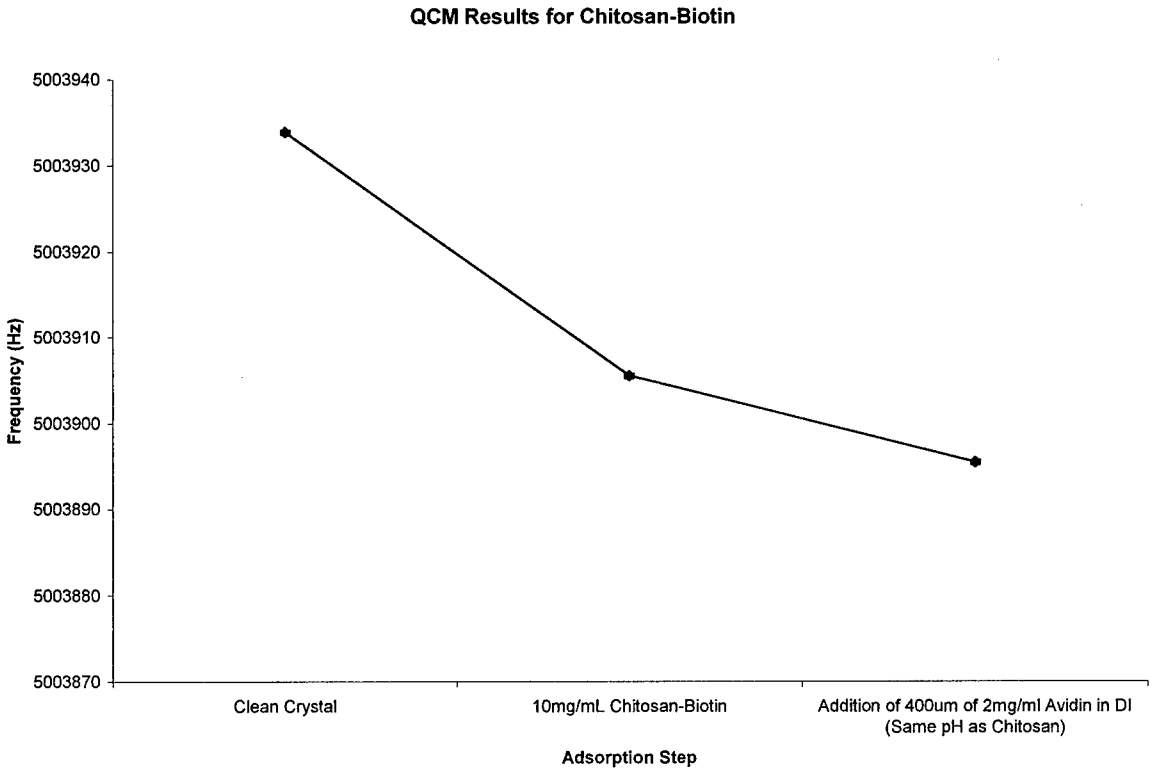

Figure 11: QCM Data for Chitosan-Biotin Material

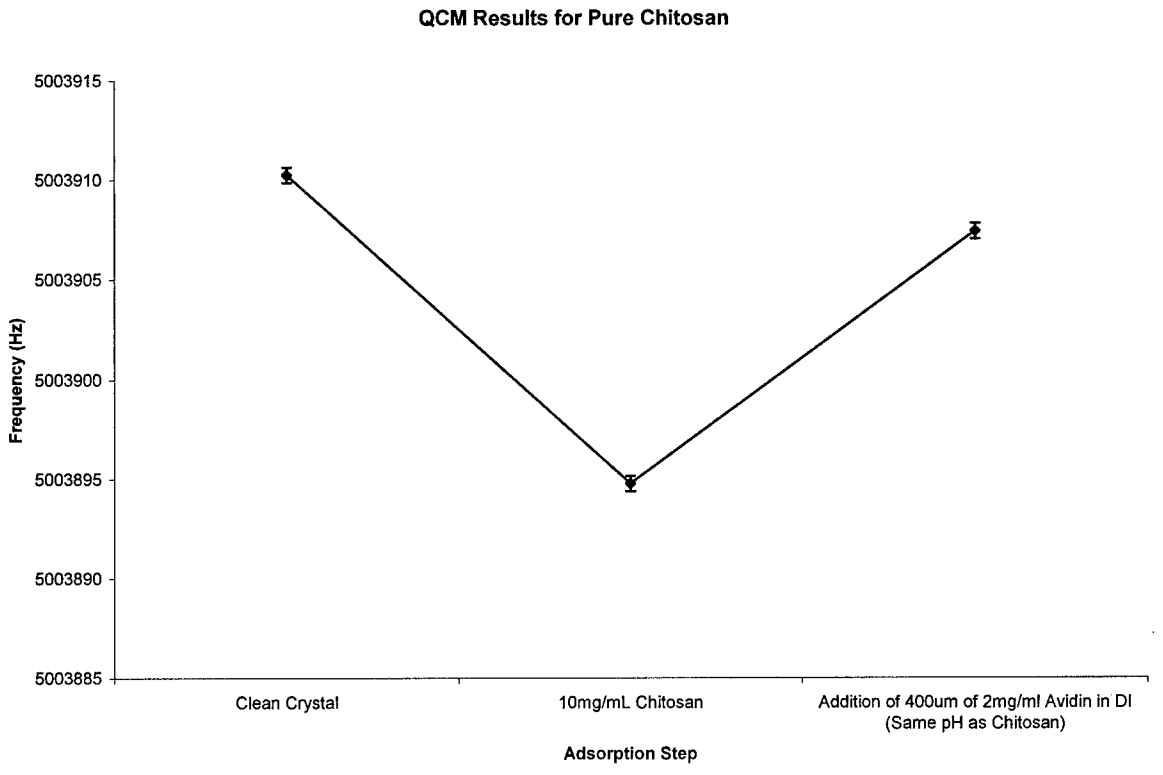

Figure 12: QCM Data for Pure Chitosan

Once the biotin/avidin immobilization method is accomplished, the enzyme stability of each previously mentioned GOx addition method will be assessed with leaching tests performed on samples prepared by each technique. FITC-GOx will be used to facilitate analysis of protein loss with fluorescence spectroscopy. This testing will involve exposing samples to PBS ranging from pH 5.5 to pH 7.4 in microwell plates; they will be exposed to the PBS solutions for 48 hours to allow for swelling equilibrium. After equilibrium is reached, samples will be removed from the bulk solution surrounding each sample, and UV/Vis absorbance and fluorescence scans will be used to assess the amount of FITC-GOx in the PBS solution. The presence of the fluorescent molecule on the enzyme will facilitate absorbance and fluorescence measurements. Biotinylation of PAA will also be attempted after successful chitosan biotinylation. The implementation of the biotin/avidin interaction method in GOx addition methods should provide more stable anchoring of GOx in the hydrogel material. We note that the incomplete status of this aspect of the project is offset by the advances in other areas of the project that have progressed into Tasks outlined originally for Year 2. Return to this area of the project is not essential to success of developing useful systems, but is necessary to optimize efficiency and stability of the enzyme in the gels. It was deemed most appropriate to study the fundamental properties and processing limitations of chitosan gels in more depth before attempting additional experiments with macrogels.

b. Develop pH-sensitive hydrogel with GOx-coated nanoparticle inclusions, and assess loading efficiency, enzyme activity, and stability. (Months 3-5)

Overview/Objectives

It became obvious that direct enzyme loading led to poor stability of encapsulation. Immobilizing GOx in nanofilm coatings on nanoparticles was proposed as a means to improve the stability of enzyme entrapment in the hydrogels, using the larger relative size of the nanoparticles to increase the likelihood of physical entanglement in the gel matrix. The objective of this aspect of the project was to compare the stability of the glucose response using GOx-coated nanoparticles to that observed for native enzyme.

Methods

Hydrogel film stability experiments were conducted on a microcantilever coated by the GOx doped hydrogel after one month of storage in a 0.01 M NaCl solution. Similarly, glucose oxidase-coated nanoparticles were introduced in a hydrogel on a cantilever, and the device was stored in the same saline solution. For nanoparticle modification, GOx was assembled in nanofilm coatings on 750 nm particles using the layer-by-layer electrostatic assembly process outlined in Figure 13. Using the reversal of surface charge (ζ-potential) that occurs at each step, the anionic enzyme was assembled in multilayers in alternation with poly(allylamine hydrochloride) (PAH) (polycation). A total of three bilayers of GOx/PAH were assembled, and enzyme activity was confirmed by colorimetric assay.

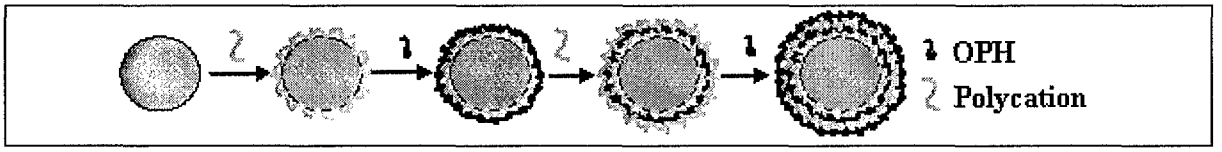

Figure 13. Scheme of polycation/anionic enzyme (OPH) alternate assembly on a spherical nanoparticle

Results

For direct-added GOx, the cantilever deflection in response to the presence of glycose decreased to less than 25% of that of fresh-made microcantilever, indicating a significant loss of GOx from the gel. However, preliminary experimental results showed that the cantilevers lost their bending response to glucose gradually over months in a similar speed as that of pure GOx doped hydrogel.

Conclusion

It was anticipated that GOx films on nanoparticles will provide a better means of encapsulation of the active enzyme. Unfortunately, use of fairly large dimension (~100X larger than GOx) particles had no apparent effect on the stability. This was surprising, but given the magnitude of the swelling response, it can be accepted that even 100X increase in size is insufficient to physically trap the particles in the gel. To further study this, larger particles (micron-size) and alternative surface charge and hydrophobicity will be compared to the results obtained for native GOx.

c. Confirm and quantify glucose-sensitive swelling behavior of hydrogels; identify most sensitive and stable system to be used in developing readout methods (Months 4-6).

Glucose sensitivity: Chitosan

Overview/Objectives

Chitosan gels, previously shown to exhibit pH-sensitive response, must be modified to

contain an enzymatic element to exhibit a glucose-sensitive response. Following modification of the chitosan with GOx using the direct addition method, swelling experiments were used to determine steady-state swelling characteristics of the gels due to the presence of the enzyme and exposure to glucose. It was hypothesized that gel swelling would increase with glucose concentration due to the acidic product, resulting in protonation of amine groups and subsequent water uptake by the gels. Furthermore, a response that is consistent over different glucose concentration and time was expected.

Methods

Chitosan gel discs were prepared as described above for pH-sensitivity experiments, with the addition of GOx prior to ionic gelation. After drying, samples were rehydrated in phosphate buffered solution with a pH of 7.0 (PBS 7.0) for 24 hours. After rehydration, the prepared GOx/Chitosan/Gelatin hydrogel samples were weighed and moved into pH 7.0 PBS solutions with known concentrations of β-D glucose (0 to 50mM) in random order. After 24 hours in each glucose-PBS 7.0 solution, the samples were weighed again, and the percent weight change for each sample was calculated. This was accomplished by comparing the weight of the material in PBS 7.0 solutions with no glucose to the weight of the material after being exposed to glucose containing solutions using.

$$\%\_Change = (W_{gluc} - W_{0mM}) / W_{0mM}$$

Results and Discussion

Data from twenty hydrogel samples in different, known concentrations of glucose were averaged, and plotted in each experiment. The results of the experiment are graphed in Figure 14 and Figure 15:

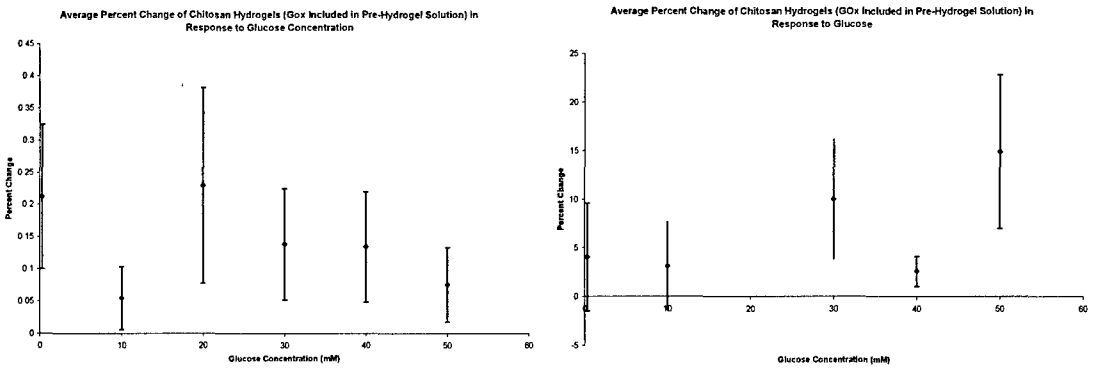

Figure 14 and Figure 15:
Chitosan/gelatin hydrogel glucose sensitivity experiments.

Theoretically, the hydrogels should absorb a consistent amount of water with respect to glucose concentration; however, the data show an inconsistent behavior. There is a decrease in percent weight change versus glucose concentration above 20mM, whereas the weight change below 20mM was inconsistent. Overall, the variation in the data was extremely large. Both of these issues were attributed to hydrogel sample dissolution due to breakage during handling, similar to what was noted above for the pH-sensitivity experiments. Once rehydrated, the dried samples became extremely delicate and difficult to handle; during movement from solution to solution, the gel samples would often break apart, complicating the weighing process and influencing the resulting weight change of the hydrogel. The frequency of breakage was found to

increase with higher water content.

Conclusions

Without crosslinking or other treatment, large-scale chitosan/gelatin gels of this form were unstable and data collected from these systems are simply unreliable for any conclusions. Additional experimentation to determine the swelling characteristics of the same gels, on the microscale, was completed with much greater success, as described under Tasks 2 and 3.

Chitosan basic properties analysis

Overview/Objectives

Many studies have been done to study the swelling behavior of various pH-sensitive hydrogels. The most common method used to determine the swelling behavior of hydrogels is as we described above: it involves weighing the dried material, immersing it in a solution of known pH for a specified time, removal from pH controlled solution, blotting the sample to remove surface liquid, and re-weighing. [19] Disadvantages of this method include the difficulty of controlling the amount water removed from the gel, and dissolution of soft swollen gel due to repeated handling during measurements. Other typical measurement methods include calculating the volume change by measuring the change in diameter of gel discs[20] or measuring drug release from the hydrogel matrix during exposure to different pH solutions[21]. It is commonly reported that the swelling of ionically-crosslinked chitosan hydrogels exposed to acidic pH, below pH 4, is significant, while under neutral conditions the swelling of the gel is less significant.[8,9] Therefore, the swelling behavior of chitosan hydrogels in physiological pH range, which is very important in this application, is still unclear.

Given the difficulty in handling and lack of consistency in results form chitosan/gelatin swelling systems described above, further characterization of basic chitosan behavior in different pH environments was performed. The objective of this part of our study was to investigate the swelling mechanism of chitosan/gelatin hydrogel crosslinked with TPP in physiological pH range with turbidimetric titration methods, which give insight into the interactions among TPP, chitosan and gelatin molecules in solution.

Turbidimetric Titration

Methods

Low molecular weight chitosan (50,000 MW), gelatin (type B, 225Bloom), sodium tripolyphosphate (TPP), phosphate buffered saline (PBS tablets), and 1H,2H,2H-perfluorodecanethiol (PFDT) were obtained from Sigma. Turbidity measurements were monitored with transmittance measurements using a Perkin-Elmer Lambda 45 UV-Vis Spectrometer. The interactions of chitosan, gelatin and TPP molecules were investigated by turbidimetric titration. The dependence of the polymer solution turbidity on pH was obtained according to reported methods.[22] Briefly, 0.1M NaOH was added into the solution at constant ionic strength and constant concentration. Gelatin, chitosan and TPP solutions were prepared independently and filtered with 20μm nylon membranes (MAGNA) prior to mixing. Upon addition of base, the solution was gently stirred until a stable transmission reading (%T) was obtained. A digital pH meter was used to monitor the solution pH. Transmittance was monitored at 420nm with an UV-Vis spectrometer and the turbidity was calculated in terms of 100-%T.

Results and Discussion

The results of the turbidity titration curves of gelatin, chitosan and gelatin/chitosan mixture solutions are shown in Figure 16. Three obvious turbidity change regions are revealed by the curve of gelatin/chitosan mixture: T_1, T_2 and T_3. The point of T_1 (between pH 4 to 5) is not as clear as the other two points. At pH values less than T_1, the turbidity of the solution is nearly constant, and the solution is clear. As the pH value is increased above T_1, the turbidity of the solution slowly increased. Above T_2, between pH 6 to pH 7.2, the turbidity of the solution increased quickly. As the pH of the solution is increased above T_3, the substantial increase in turbidity indicates the presence of a coacervate.

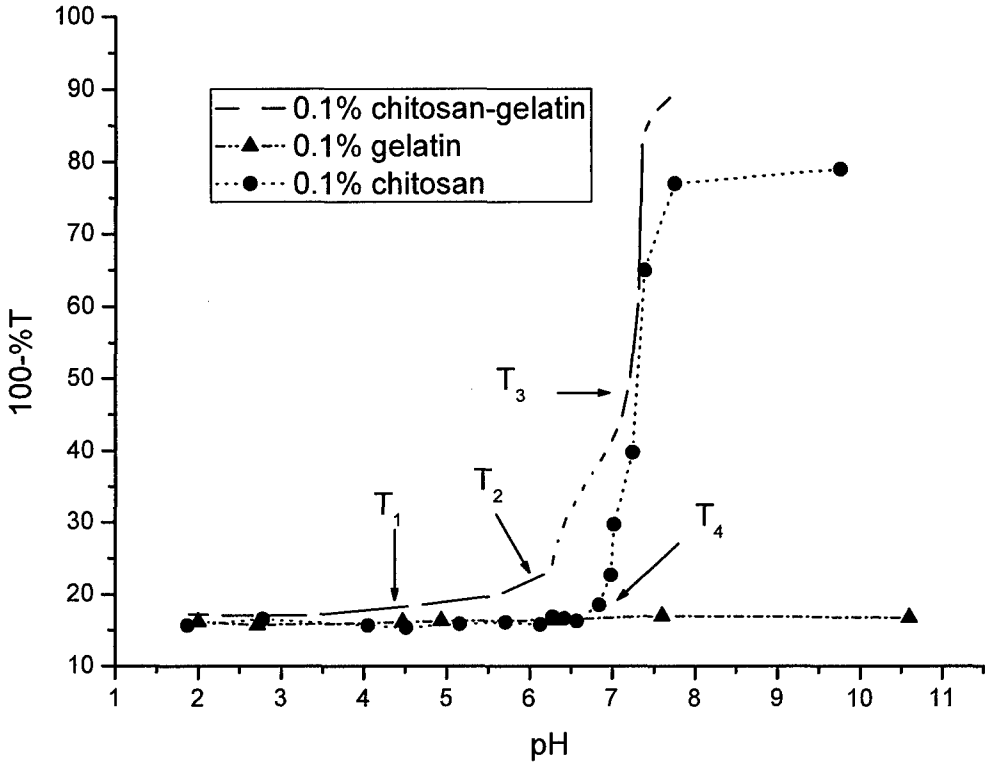

Figure 16: Turbidity titration curves of gelatin, chitosan and gelatin/chitosan mixture solutions at 420nm

This is likely due to the presence of gelatin which has a pI of 4.5-5.0. At a pH value lower than the pI, gelatin molecules have a positive charge, while they possess a net negative charge at pH higher than the pI. Furthermore, the pK_a of chitosan is around 6.5; therefore, at pH values lower than gelatin's pI, both gelatin and chitosan molecules have an overall positive charge. The repulsive forces between the positively charged gelatin and positively charged chitosan prevent the formation of complexes, and the two kinds of molecules exist separately within the solution. When the pH is above gelatin's pI, but below chitosan's pKa (between 4 and 6), the gelatin molecules have negative charge, which can react with the positively charged-chitosan to form a complex. From previous reports, the net charge density of gelatin is relatively low; for example there are only 15 ionized groups per 10^5 grams of gelatin at pH 6.5.[23] Therefore, even as gelatin reacts with chitosan, the complex they form still has a high positive charge like the free

polyelectrolyte, and displays a pH-dependent mobility that decreases to zero at the point of coacervation. The positive charge between the complexes and the thermodynamic mobility of the complexes keeps the solution stable. Thus, the formation of T_1 results from the pI of gelatin influencing the mixture. At a pH near the pKa of chitosan (pKa = 6.5), the positive charge density of chitosan decreases dramatically. Some complexes conjugate together to form larger particles in order to reach a stable balance in the solution, which is due to a decrease in charge density on the complex surface, and results in an increase of solution turbidity. Thus, the appearance of T_2 is the effect of pKa of chitosan on the mixture solution.

Compared with the curve of chitosan/gelatin mixture, the curve of pure chitosan shows only a single inflection point (T_4), where the chitosan molecule loses its positive charge and begins to aggregate. In contrast, the gelatin curve exhibits no obvious change, which suggests that the pH change in this range does not influence the gelatin solution's behavior. Gelatin is one of the few proteins that has random coil configurations, and gelatin behavior in solution follows the Flory-Huggins lattice solution theory.[20] In addition, the charge density of gelatin molecule is relatively low, so minimal differences in ionization are expected.

The results of turbidity titration of TPP/polymer systems are shown in Figure 17. The curves of TPP/chitosan and TPP/chitosan/gelatin display the same overall trend. Both of them have two change points at T_1', T_2' and T_3', T_4'. At a pH below T_1' (T_3'), the turbidity increases dramatically with increasing pH, and at a pH above T_1' (T_3'), but below T_2' (T_4'), the turbidity increases slowly with pH. At a pH above T_2' (T_4'), the turbidity decreases due to precipitation.

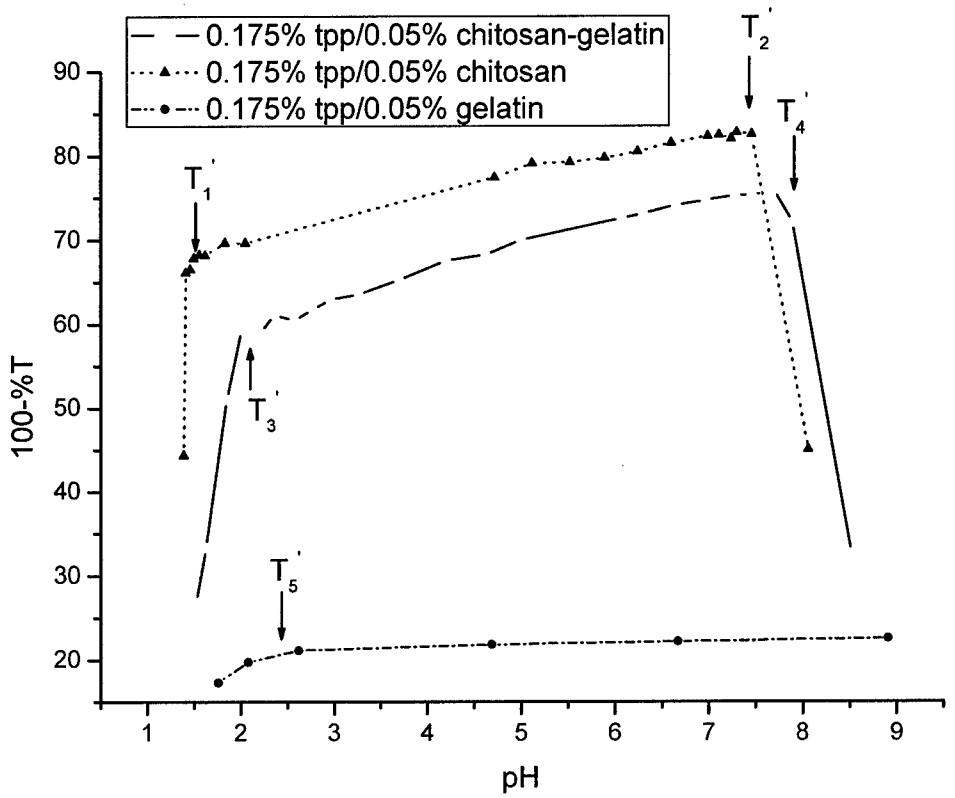

Figure 17: Turbidity titration curves of TPP/gelatin, TPP/chitosan and TPP/gelatin/chitosan mixture solutions at 420nm

From previous reports[24], it is believed that the negative charge of TPP decreases dramatically below pH 1.9. The charge density of chitosan does not change much in this pH range, therefore turbidity effects are likely due only to TPP ionization. More ionic groups of TPP react with the positively charged amine group of chitosan to form the complex, which results in increased turbidity. At pH values above 2, the ionic density of TPP increases slowly, which is reflected in the change of turbidity. In the range of pH 2-7, the turbidity of the solution increases slowly, and the complexes keep a positive charge. Therefore, T_1' (T_3') is the effect of the change of NaTPP charge density.

At the point T_2' (T_4'), precipitation is observed in the solution. At this time, most of the amine groups on chitosan chains react with TPP ions, and the free positive charge of the complexes decrease to a very low level, since the solution pH is above the pKa of chitosan. Thus the stability of the solution is destroyed and precipitation occurs. Since the gelatin has low charge density, the degree of TPP reacted with gelatin is low, as shown in Figure 17. Small increases in %T can be observed in the gelatin curve at a pH below T_5', which is the result of the increase in charge density of TPP. In this pH range, positively charged gelatin molecules can react with TPP ions, but the overall effect is small.

Taken together, the turbidity titration test results suggest that in the TPP/gelatin/chitosan system, the crosslinking structure is mainly formed by the reaction between chitosan and TPP.

Gelatin molecules can form polyelectrolyte complexes with chitosan molecules, resulting in entrapment of the chitosan structure with electrostatic bonds. In addition, gelatin has the unique characteristic of temperature-dependent sol-gel change, which is useful in making a uniform hydrogel and keeping the gel shape.[21] Therefore, this method was used in this study. First, the chitosan and gelatin were mixed above the gelatin gelation point (25°C). The pre-hydrogel solution was then cooled to a temperature below gelatin's gelation point to form a solidified gel. Then the crosslinking process occurs by addition of TPP under gel conditions, which could reduce precipitation formed by the direct reaction between TPP and chitosan, and is capable of forming a uniform gel.

Conclusions

In this study, the interactions among the chitosan, gelatin and TPP system were investigated to gain insight into the use of chitosan as a pH-sensitive element of a smart sensor. The results suggest that, in the TPP/gelatin/chitosan system, the crosslinking structure of the complexes was mainly formed by the reaction between the amino groups of chitosan and TPP ions. Gelatin molecules could form polyelectrolyte complexes with chitosan molecules in order to entrap the chitosan structure by electrostatic bonds, resulting in increased stability. The findings have provided a basis for understanding the rough dynamic range expected for chitosan-based smart gels.

***Task 2.*To develop and characterize hydrogel-coated microcantilevers to transduce swelling in response to glucose (Months 7-24):**

a. Develop procedure for depositing glucose-sensitive gels on microcantilevers (Months 7-12).

Poly(acrylamide) System

Overview/Objectives

Microcantilevers provide a sensitive platform for chemical and biological sensors[25] and can provide improved dynamic response, greatly reduced size, high precision, and increased reliability. These systems can be integrated onto micromechanical components with on-chip electronic circuitry. Since pH-sensitive hydrogels swell in response to pH and the hydrogel volume is a function of external pH, it is expected that the swelling of the hydrogel immobilized on a microcantilever will cause the cantilever to bend.[26] The direct addition method described above (Task 1) was applied in this case to acrylamide gels on microcantilevers to assess the ability to immobilize the enzyme in the gel on an opto-mechanical readout system.

Methods

Commercially-available silicon microcantilevers (Veeco Instruments, CA) were used in all experiments. The dimensions of the V-shaped microcantilevers are 180 μm in length, 25 μm in leg width, and 1 μm in thickness. One side of the cantilever was covered with a thin film of chromium (3nm) followed by a 20 nm layer of gold, both deposited by e-beam evaporation. The other side of the microcantilever is silicon with a thin naturally grown oxide layer.

The chemicals used in these experiments including NaCl, D-glucose, GOx (EC 1.1.3.4,

Type VII-S, from Aspergillus niger, 166,500 units/g solid), 2-dimethylamino ethyl methacrylate (DMEM), acrylamide (AMD), the cross-linker N,N'-methylenebisacrylamide (bis-AMD), and the UV photo-initiator diethyoxyacetophenone (DEAP), were used as received from Aldrich. High-purity de-ionized water was obtained with a Milli-Q water system (Millipore). The pH of the deionized water was 6.82. The pH of a 10^{-2} M solution of NaCl was 7.0. The glucose solutions used in our microcantilever deflection experiments were prepared in a 10^{-2} M solution of NaCl. The pH of all these solutions was maintained at 7.0.

In order to selectively attach the hydrogels on one surface of a microcantilever, PFDT was introduced on the gold-coated surface to block the attachment of the hydrogel.[27] Cantilevers were coated with PFDT by placing the cantilevers in 5 x 10^{-3}M PFDT/ethanol solution for 24 hours, and then rinsing with ethanol three times. The microcantilevers were placed on a quartz slide, and separated from the quartz surface by a 15μm parafilm spacer so that there was a 15μm distance between the microcantilever tip and the quartz surface. The slide was then dipped into a precursor solution containing 2.1mmol (0.15g) of AMD, 0.27 mmol (45mg) of DMEM, 12 mg GOx, 0.072mmol (11mg) of bis-AMD, and 0.072mmol (15mg) of DEAP dissolved in 3 ml of water. The crosslinking procedure for the hydrogel film was the same as previously reported. The resulting hydrogel film bound to the cantilever was exchanged and equilibrated in a 10^{-2} M solution of NaCl for 24 hours.

The deflection experiments were performed in a flow-through glass cell (Digital Instruments, CA) such as that used in atomic force microscopy. The V-shape microcantilever was immersed in a 10^{-2} M NaCl electrolyte solution. Initially, the NaCl solution was circulated through the cell using a syringe pump. A schematic diagram of the apparatus used in this study was previously reported.[28] Since a change in the flow rate induces noise in the cantilever bending signal due to turbulence, a constant flow rate of 4 mL/h was maintained during the entire experiment. Experimental solutions containing the electrolyte and the glucose were injected directly into the slowly flowing fluid stream via a low-pressure injection port/sample loop arrangement. This arrangement allowed for continuous exposure of the cantilever to the desired solution without disturbing the flow cell or changing the flow rate. Since the volume system was only 0.3ml, a relatively fast replacement of the liquid in contact with the cantilever was achieved.

Results and Discussion:

As noted above, it was anticipated that GOx could be used to oxidize glucose to gluconic acid, which is capable of promoting electroosmotic swelling of the gel. A 15 μm thick layer of a GOx-doped gel, coated on the surface of a microcantilever, was initially exposed to a constant flow (4mL/h) of a 10^{-2} M solution of NaCl. When an 8 mM concentration of glucose solution was injected into the fluid cell, the microcantilever bent upwards towards the gold side as shown in Figure 18. Glucose was added at the marked time. A 2.0 mL aliquot of 10 mM glucose solution was switched into the fluid cell. It took approximately 30 min for the injected glucose concentration to flow through the fluid cell, at which time the NaCl electrolyte solution was circulated back through the cell. The deflection of the microcantilever reaches a maximum of 160 nm approximately 25 min after the injection. After 30 min, the microcantilever deflection gradually returns to its original position as the solution composition returns to the original 10^{-2} M NaCl solution. This confirmed that the microcantilever bending is fully reversible; the sensor can be self-regenerated once the products are diffused out of the gel. The gel was found to be stable under the testing conditions, with no observable hysteresis or loss of gel from the cantilever surface.

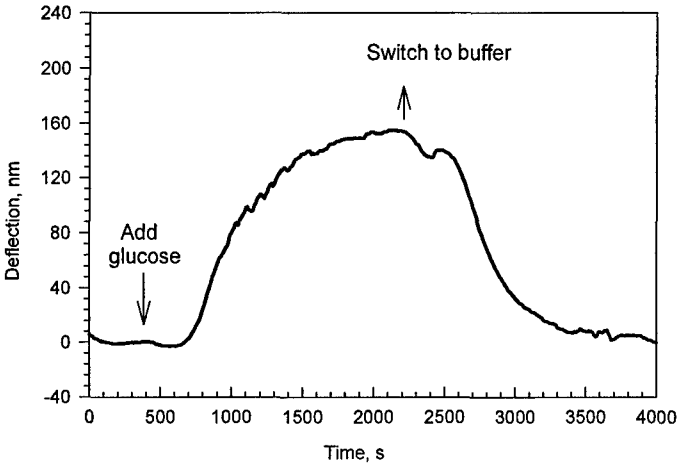

Figure 18: Bending response as a function of time for a silicon microcantilever coated with a 15μm thick layer of GOx-doped hydrogel upon injection of a concentration of 8mM glucose solutions in 0.01M NaCl background electrolyte solution

Conclusions

Cantilevers with glucose-sensitive poly(acrylamide) gels were prepared by functionalization of one side of the lever, and these were demonstrated to reversibly respond to glucose. The gel/microcantilever system itself is sensitive and stable.

Chitosan System

Overview/Objectives

Many studies have been performed to study the swelling behavior of various pH-sensitive hydrogels. The most common method used to determine the swelling behavior of hydrogels involves weighing the dried material, immersing it in a solution of known pH for a specified time, removal from pH controlled solution, blotting the sample to remove surface liquid, and re-weighing.[29] Disadvantages of this method include the difficulty of controlling the amount water removed from the gel, and dissolution of soft swollen gel due to repeated handling during measurements. Other typical measurement methods include calculating the volume change by measuring the change in diameter of gel discs[30] or measuring drug release from the hydrogel matrix during exposure to different pH solutions[31]. It is commonly reported that the swelling of ionically-crosslinked chitosan hydrogels exposed to acidic pH, below pH 4, is significant, while under neutral conditions the swelling of the gel is less significant. Therefore, the swelling behavior of chitosan hydrogels in physiological pH range, which is very important in this application, is still unclear.

As noted above, a second swelling hydrogel transduction system was also developed using chitosan as the environmentally-sensitive component. The objective of this part of the study was to investigate the swelling mechanism of chitosan/gelatin hydrogel crosslinked with TPP in physiological pH range by coating the hydrogels on microcantilevers, and then exposing the hydrogel cantilevers to solutions with different pH ranging from 6 to 7.45.

Materials and Methods:

The cantilevers used experimentally were silicon microcantilevers commercially available from Veeco Instruments. The dimensions of the V-shaped microcantilevers were 200μm length, 20μm width, and 1μm thickness. One side of the cantilever had a thin film of chromium (3nm) followed by a 20nm layer of gold deposited by electron-beam evaporation. The other side of the cantilever was a thin, naturally grown oxide layer.

Chitosan (2% w/w) and gelatin (2% w/w) were mixed together, and the slide containing the cantilever was dipped in the mixture and cooled to 4°C for 3h, similar to the procedure used for poly(acrylamide) gel immobilization. Then TPP solution was added and kept overnight. The coated microcantilevers were then stored in 0.01M PBS solution pH7.45 for 24h. A schematic of the hydrogel-coated cantilever is shown in Figure 19.

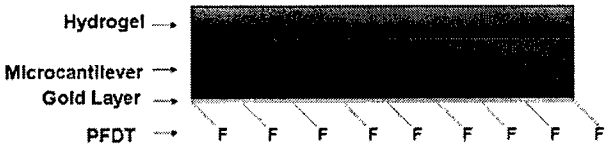

Figure 19: Schematic of chitosan/gelatin coated microcantilever

All experimental solutions were adjusted to have the same buffer concentration and ionic strength with different pH. The microcantilever response was measured in a flow-through glass cell (Digital Instruments, CA) arranged in an atomic force microscope. Initially, the microcantilevers were exposed to 0.01M PBS solution pH7.45 by pumping it through the cell with the aid of a syringe pump at a flow rate of 40ml/hr. After a base line reading was established, 2ml of 0.01M PBS at a different pH was pumped through the sample cell. Then, after 3min, the base line PBS solution (pH=7.45) was circulated back into the fluid cell. Bending was measured by a change in the position of reflectance of a laser beam on to a four-quadrant diode.

Results and Discussion

In this study, microcantilevers were used to provide a sensitivity test on pH-induced swelling behavior of chitosan/gelatin hydrogels in the physiological pH range from 6 to 7.45. A 15μm thick TPP crosslinked chitosan/gelatin hydrogel coated microcantilever was initially exposed to a constant flow (40mL/h) of basic line PBS (pH=7.45). When solutions with pH's other than 7.45 were injected into the fluid cell, the microcantilever reacted by bending. The basic line buffer solution (pH=7.45) was then circulated back into the fluid cell, and the microcantilever deflection gradually returned to its original position. The speed of the bending response was also dependant on the pH change, and was calculated as –dB/dt from the slope of the bending.

The bending response of the gel curing in pH 6, 3.5% (m/v) TPP solution to changing external pH is shown in Figure 20 and Figure 21. The response speed graph of the gel to one pH value stimuli is also shown in Figure 22. The results suggested that the response of gel curing at pH 6 has a transient section early in the experiment (Figure 20) and a steady state reached afterward (Figure 21). As shown in Figure 20, the gel was exposed to pH 7.45 PBS solution to

establish the baseline value. pH 6.13 PBS was then injected into the cell, and a small negative bending was observed. Next, pH 7.45 PBS solution was introduced and the bending deflection started to return. However, it did not return to the original baseline; a positive bending was observed. The two different PBS solutions of pH 6.13 and pH 7.45 were then injected into the cell alternatively.

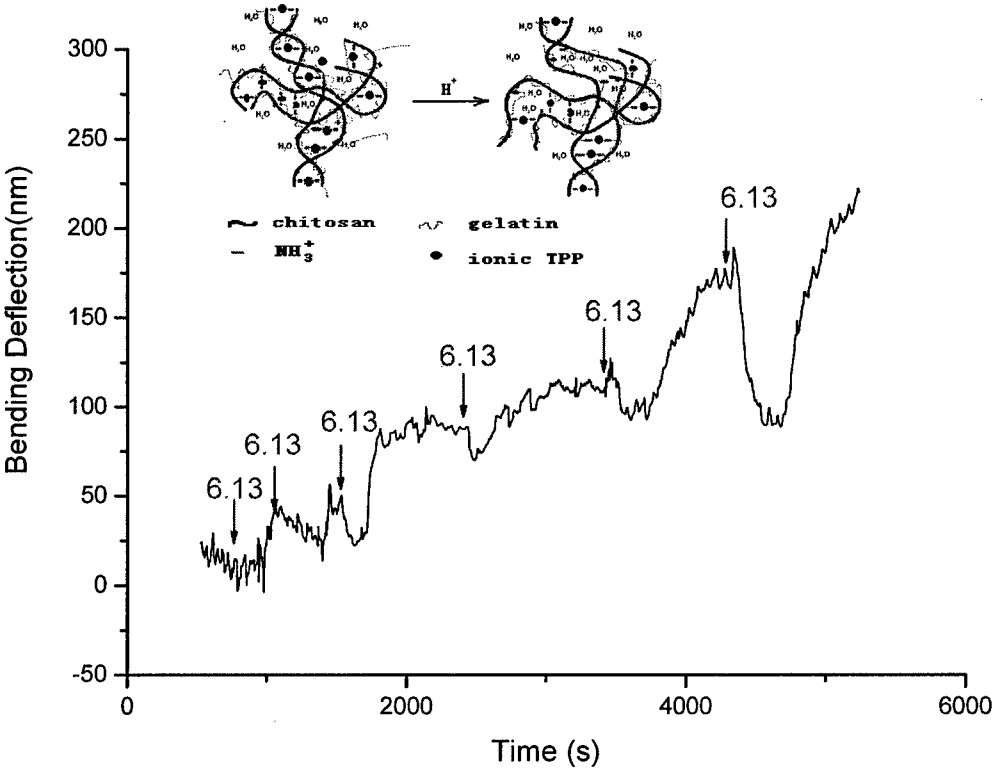

Figure 20: The transient bending response as a function of time for chitosan/gelatin gel (C:G=1:1, 3.5% TPP at pH=6.0) coated microcantilever, upon injection of a 0.01M PBS at pH 6.13, basic line was 0.01M PBS pH 7.45. The injection time is indicated with arrows.

The shape of the bending peaks of the transient gel is different from the bending peaks of the gel in steady state region as shown in Figure 21. It indicates that the hydrogel swells a small amount while the low pH solution was injected and then shrank when exposed to the higher pH solution. While this procedure was repeated, the swelling of gel increased.

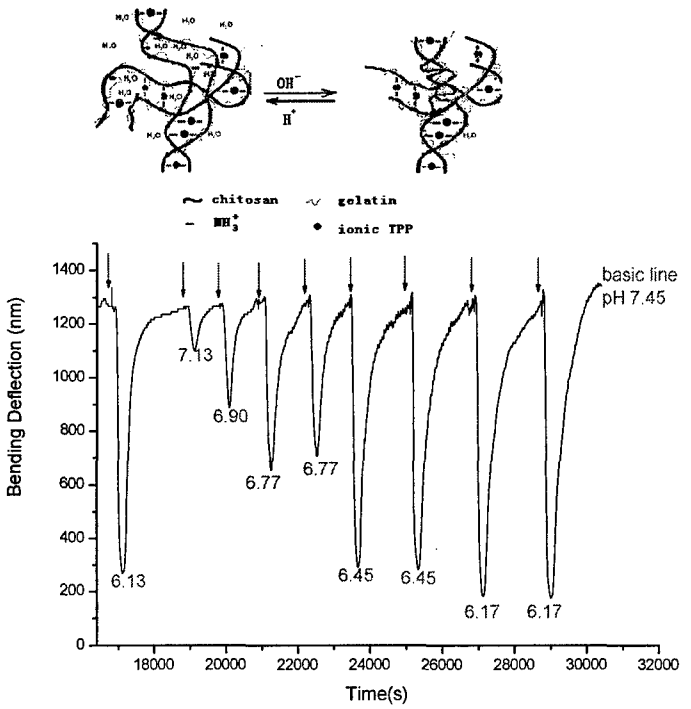

Figure 21: Steady bending response as a function of time for chitosan/gelatin gel (C:G=1:1, 3.5% TPP at pH=6.0) coated microcantilever, upon injection of a 0.1M PBS at various pH. The injection time is indicated with arrows.

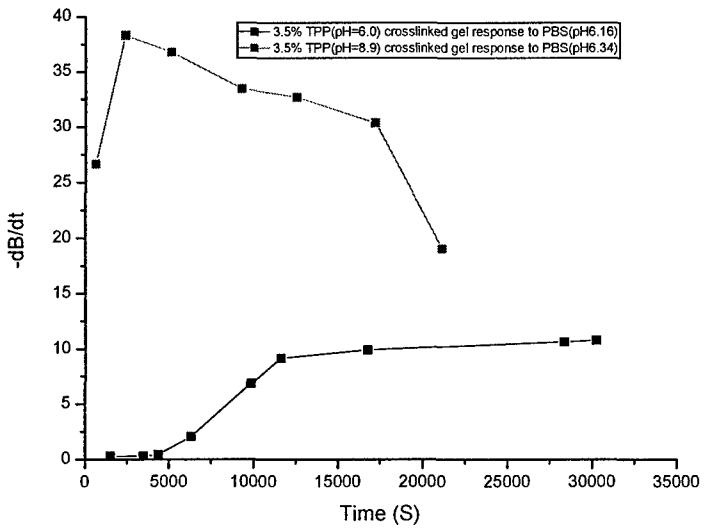

Figure 22: The speed of the bending response (-dB/dt) of the chitosan/gelatin hydrogel crosslinked by 3.5% TPP at pH 6.0 and 8.9

In Figure 22, the increase of the response speed at the beginning was also determined. The transient pH-response of the gel indicates that the structure change of the gel occurs inside the hydrogel, as illustrated in Figure 20. A structure with high crosslink density is formed after the gel is prepared in pH 6 TPP solution. As the gel is exposed to low pH solution, a small number of bonds between the NaTPP and amino group of chitosan are broken, due to the competitive reaction between H^+ and NH_3^+ with TPP ions, and an increased amount of free NH_3^+ groups are left as a result. The gel swells because of increased electrostatic repulsion between the cationic chains; at the same time, the polymer chains become more hydrophilic, contributing to the increased charge, thus leading to increased hydration of the polymer chain. When a more alkaline solution is introduced, the NH_3^+ groups become neutralized by OH^- and form NH_2, which decreases the repulsion force between the chitosan chains. In addition, the hydrophobicity of the gel increases, because more NH_2 groups are presented on the chitosan chains. The hydrophobic effect causes the molecular chains to aggregate and water molecules between the chains are pushed out of the structure. Therefore, the hydrogel shrinks when the external pH increases, because there are more NH_3^+ groups available after one pH-stimuli response, the hydrogel shrinks more, which causes decreased volume.

After repeated swelling and shrinking, the swelling of the gel became steady (Figure 21). At this state, the microcantilever coated with the hydrogel shows a sensitive and repeatable pH response to different pH. As shown in Figure 22, the bending response speed of the hydrogel coated cantilever to same pH could stabilize after a transient period. In the steady state, the microcantilever deflection increases as the pH decreases from 7.45 to 6.1, with a significant sensitivity of approximately 1000nm per pH unit. The response speed as a function of pH is nearly linear, as shown in Figure 23.

These results indicate that the chemical structure formed by the interaction between chitosan molecule and TPP ions do not change when the gel enters the steady state. The results of turbidity tests suggest that the crosslinking structure of the TPP/gelatin/chitosan system is mainly formed by the reaction between chitosan and TPP. Since the gel maintains a stable and consistent reversible response, the swelling of the gel is mainly attributed to chain-relaxation of chitosan-TPP complex by the protonation of the unbound $-NH_2$ groups, and not by the scission of ionic-crosslinked chain. The entering H^+ ions protonate the free amino groups on the chitosan molecule chain, instead of competitively reacting with TPP ions. The protonation and deprotonation of the free amino groups changes the repulsion between the same charged groups on the chitosan molecule, which results in the volume change of the hydrogel, and the volume change is reflected by the bending of the microcantilever. Since the gel crosslinking structure is relatively steady in this stage, the bending of the microcantilever is reversible and reproducible. In this study, the external pH change was controlled from 6.14 to 7.45, which is near the pKa of chitosan. In this pH range, the positive charge density of chitosan molecule increased dramatically as external pH decreased, as shown in the turbidity results. Therefore the swelling of the gel increases as external pH decreases, and the bending deflection increases as the external pH decreases.

pH of TPP Solution

It has been reported that the ionic interaction of chitosan with TPP is pH-dependent. Chitosan beads cured in TPP solution at a pH value lower than 6 were ionic-crosslinking controlled, whereas chitosan beads cured in pH at 8.9 were coacervation-phase inversion controlled, accompanied with slight ionic-crosslinking dependence.[32] A similar effect on

hydrogel swelling behavior of structure difference caused by different prepared conditions appeared in this study.

Compared to the plot of gel curing in pH 6.0 TPP solution (GEL 6.0) in Figure 22, the plot of gel curing in pH 8.9 TPP solution (GEL 8.9) was completely different. The bending deflections of GEL 8.9 were much larger than that of GEL 6.0.

Because of different crosslinking mechanisms, GEL 8.9 has relatively low crosslinking density. So at the beginning, the structure of the hydrogel is loose. There are more free amino groups on the chitosan molecule in GEL 8.9, compared to that in the GEL 6.0; therefore, it has high pH response at beginning. But this kind of crosslinking structure is not durable, due to low crosslinking density. After a relatively steady section, the response speed of GEL 8.9 drops quickly. The crosslinking density decreases, which is caused by chain scission. The hydrogel is dissolved in some degree. The chain scission is not the main reaction happening during swelling of chitosan in the pH range from 6 to 7.45; after long experiment times, the accumulated effects will be determined.

Ratio of Chitosan to Gelatin

The ratio of chitosan to gelatin (C:G) in the precursor mixture also influences the swelling behavior of the hydrogels and the deflection of the coated microcantilevers. The steady response speed of chitosan/gelatin hydrogel with different ratio of C:G as a function of pH is shown in Figure 23. All of these three different batches of hydrogel had nearly linear bending response speed as a function of pH. The gel with higher C:G ratio had higher pH sensitivity.

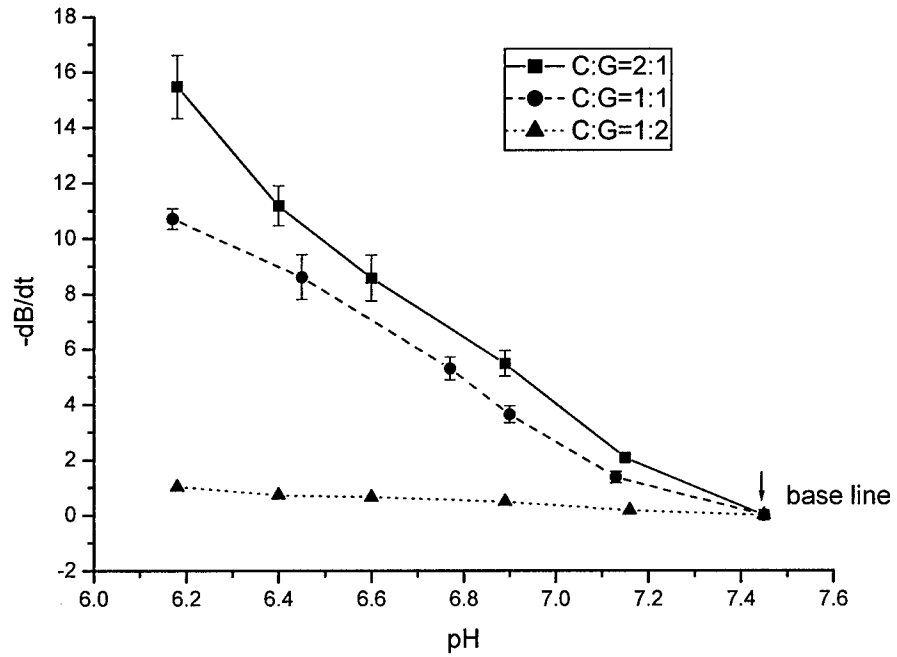

Figure 23: The steady response speed (-dB/dt) of chitosan/gelatin with different ratio of C:G (crosslinked with 3.5% TPP pH=6.0) coated on the microcantilever as a function of pH(Experiments were run in triplicate per sample. All data were expressed as means±standard deviation(SD) for n=3).

Higher C:G means there are more chitosan molecules in the structure; thus there are more free amino groups provided in the gel, if other experimental conditions are identical. As previously mentioned, the swelling of gel is dependant on the protonation of amino groups in the structure. Therefore, the hydrogel with a higher molar ratio of amino groups induces faster bending response speed of the coated microcantilever, compared to that of gel with lower amino group concentration.

Concentration of TPP Solution

The steady pH-response speed of chitosan/gelatin gel crosslinked by 10% (GEL 10) or 3.5% TPP solution (GEL 3.5) at pH 6.0 is shown in Figure 24. GEL 3.5 has higher pH sensitivity than GEL10, and it has a more linear response when compared to GEL10.

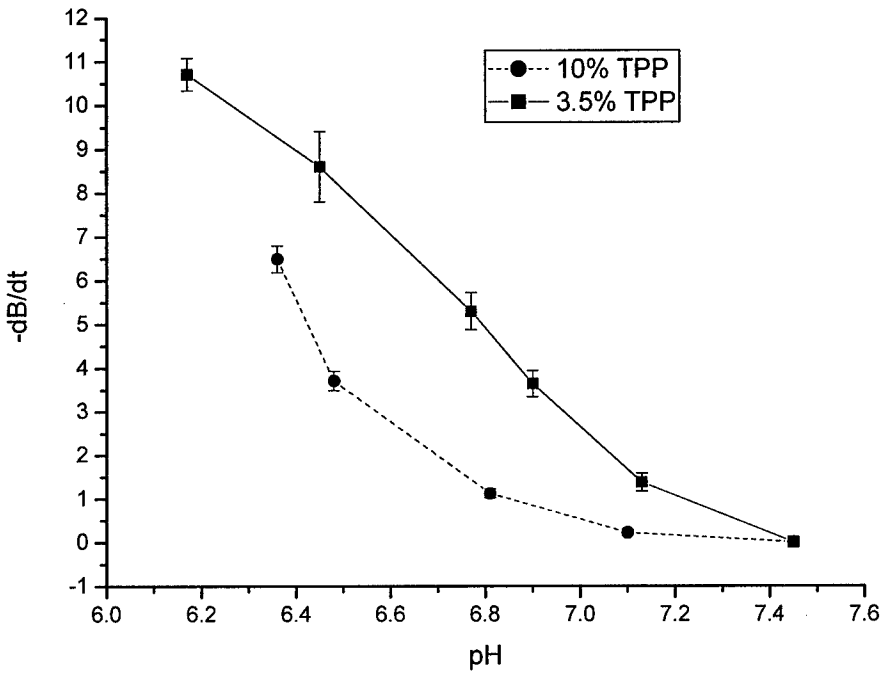

Figure 24: The steady response speed (-dB/dt) of chitosan/gelatin crosslinked by 3.5%TPP or 10% TPP solution at pH 6.0 coated on the microcantilever as a function of pH. (Experiments were run in triplicate per sample. All data were expressed as means±standard deviation(SD) for n=3)

Swelling of the gel is mainly influenced by ionic interactions between chitosan chains, which depends on the crosslinking density set during the formation of the network. An increase in crosslinking density induces a decrease in swelling and pH sensitivity by improving the stability of the network. GEL 10 has higher crosslinking density than GEL 3.5, thus there are less free NH_3^+ groups available on the chitosan chain. The volume change of the hydrogel caused by the protonation of the amino group is decreased.

Conclusions

The swelling of chitosan/gelatin semi-interpenetrating hydrogels ionic crosslinked with TPP were investigated by coating the gels on one side of a microcantilever. Due to the volume change of the hydrogels, the microcantilever sensors deflected upon exposure of the constructs to varying pH from 6 to 7.45. The effects of the pH of the TPP solution, the concentration of TPP solution, and ratio of chitosan to gelatin on the pH sensitivity of this hydrogel were considered. Swelling of this kind of hydrogel was mainly influenced by the chain relaxation of chitosan–TPP complex caused by the protonation of free amino groups in chitosan, which depends on the crosslinking density set during the formation of the network. An increase in crosslinking density induces a decrease in swelling and pH-sensitivity.

The hydrogel (G:C=1:1, 3.5% TPP solution pH 6.0) was used as the typical hydrogel in this study. At steady state, the microcantilever coated with this hydrogel shows a sensitive and repeatable pH response to different pH. A significant 1000nm/pH unit bending response was observed in pH range from 6.1 to 7.45; the deflection of the microcantilever increased as the pH decreased; and the response speed as a function of pH is nearly linear. It can be concluded from this study that the microcantilevers can be used as a platform for testing environmentally-sensitive polymers, and the chitosan-coated microcantilever is a promising candidate as biological sensor when molecular recognition agents, such as antibodies or enzymes, are immobilized in the gel.

b. Characterize the sensitivity, response time, and repeatability of cantilever deflection (within and between devices) due to glucose (Months 13-18).

Poly(acrylamide) System

Overview/Objectives

The performance characteristics of the devices were evaluated using short-term experiments and one-month stability tests. In this part of the project, the primary goals were to determine the swelling behavior of the gels in terms of repeatability, glucose sensitivity, specificity of the response to enzyme products, and to develop a mathematical description of the gel swelling and compare the theoretical properties with experimental observations. The latter aim has particular importance in the future optimization of the sensors for maximum sensitivity and operating range.

Methods

Using the procedures highlighted in Task 2a above, glucose-sensitive cantilevers using the poly(acrylamide) system were repeatedly exposed to a 2 mM solution of glucose of the same cantilever modified with the hydrogel. Next, deflection was measured as a function of glucose concentration. Finally, similar gels without addition of the glucose oxidase were exposed to glucose solutions to compare the relative swelling response with and without the substrate-specific enzyme.

Results

Repeated exposure to 2mM glucose solution caused consistent deflection amplitudes and bending rates, as shown in Figure 25. The standard errors of maximum bending and average forward and reverse slopes were within 10%, indicating good short-term reproducibility.

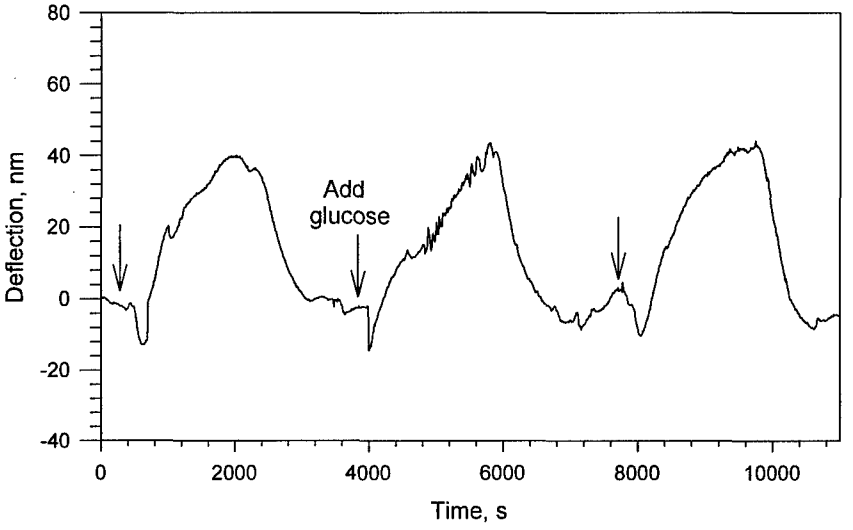

Figure 25: Three replications of the bending response as a function of time following injection of a solution of 2mM glucose in 0.01M NaCl solution (the injection points are indicated with arrows). The silicon microcantilever was coated with a 15μm thick GOx-doped poly(acrylamide) hydrogel.

Figure 26 shows the bending response of a GOx-containing-hydrogel modified microcantilever to various concentrations of glucose. The maximum microcantilever deflection was increased as the concentrations of glucose increased. Since the normal human blood glucose concentration is in the range of 4 to 6 mM (~80-120 mg/dL) and diabetics may experience 8 mM (~160 mg/dL) or higher, we have initially focused on measurement of glucose in the range of 1 to 10 mM. The plot shows that this microcantilever can be used for the measurement of glucose with a concentration between 1 to 10 mM in a solution with NaCl background electrolyte.

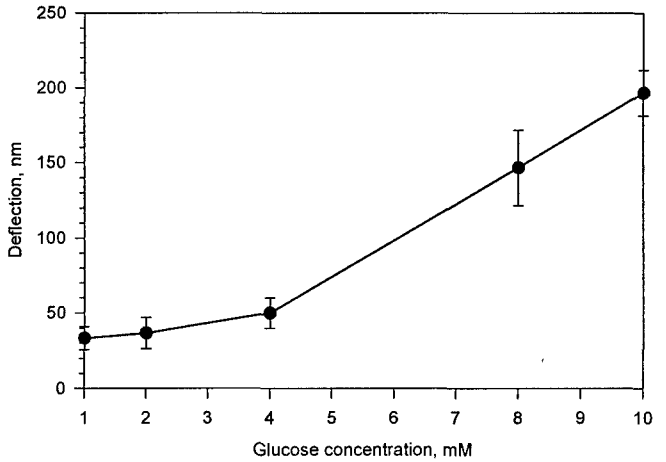

Figure 26: Maximum bending amplitude for a microcantilever coated with a GOx-containing hydrogel as a function of the change in concentrations of glucose

A control experiment was performed with a microcantilever coated with a 15 μm thick hydrogel without GOx, as shown in Figure 27. No deflection of the cantilever was observed upon exposure of glucose to the gel without GOx. These results confirm that that GOx is the active, specific component for the glucose measurement using the hydrogel modified cantilever. The hydrogel swells upon oxidation of glucose to gluconic acid by GOx, and the GOx provides a specific molecular recognition element.

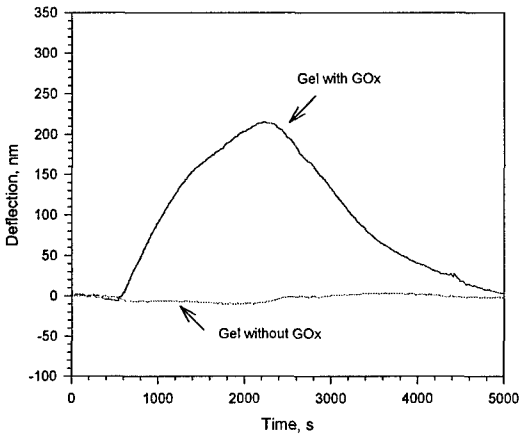

Figure 27: Bending response as a function of time, t, for silicon microcantilevers coated with and without GOx doped hydrogel on the gold surface after injection of a solution of 0.01M glucose in 0.01M NaCl. The microcantilevers were pre-equilibrated in the 0.01M NaCl solution before injection of the glucose solution.

Mathematical Modeling

The expansion and contraction of gels allow chemical or electrical energy to be converted into mechanical work. Although several hydrogel-based microcantilever sensors were reported in 2003 and 2004, no mathematical description of the volume-change-induced microcantilever bending has been given. Using basic mechanical properties, we have derived an equation to correlate the volume change of a surface-immobilized gel with microcantilever bending. Figure 28 is a schematic presentation of a side and front view of a hydrogel-modified microcantilever that is deflected due to gel swelling.

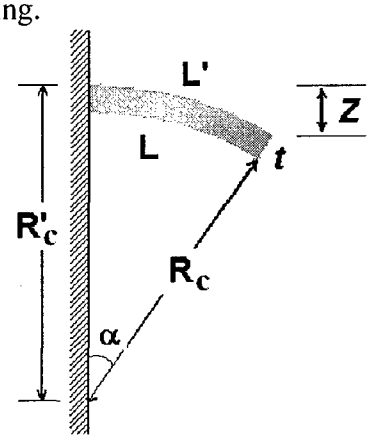

Figure 28: Schematic representation of side and front view of a rectangular microcantilever

The side-view swelled hydrogel area A can be written as

$$A = \alpha\pi(R_c'^2 - R_c^2) \quad (1)$$

Since $\alpha = L/2\pi R_c$, and

$$R_c' = R_c + T + \Delta T \quad (2),$$

Equation 1 can be rewritten as

$$A = \frac{L}{2R}((R_c + T + \Delta T)^2 - R_c^2) = \frac{L}{2R_c}(2(T + \Delta T)R_c + (T + \Delta T)^2) \quad (3)$$

where T is the hydrogel thickness before exposure to glucose solutions, ΔT is the hydrogel thickness change after exposure to glucose solutions, R' and R are the radii of curvature of the bending of the cantilever's top and bottom surfaces, respectively.

In these experiments, in general, the microcantilever bending (z) is less than 1 μm and is relatively much smaller than microcantilever length (L = 180 μm), so the R_c is much larger than $T + \Delta T$, thus, $(T + \Delta T)^2$ can be neglected, so

$$A \approx L(T + \Delta T) \quad (4)$$

The volume of expanded hydrogel approximately equals to

$$V' = L(T + \Delta T)(W + \Delta W) \quad (5)$$

where W is the width of the cantilever, ΔW is the width increase of the cantilever. We approximate $\Delta W/W = \Delta T/T = \Delta L/L$, so Equation 4 becomes

$$V = LTW(1 + \frac{\Delta L}{L})^2 = V_s(1 + \frac{\Delta L}{L})^2 \quad (6)$$

V is the volume of swelled gel after exposure to glucose, and V_s is the original volume prior to glucose exposure. Thus,

$$\Delta L = L(\sqrt{\frac{V}{V_s}} - 1) \quad (7)$$

Since the arc angle (α) was very small because of the small z,

$$L'^2 + (R_c' - z)^2 = R_c'^2 \quad (8)$$

Thus,

$$L'^2 = 2zR_c' - z^2 \approx 2zR_c' \qquad (9)$$

Similarly,

$$L^2 \approx 2zR_c \quad (10)$$

Combining Equations (2), (9), and (10) reveals that

$$\Delta L = L' - L = \sqrt{2zR_c'} - L = \sqrt{L^2 + 2z(T + \Delta T)} - L \qquad (11)$$

By combining Equations 11 and 7, the deflection of the cantilever can be quantitatively expressed as[33]

$$z = \frac{2\Delta L * L + \Delta L^2}{2(T + \Delta T)} \approx \frac{\Delta L * L}{T + \Delta T} = \frac{L^2(\sqrt{V/V_s} - 1)}{T\sqrt{V/V_s}} = \frac{L^2}{T}(1 - \sqrt{V_s/V}) \qquad (12)$$

Finally, Equation 12 can be rewritten to

$$\frac{V}{V_s} = (\frac{L_2}{L_2 - zT})^2 \qquad (13)$$

The corresponding volume change ratio V/V_s of the hydrogel can be determined from cantilever deflection according to Equation 13 and the dependence of the V/V_s on the glucose concentration is shown in Figure 29.

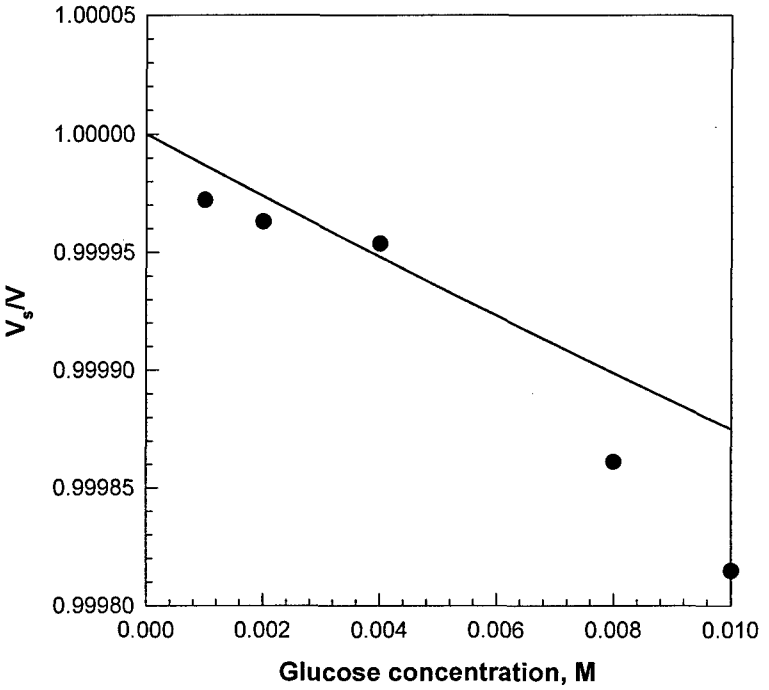

Figure 29: The volume change ratio V/V_s of the hydrogel on the glucose concentration determined from cantilever deflection (closed circle) and calculated from a hydrogel swelling model (line).

Thermodynamic analyses can theoretically produce more accurate and precise characterization of biomolecular interactions. Understanding these processes and correlations will be helpful in predicting microcantilever bending responses and improving the cantilever sensors.

In an osmotic swelling experiment, the measurable quantities involve derivatives of the free energy[34], the swelling behavior with Π_{elas} of a gel can be calculated using rubber elastic theory, Π_{mix} can be calculated using the Flory-Huggins model,[35] and Π_{ion} can be calculated using classical Donnan equilibrium theory,[21]

$$\Delta\Pi_{mix} = -\frac{\partial \Delta G_{mix}}{\partial V} = -\frac{RT}{V_s}[\ln(1-\frac{V_D}{V}) + \frac{V_D}{V} + \chi(\frac{V_D}{V})^2] \quad (14)$$

$$\Delta\Pi_{elas} = -\frac{\partial \Delta G_{elas}}{\partial V} = -\frac{RT * n_{cr}}{V_n}[(\frac{V_s}{V})^{1/3} - \frac{1}{2}\frac{V_s}{V}] \quad (15)$$

$$\Pi_{ion} = RT(C_+ + C_- - C_+^* - C_-^*) \quad (16)$$

where Π_{tot} is the swelling pressure of the hydrogel, Π_{mix}, Π_{elas}, and Π_{ion} are the mixing, elastic, and ionic contribution of Π_{tot}. Here, R is the universal gas constant, T is the temperature, χ is the Flory-Huggins interaction parameter for the polymer network and the solution, V_s is the molar volume of the water (18 mL), n_{cr} is the effective number of crosslinked chains in the network, V

is the existing volume of the hydrogel, V_s is the volume of the network before exposure to glucose, V_D is the volume of the dry polymer network (we measured $V_D = 0.03V_s$), C_+ and C_- are the concentration of mobile cations and anions inside the gel, and C^*_+ and C^*_- are the concentration outside the gel. In the case here we will use the simplifying conditions that all ionic species are singly charged and the anion/cation stoichiometry is unity. Some of these data can be obtained from literature; for instance, n_{cr}/V_m=1.46x10^{-3} M and χ=0.49 for polyacrylamide.[36]
Equation 16 can be written as

$$\Pi_{ion} = RT(\frac{iC_p}{Z_-} - v_i(C^*_s - C_s)) \qquad (17)$$

where i is the degree of ionization of the polymer monomer units, C_p is the concentration of monomer units inside the gel, Z_- is the valence of the counterelectrolyte (Z_- = 1), v_i is the sum of cation and anion stoichiometries of the ionized electrolytes (v_i = 2), C_s and C_s* is the concentration of mobile ions in and out of the gel, respectively.

In the designed hydrogel, the only ionic species bound to the gel were protonated amino groups (R_3NH^+). The mobile ions are gluconate, OH^-, H_3O^+ and H^+. The concentration of OH^-, gluconate anions, R_3NH^+, can be calculated using the equilibrium equations:

$$[R_3NH^+] = \frac{[H^+][R_3N]_0}{K_a + [H^+]}, \qquad (18)$$

where K_a is the equilibrium constant for R_3NH^+ formation (3.4x10^{11} M^{-1}), $[R_3N]_0$ is the original concentration of amino bound on the hydrogel network (0.09 M).

We originally anticipated that the production of gluconic acid will protonate the tertiary amine group, leading increases in electrostatic repulsion between polymer chains and a resultant expansion of the hydrogel network. The equilibrium equation 18 shows that after the hydrogel is equilibrated in a pH = 7.0 solution, 99.96% of the R_3N were in the protonated state. Our calculation showed that the further protonation of R_3N at lower pH due to the formation of gluconic acid does not have significant contributions to the cantilever bending and can be neglected. Thus, the Equation 17 can be expressed as

$$\Pi_{ion} = RT([R_3N]_0 - 2(C^*_s - C_s)) \qquad (19)$$

At swelling equilibrium for an unconfined hydrogel, Π_{tot} must equal zero.

$$\Pi_{tot} = \Pi_{mix} + \Pi_{elas} + \Pi_{ion} = 0 \qquad (20)$$

So, Equation 14-20 can be combined to

$$\frac{1}{V_s}[\ln(1 - \frac{V_D}{V}) + \frac{V_D}{V} + \chi(\frac{V_D}{V})^2] + \frac{n_{cr}}{V_n}[(\frac{V_s}{V})^{1/3} - \frac{1}{2}\frac{V_s}{V}] = [R_3N]_0 - 2(C^*_s - C_s) \qquad (21)$$

The concentration difference in and out of the gel, $2(C_s\text{-}C_s^*)$, including gluconate and H_3O^+ generated, can be determined by the GOx reaction rate and the diffusion rate of the ions in the hydrogel. At equilibrium, the reaction rate in the hydrogel can be determined by the Michaelis-Menten equation[37]

$$V = \frac{k_2[E][S]}{k_M + [S]} \qquad (22)$$

where k_2 is the second rate constant for reaction of the GOx enzyme with the glucose (800 M^{-1}), and $[E]$ is the concentration of the enzyme in the hydrogel (6.4×10^{-5} M).

We can roughly calculate the hydrogel swelling by assuming the glucose concentration in the hydrogel is the same as that in the solution because of the fast follow rate of glucose (6.9×10^{-6} cm^2/s). This assumption could provide us a rough estimate of hydrogel swelling upon exposure to glucose.

The presence of glucose produces H_3O^+ within the hydrogel film. The excess $[H_3O^+(x)]$ diffuses out of the gel until a steady state is reached wherein the production and the diffusion losses of $[H_3O^+(x)]$ balance each other,

$$D_{H_3O^+} \frac{d^2[H_3O^+(x)]}{dx^2} = V \qquad (23)$$

where D_{H3O+} is the diffusion coefficient of H_3O^+ in the gel (5.85×10^{-5} cm^2/s). Solving Equation 23 determines the concentration of H_3O^+

$$C_s\text{-}C_s^* = [H_3{}^+O] = \int_0^T [H_3{}^+O](x)dx = \frac{k_2[E][S]T^2}{2D_{H_3O^+}(k_M + [S])} \qquad (24)$$

where T is the half of the thickness of the hydrogel.

The corresponding volume change ratio V/V_s of the hydrogel can be calculated from Equation 21. The calculated dependence of the V/V_s on the glucose concentration is also shown in Figure 30, and can be used to compare with the measured data. Although this model is only a rough approximation of the system properties, the curvature of the calculated fit matches the experimental results very well. Thus, this model can be used to design systems with desired sensitivity and response range.

Stability Tests

Hydrogel film stability experiments were conducted on a microcantilever coated by the GOx doped hydrogel after one month of storage in a 0.01 M NaCl solution. The cantilever deflection decreased to less than 25% of that of fresh made microcantilever (Figure 30), indicating a significant loss of GOx from the gel, either in enzymatic activity. Unfortunately, the long-term stability of this system was severely compromised by either leaching of enzyme from the gel, or loss of catalytic activity due to protein denaturation. The nature of the loss is currently under investigation by direct measurement of leaching from gels and activity measurements using time-dependent oxidation of dye by substrate-saturated enzyme.

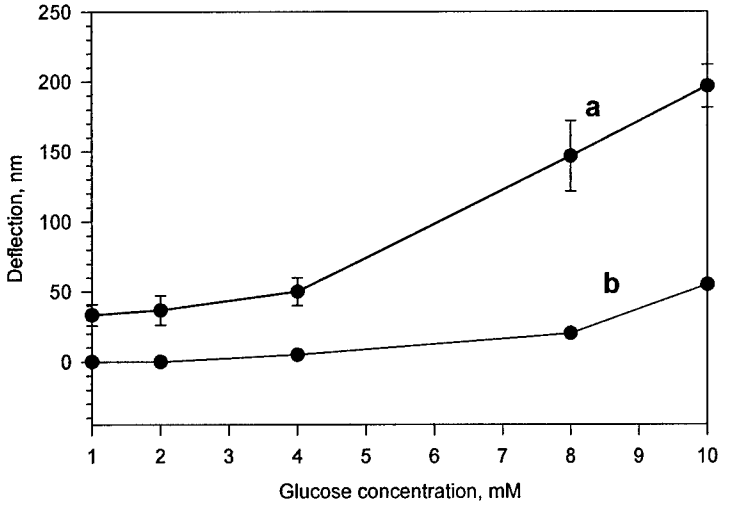

Figure 30: Maximum bending amplitude for a microcantilever coated with GOx-containing hydrogel as a function in the change in concentrations of glucose after a) one day, b) 30 days of equilibration in a 0.01M NaCl solution.

Conclusions

Preliminary experiments with functionalized microcantilevers suggest that these devices have the necessary sensitivity to transduce small changes in glucose by beam deflection induced by acidic reaction products. The short-term reproducibility of the measurements appears excellent, and is currently being further characterized. Simple mathematical models described the behavior reasonably well, and these will be useful in designing cantilevers and gels to tailor response properties to the necessary sensitivity and range. Unfortunately, however, the loss of GOx or GOx activity observed with the current fabrication approach is unacceptable for practical use (details in Task 2b). Improvement of the sensor stability is under investigation by covalent enzyme attachment to the gel and through doping with GOx-covered nanoparticles (Task 1). At this juncture, the chitosan-modified cantilevers have not yet been tested with GOx for glucose sensing. This work will be beginning immediately following the completion of the annual report and submission of manuscripts on the chitosan pH-sensitive cantilevers and glucose-sensing poly(acrylamide) cantilevers.

b. *Study long-term stability of measurement system, and effects of interferences on glucose measurement accuracy (Months 19-21).*

As was noted under Task 2a, the stability of the PA gels prepared by direct addition of GOx was found to be poor. This aim will be pursued in the current performance period (Grant-Year 2) to improve this aspect of sensor performance.

c. *Produce optimized transducer for glucose using feedback from steps a-c, fully characterize sensor properties. (Months 21-24)*

This aim will be pursued in the current performance period (Grant-Year 2) using the results of experimental and theoretical work.

Task 3. **To develop and characterize fluorescent hydrogels that produce shifting spectral properties due to energy transfer changes induced by gel swelling (Months 7-24):**

a. Develop and characterize labeling procedures (Months 7-9).

Overview/Objectives

The ability to stably and controllably attach fluorescent molecules to functional groups on the environmentally-sensitive gels is paramount to the eventual application of these materials as RET-transduced sensors. The primary objective for this phase of the work was to establish basic protocols for conjugation of gel polymers with fluorescent tags.

Methods

Chitosan is a copolymer of β-(1→4)-linked-2-acetamido-2-deoxy-D- glucopyranose and 2-amino-2-deoxy-D-glucopyranose. The primary amine group of D-glucosamine residues in chitosan can be conjugated with amine-reactive dyes, such as succinimidyl esters (Alexa Fluor 647™, CY5®), isothiocyanates (FITC, TRITC), and sulfonyl chlorides (pyrene 8-hydroxy-1,4,6-trisulfonyl chloride (HPTS)). Two grams of chitosan were dissolved in 100 ml of 1% (w/v) acetic acid to produce a 2% (w/v) solution of chitosan. 1mg of dye was dissolved in 400μl DMF, and then slowly added to 5ml of the chitosan solution, and then stirred for 4 hours in the absence of light at room temperature. Labeled chitosan was precipitated in acetone, washed in acetone, and then re-dissolved in 5ml 1% acetic acid. FITC, TRITC, CY5®, and Alexa Fluor 647™ were used as the dyes to labeled chitosan separately. FITC/TRITC, TRITC/ CY5®, or TRITC/ Alexa Fluor 647™ dye pairs could be used as the RET pairs.

PAA was labeled with 5-dimethylaminonaphthalene-1-(*N*-(5-aminopentyl))sulfonamide (dansyl cadaverine) (D113), a fluorescent dye that absorbs light around 335nm, and emits light around 518nm. This molecule was used only as a model amine-containing dye for establishment of basic labeling procedures, and was not intended for use as a sensor component. D113 labeling was accomplished through an amine-carboxyl bond; the D113 contributes the amine group to bond onto the carboxyl moiety available on the acrylic acid monomer.[38] Acrylic acid monomer was mixed with EDC for 4h, then D113 (1mg/mL in ethyl alcohol) was added into the prepared acrylic acid solution. The mixture was kept overnight at 4°C, and the resulting labeled acrylic acid solution was then used in the pre-polymerization solution in place of unlabeled acrylic acid

for gel construction, as described in Task 3b.

The absorbance spectra of labeled polymers were measured with a Perkin-Elmer Lambda 45 UV-Vis Spectrometer. The labeling ratio was calculated according the equation:

$$\mathrm{DOL}=\frac{A_{\max}\times MW}{[monomer]\times L\times \varepsilon_{dye}},$$

where DOL refers to the molar ratio of dye to monomer units, the "degree of labeling", MW is the polymer's monomeric unit molecular weight, ε_{dye} is the extinction coefficient of the chromophore at the wavelength where absorbance is maximum ($A_{\max}$), and L is the measurement pathlength (1cm).

Results

The measured values for FITC-chitosan were found to be:

A_{494nm}=0.153276
MW=161
[D-glucosamine]=0.77g/L
ε_{dye}=68000$cm^{-1}M^{-1}$
DOL=4.71×10^{-4}

Therefore , the labeling ratio of FITC:chitosan was found to be approximately one FITC molecule per 2100D-glucosamine residues of chitosan. This low level of labeling was desirable for maintaining pH-sensitivity of the gel while providing sufficient fluorescence brightness.

TRITC-chitosan:

A_{552nm}=0.224499
MW=161
[D-glucosamine]=0.077g/L
ε_{dye}=84000$cm^{-1}M^{-1}$
DOL=5.58×10^{-4}

Thus, the labeling ratio of TRITC:chitosan was approximately one TRITC molecular per 1750 D-glucosamine residues of chitosan.

Similar DOL figures were obtained for Cy5 and AF 647.

Conclusions

The DOL achieved was very low, yet sufficient fluorescence signals were obtained. This is a very positive result, as the low labeling is sufficient to obtain measurable fluorescence but sufficiently low to avoid substantial change in the number of ionizable functional groups available to interact with protons and induce structural changes in response to changing pH. Full characterization of DOL, and the influence of labeling ratio on swelling properties and RET transduction will be completed in Year 2.

Once proper PAA/PAM tetramethylrhodamine-5-(and-6)-isothiocyanate (TRITC), CyDye® 5 NHS-ester (CY5®) and Alexa Fluor 647™ labeling procedures are outlined, the labeled hydrogel material will be investigated with microsphere particles made from the labeled material or by attaching the labeled material to optical fiber and observing spectra during

exposure to PBS of different pH. Microsphere particles will be made from the labeled PAM/PAA materials, and will be used to evaluate the spectral properties of the materials in response to environmental stimuli. Both of these approaches offer specific advantages: microspheres offer fast response to stimuli across the entire excited volume of a small environment and provide an average spectral response from the entire excited volume, while the optical fiber architecture allows for photobleaching correction and observance of the transient response of the material in a localized environment at the fiber tip, even though the response will occur less rapidly and the dip-coating fabrication result is less consistent than the emulsion approach.

b. Assess spectral and structural properties of crosslinked gels, homogeneity of dye distribution, identify appropriate protocols to obtain gels with strong signals from both donor and acceptor at neutral pH. (Months 10-15)

Effect of dye on poly(acrylamide) swelling

Overview/Objectives

As described above, the PAM/PAA system was experimentally verified to exhibit strong pH sensitivity; however, for RET readout systems, this behavior must be preserved following addition of the fluorescent tags. This phase of the work was aimed at repeating pH-swelling experiments to compare the swelling properties of labeled gels to unlabeled systems.

Methods

The labeled acrylic acid was used in the pre-polymerization solution in place of unlabeled acrylic acid for construction of gels in custom cylindrical molds, as previously described. These fluorescent-labeled hydrogel discs were immersed in PBS solutions of known pH for 24 hours, then weighed as described in previous sections to assess swelling change.

Results

The PAA-D113/PAM hydrogel slab pH sensitivity results showed an approximately linear response to pH between 5.3 and 7.9 (Figure 31). Interestingly, the labeled hydrogels broke less than the unlabeled PAA/PAM hydrogels throughout the experiment. This suggests a changed in the crosslinked gel structure owing in part to the presence of the modification of some carboxyl moieties with the fluorophores. Fluorescence measurements were unsuccessful because the discs were too thick for the right-angle measurement UV-excitation systems currently available. A fiber-optic reflection measurement system is currently being constructed that will enable measurements of this type in the future.

Conclusions

The attachment of fluorophores did not deleteriously affect the gel swelling properties. The sensitivity to pH was retained, and the mechanical integrity of the gels apparently increased as well. Thus, no concerns over the applicability of RET measurements with the PAA/PAM system were raised during these experiments. Further work with the longer wavelength RET pairs required for true swelling transduction is now in progress, and preliminary work suggests similar behavior to that observed for D-113; thus, all indications are that successful pH-sensitive gels can be constructed and demonstration of monitoring swelling using RET will be feasible in short order.

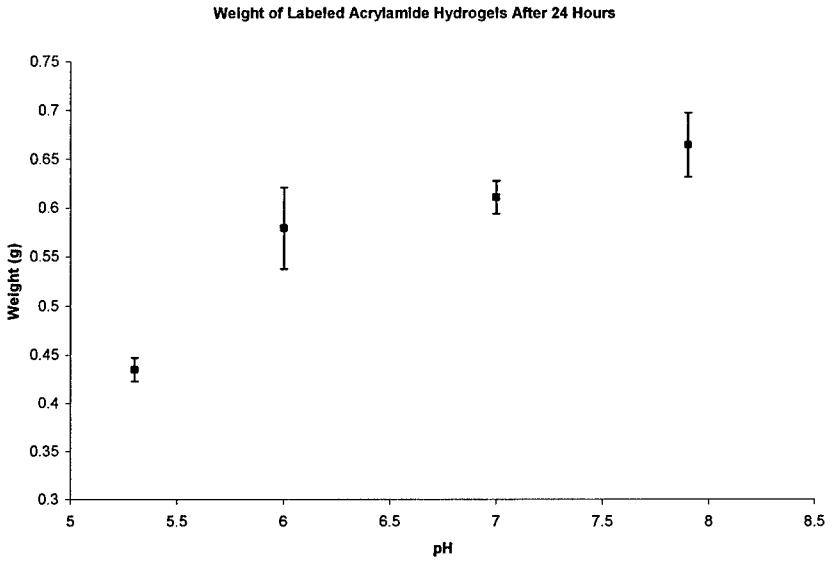

Figure 31: Results from PAA-D113/PAM Hydrogel pH-Sensitivity Experiments

Chitosan swelling systems

As mentioned above, ionic crosslinked chitosan/gelatin hydrogel can be used as pH-sensitive hydrogels. The swelling behaviors of hydrogel microspheres are ideal system for developing fluorescent resonance energy transfer-based chemical and biological sensors due to the small dimensional changes expected that require high sensitivity measurements. In this phase of the work, three overall goals were pursued: 1) Construction of stable chitosan microspheres; 2) producing dual-labeled chitosan gels with appropriate dye ratios for observation of two emission peaks due to RET; and 3) demonstration of pH- and glucose-sensitivity of chitosan-based microspheres.

Objectives/Overview

A first goal was to develop a suitable protocol for construction of chitosan microspheres in the size range of 5-20μm. This is an appropriate size for dermal implantation of these biocompatible spheres. The effects of crosslinking ions, gelatin, and stirring conditions on the resulting microspheres were initially studied, following by efforts to enhance the structural stability of the spheres using surface nanofilm coatings and covalent crosslinking. Detailed methods for each of these aspects are given in the respective sections below.

Methods

Gelatin was dissolved in an acetic acid (1% v/v) solution of chitosan at 37°C while stirring to create a 2% (w/v) gelatin solution. The component concentration in the solution (w/v) was 2% chitosan and 2% gelatin; 5ml of solution was emulsified in 50ml liquid paraffin oil containing 1ml Tween 80 for 15 minutes under mechanical stirring. The emulsion was cooled to 4°C while stirring for 15min, and then 50ml sodium sulfate solution was added, and stirred was continued for 1-3 hours. The microspheres were collected by centrifugation and washed 3 times with sodium sulfate solution.

Results and Discussion

Effects of Sodium Sulfate

In most of the studies wherein chitosan microspheres were prepared via a droplet extrusion technique, the TPP ions were used as counterions for the gelation of chitosan; however, when TPP was added to the w/o emulsion in this study, weak chitosan microspheres without a spherical shape were obtained (Figure 32).

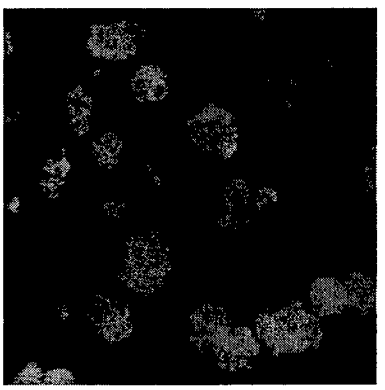

Figure 32: CLSM image of TPP cross-linked chitosan/gelatin microspheres.

Based on an earlier study, it was hypothesized that the sulfate ion could be used as a crosslinker.[39] Due to its strong acidic characteristics, each sulfate molecule carries more than one charge in the pH region 1.0 to 9.0. The ionization degree of chitosan decreases at a pH higher than pH 6.0; therefore, the electrostatic interaction of sulfate/chitosan may exist in the pH range between 1.0-7.5. In this study, the pH of the reacted solution was 6.0.

The amount of sodium sulfate added to the w/o emulsion was a critical factor. When 15ml 2% sodium sulfate was added to the mixture, very soft beads without spherical shape were obtained. On the other hand, while the amount of the sodium sulfate solution increased to 50ml, microspheres with good spherical shape and higher densities were obtained (Figure 33). The reason for this was that there was not enough sodium sulfate solution to cover the liquid droplets in the w/o emulsion. As more sodium sulfate was added, higher density of microspheres was obtained. However, if the volume of sodium sulfate solution added is too high, there is a destabilizing effect on the emulsion as a result of an increase in the volume ratio of the water/oil phase, which leads to coalescence of the droplets in the w/o emulsion.

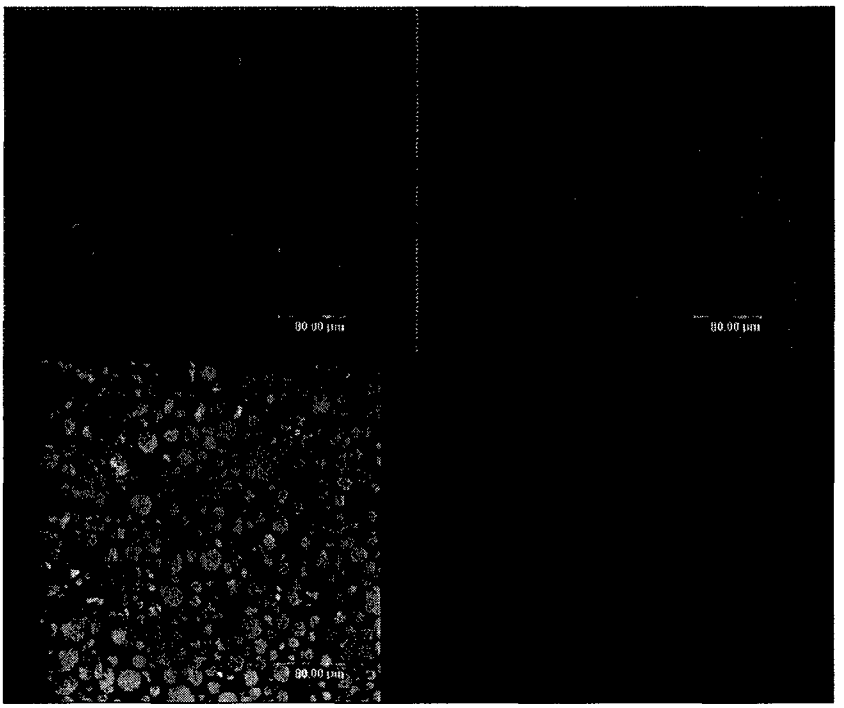

Figure 33: CLSM image of chitosan/gelatin microspheres cross-linked by sodium sulphate. (chitosan was labeled with FITC and TRITC)

In order to improve the mechanical properties of the microspheres, the concentration of sodium sulfate solution was increase from 1% to 7%. When 1% sodium sulfate was added in the emulsion, very soft microspheres were harvested. 7% sodium sulfate could make much harder microspheres, due to the increased crosslink density, but the concentration of the sodium sulfate higher than 7% results in coalescence of the droplets, because the increase of the ionic strength of the emulsion destabilizes the emulsion. The microspheres crosslinked by 5% sodium sulfate were smaller and denser than those crosslinked by 2% sodium sulfate (Figure 34).

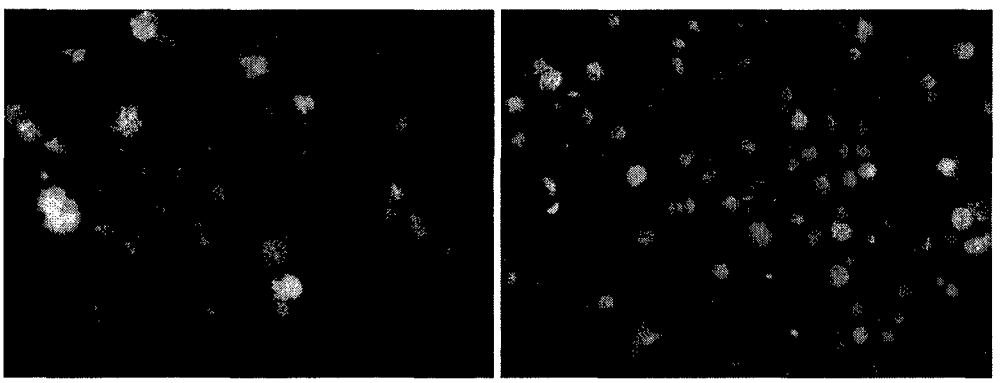

(a) **(b)**

Figure 34 (a and b): Fluorescence microscope images of chitosan/gelatin microspheres cross-linked by different concentration of $NaSO_4$. (a) 2% $NaSO_4$ (X 200) (b) 5% $NaSO_4$ (X 200)

The rate of addition of sodium sulfate solution to the emulsion is also important. When 50ml sodium sulfate solution is added quickly, no microspheres were obtained. The reason behind this result was the sudden increase in the volume ratio of water/oil phase could destroy

the emulsion balance and result in coalescence of the droplets. Thus, while 50ml solution was dropped in the emulsion over a 60 minute period, crosslinking of the droplets occurs before the destabilizing effect caused by the increase in volume of water phase, and spherical microspheres were obtained.

Effects of Stirring Condition

Microspheres were prepared separately after 1, 2, 3 or 4 hours of stirring subsequent to crosslinker addition. The microspheres formed after 2,3 and 4 hours of stirring were discrete and spherical, while those formed after 1h of stirring were soft, and a degree of aggregation was observed. Prolonging the stirring time did not affect the size distribution or the size of the microspheres. It indicates that after 2 hours of stirring, the ionic crosslinking was completed.

In this study, three different stirring speeds were investigated: 700, 2000 and 3000rpm. With the stirring speed increased, the diameter of the microspheres decreased, and the size distribution became narrower (Figure 35). The size and size distribution of the microspheres depends on the turbulent force throughout the emulsion. A higher speed of stirring increases the turbulent force, thereby reducing the size of the dispersed droplets and resulting in the formation of smaller microspheres.

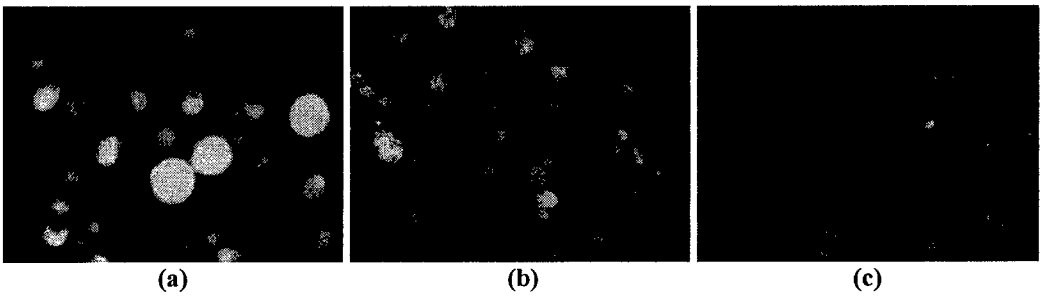

(a) (b) (c)

Figure 35 (a, b, and c): The fluorescence microscope image of chitosan/gelatin microspheres made under different stirring speed.(X 200) (a) 700rpm (b)2000rpm (c)3000rpm

Effects of Gelatin

Gelatin is a linear, flexible biomolecule that exhibits a characteristic temperature-dependent sol-gel change. Gelatin molecules interact with chitosan molecules to form polyelectrolyte complexes, which can increase the bonded-water content of chitosan network, decreasing the degree of crystallization and enhancing the flexibility of chitosan molecules. At the same time, the ionic crosslinking process took place after the droplets were coagulated under the gelatin gelation point (25°C), which was beneficial in keeping the spherical shape of the formed microspheres.

Enhancing the Stability of Ionic-Crosslinked Microspheres

As noted above, when the chitosan/gelatin microspheres crosslinked by sodium sulfate were diluted by PBS, the microspheres were not stable. Ionic crosslinked chitosan microspheres can be reinforced by additional covalent crosslinking of chitosan by glutaraldehyde. However, the addition of glutaraldehyde may decrease the biocompatibility due to the toxic formaldehyde content. As an alternative, the layer-by-layer (LbL) electrostatic self-assembly method was proposed as a means of increasing the stability of the chitosan/gelatin microspheres in PBS by providing an outer multilayer coating.

Glutaraldehyde-Enhanced Microspheres

Gelatin was dissolved in an acetic acid (1% v/v) solution of chitosan at 37°C under stirring. The component concentration in the solution (w/v) was chitosan 2%, gelatin 2%. 5ml of solution was emulsified in 50ml liquid paraffin oil containing 1ml Tween 80 for 15 min during mechanical stirring. The emulsion was cooled to 4°C while stirring for 15min, and then 50ml of sodium sulfate solution was added, and stirring was continued for 2 hours. 20ml of 0.25% (w/v) glutaraldehyde was then added to the microspheres and reacted at room temperature overnight. Slight crosslinking with glutaraldehyde was used to enhance the stability of the microspheres. The microspheres were collected by centrifugation and washed 3 times with sodium sulfate solution.

Results

Uniform microspheres were made by this method, as shown in Figure 36 and Figure 37. With an average diameter of approximately 5μm, these particles are easy to separate and manipulate using standard colloid techniques, and the size distribution is very narrow. These particles are of an appropriate size for implantation and *in vivo* use.

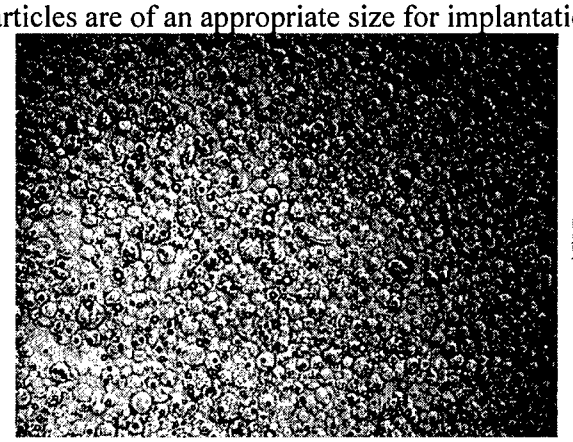

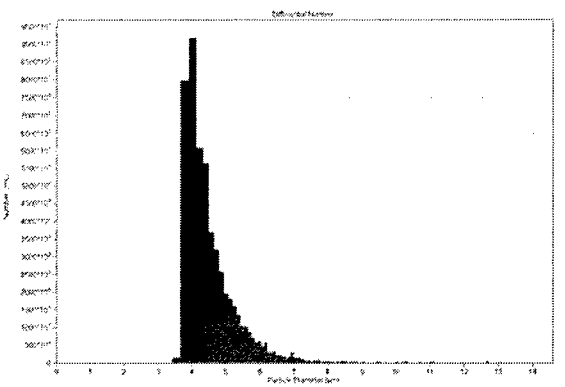

Figure 36: (Left) Optical microscope image of glutaraldehyde-enhanced chitosan microspheres. (400X)

Figure 37: (Right) Size distribution of the glutaraldehyde enhanced chitosan microspheres.

Coating the Chitosan/Gelatin Microspheres by LBL Methods

To apply nanofilm coatings for added stability, a standard procedures was employed.[40] 1ml 2% polystyrene sulfonate (PSS) (Mw: 70,000 and 1,000,000) was added to 1ml chitosan/gelatin microspheres, shaken and reacted for 15min. The mixture was then centrifuged under 3000rpm for 4 minutes and washed with DI water. This process was repeated 3 times. 0.5ml 2% poly(allylamine hydrochloride) (PAH) (Mw:70,000) was added to 200μl PSS coated microspheres, shaken and reacted for 15min. The mixture was then centrifuged and washed. As the above procedure was repeated, more layers could be adsorbed onto the microspheres.

Results and Discussion

Uncoated chitosan/gelatin microspheres and those coated by PSS/PAH and PSS were kept in PBS for 48h. The microspheres without adsorbed layers were completely dissolved, while those with adsorbed layers kept their spherical shape and size in PBS (Figure 383).

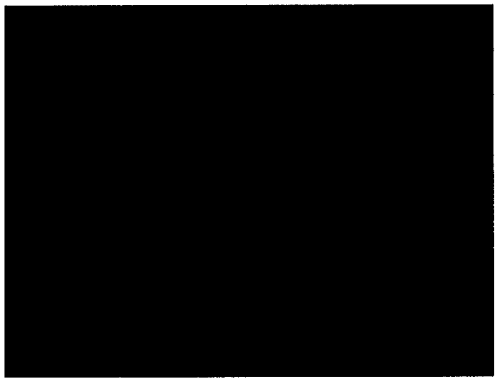

Figure 383: The fluorescence microscope images of chitosan/gelatin microspheres coated with PSS/TRITC-PAH/PSS after keeping in PBS 6.3 for 48h (X 200).

The Zeta potential of LbL coated chitosan/gelatin microspheres is shown in Figure 394. There is charge reversal after each adsorption step. The molecular weight of PSS has an influence on the structure of the coating on the microspheres. The CLSM pictures of microspheres coated with PSS 1,000,000 and PSS 70,000, respectively, and then coated with PAH-TRITC are shown in Figure 405. Compared to the ultrathin film made by PSS 1,000,000 and PAH, the fluorescence of TRITC is distributed uniformly inside the microspheres coated with PSS 70,000 and PAH. These results suggest that, compared to the mesh size of the polymer network, the size of PSS MW 70,000 molecules were small enough to allow negatively charged PSS molecules to be easily absorbed and distributed inside positively charged chitosan polymer network. Under same conditions, the molecules of PSS MW 1,000,000 were big enough to be blocked from entering the polymer network, and were adsorbed only onto the surface of the microspheres.

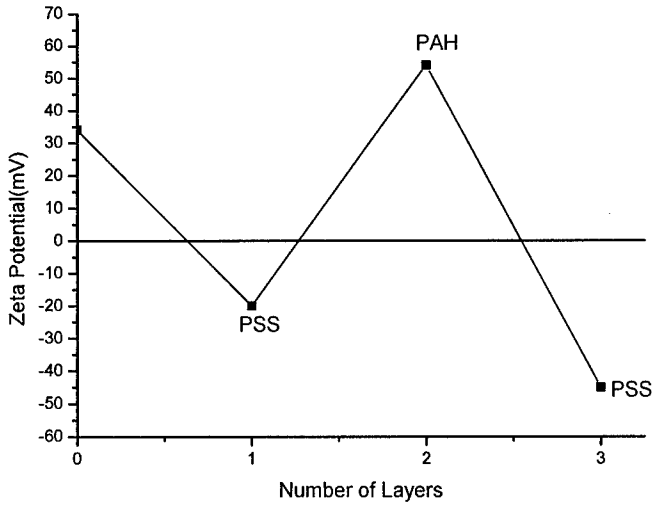

Figure 394: Zeta potential change after coated the microspheres by PSS/PAH/PSS.

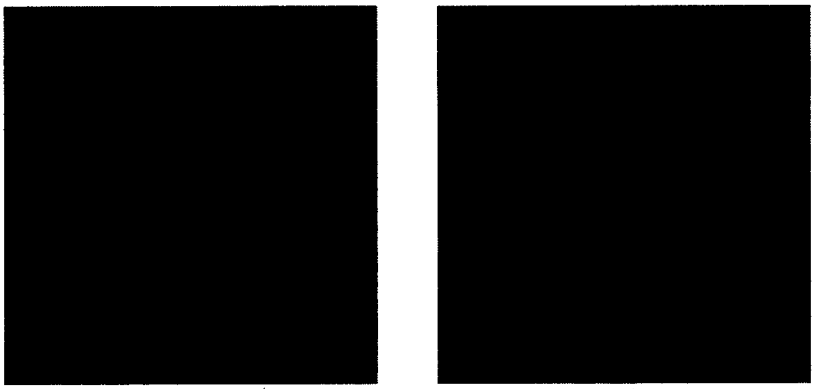

(a) (b)

Figure 405 (a and b): CLSM images of chitosan/gelatin microspheres coated with PSS 1,000,000/TRITC-PAH (a) and PSS 70,000/TRITC-PAH (b)

Conclusions

Uniform chitosan/gelatin microspheres, with diameter around 5μm, can be prepared by emulsion methods with sodium sulfate as a crosslinker. The diameter and size distribution of the microspheres can be controlled by adjusting stirring speed, concentration and amount of crosslinker. Either LbL nanofilm coating methods or low-level glutaraldehyde crosslinking can both used to enhance the mechanical property of the microspheres.

Fluorescent dye labeled microspheres

Overview/Objectives

To produce RET-readout pH-sensitive gels, ionizable polymers with a donor-acceptor pair must be combined with a static condition that provides sufficient physical proximity for energy transfer, while producing sufficient swelling to be useful in sensor applications. This phase of the work aimed at identifying appropriate dye/polymer combinations to achieve a two-peak emission from a gel irradiated along the donor excitation band.

Methods

Microspheres (1ml) were centrifuged and 100μl dye (TRITC, CY5®, Alexa Fluor 647™ or HPTS in DMF, 1mg/ml) was added; the microspheres and dye were kept overnight at 4°C, and then washed with DI-water and centrifuged to get single-dye-labeled microspheres. For dual-labeled systems, 1ml of microspheres was centrifuged and 100μl TRITC (1mg/ml DMF) was added; the microspheres were kept overnight at 4°C. The TRITC-microspheres were centrifuged and washed with DI water several times. Subsequently, 60μl of Alexa Fluor 647™ or CY5® (1mg/ml) was added and reacted for 4 hours. The dual-labeled microspheres were centrifuged and washed with DI-water.

Results and Discussion

HPTS-microspheres are shown in Figure 41. TRITC and CY5® dual-labeled microspheres are shown in Figure 42. TRITC and Alexa Fluor 647™ dual-labeled microspheres are shown in Figure 43. The dye distribution of the HPTS-microspheres was more uniform than the others. HPTS is a sulfonyl chloride dye that has a higher reactivity to amine groups than the other mentioned amine-reactive dyes; furthermore, the molecule is rather hydrophilic, and it is

likely that the penetration and distribution prior to reaction is superior to the other more hydrophobic materials.

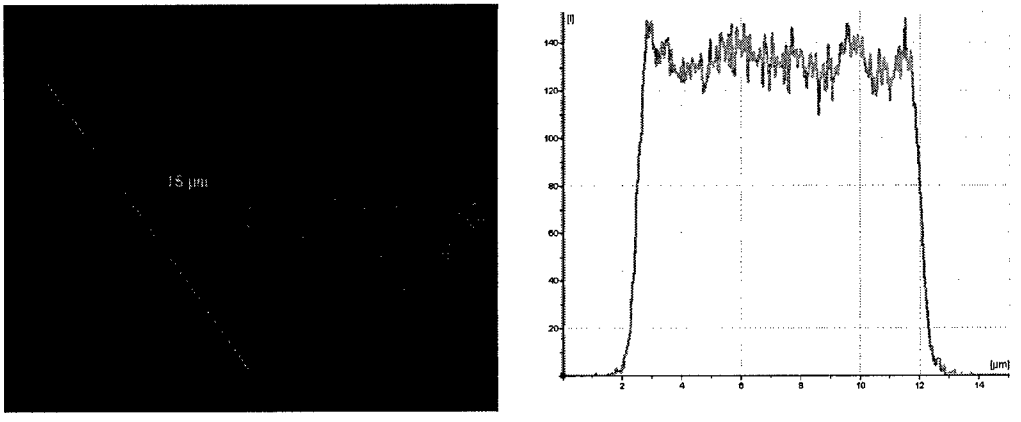

Figure 41: CLSM images and inside fluorescent dye distribution of HPTS labeled microspheres.

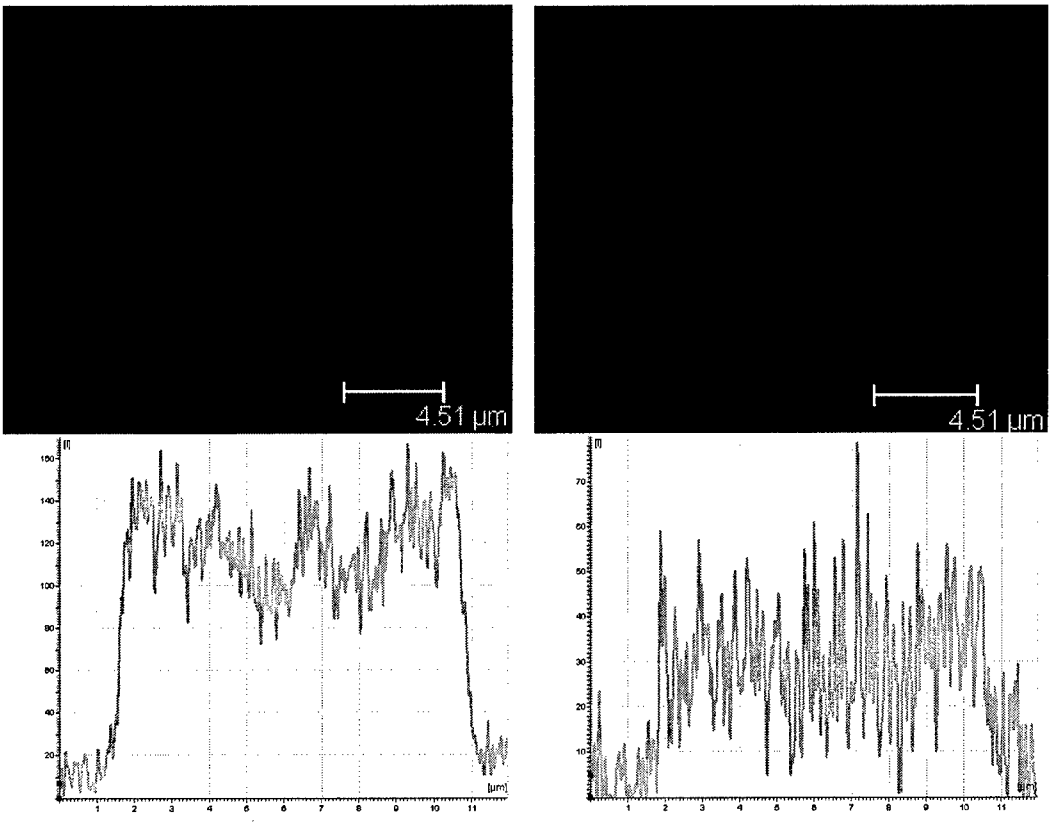

Figure 42: CLSM images and inside fluorescent dyes distribution of TRITC-Cy5 labeled microspheres.

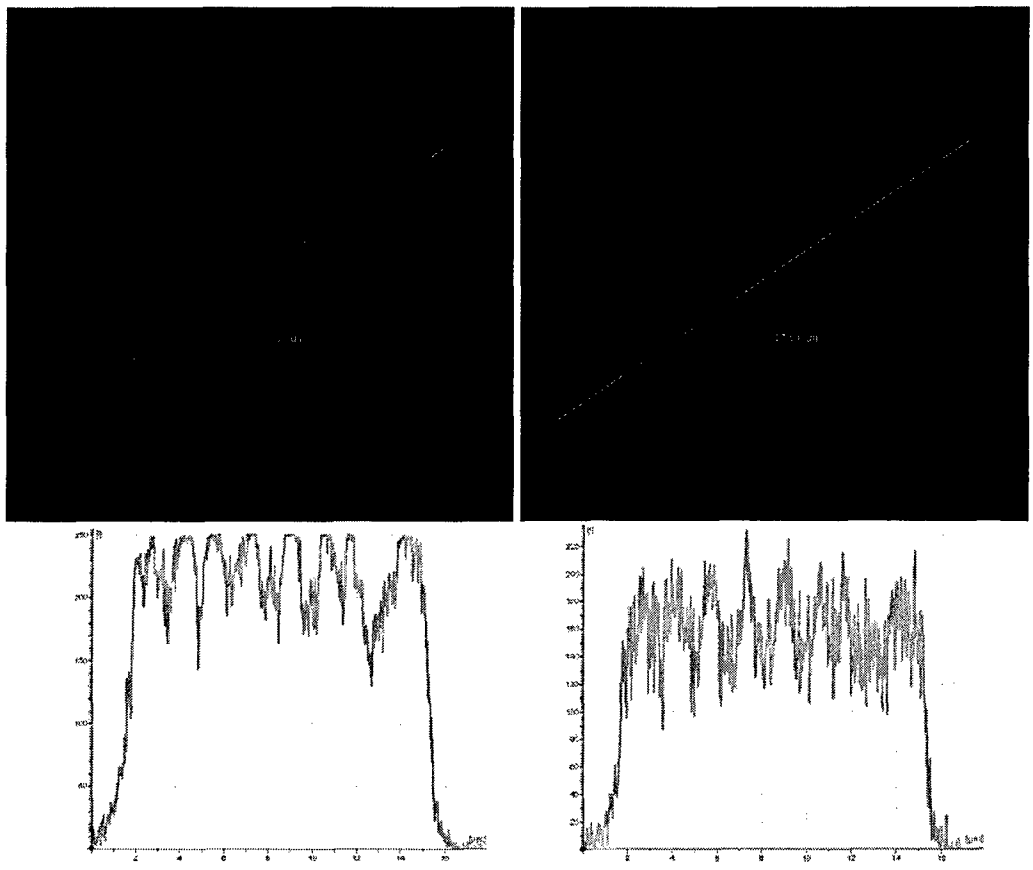

Figure 43: CLSM images and inside fluorescent dyes distribution of TRITC-Alex 647 dual labeled microspheres

Conclusions:

Fluorescent dyes can be labeled into the chitosan microspheres, and the dye distribution in the microspheres is quite uniform. No significant problems were encountered in this phase of the work. Further systematic investigation of the influence of labeling levels and optimization of signal intensity, distribution, RET spectra, and pH sensitivity will be completed in Year 2.

c. Test the RET-Based Response of Hydrogels to Glucose Changes (Months 16-18).

RET-Based Response Caused by pH of Solution

Due to the varying characteristics of the different dyes employed, several RET pairs were tested for sensitivity in the chitosan system: FITC - TRITC, TRITC-Cy5®, and TRITC-Alexa Fluor 647™.

Overview/Objectives

The primary goal of this part of the work was to construct gels with the different donor-acceptor pairs, and assess the change in fluorescence as a function of pH.

Methods

All RET experiments of FITC and TRITC-labeled chitosan/gelatin microspheres were

performed in DI water. Observations of RET response caused by pH change in solution were performed with a fluorescence spectrometer using 488nm excitation, with emission scans collected across the range of 500-600nm. 0.1M HCl was added into the solution to adjust the pH.

Results and Discussion

As the spectra change (Figure 44), FITC itself has strong pH sensitivity. Therefore, FITC cannot be used as a RET dye to test response caused by pH changes.

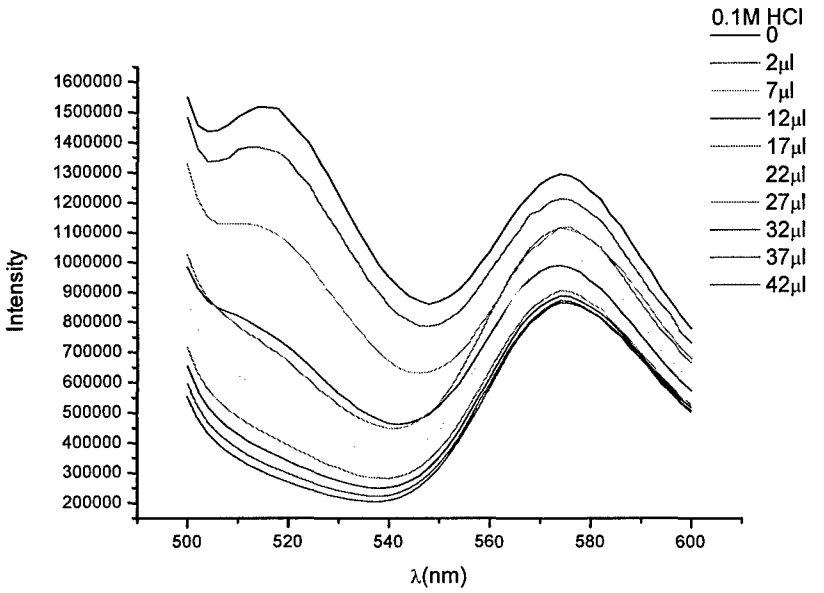

Figure 44: The fluorescent spectra of FITC and TRITC dual-labeled chitosan/gelatin microspheres, while different volume of 0.1M HCl was added into the solution to change the pH.

TRITC- CY5® Pair

Methods

All RET experiments of TRITC and CY5® dual-labeled chitosan/gelatin microspheres were performed in 0.01M PBS. Observations of RET response caused by pH change in solution were performed with a fluorescence spectrometer using 543nm excitation, with emission scans collected across the range of 560-700nm. The spectra were normalized to the TRITC peak at 572nm to accentuate the changes in the CY5® fluorescence.

Results and Discussion

The change in the CY5®/TRITC peak intensity ratio as the function of pH is illustrated in Figure 45. The CY5®/TRITC peak intensity ratio increases as the pH of the solution is increased. This experiment proves that TRITC and CY5® could be used as a pair of RET dyes. However, from the data provided by the supplier, CY5® is a slightly pH-sensitive dye. Even though it is not as sensitive as FITC, the use of CY5® as the acceptor still can make it complicated to explain the results of the RET-based response caused by pH changes.

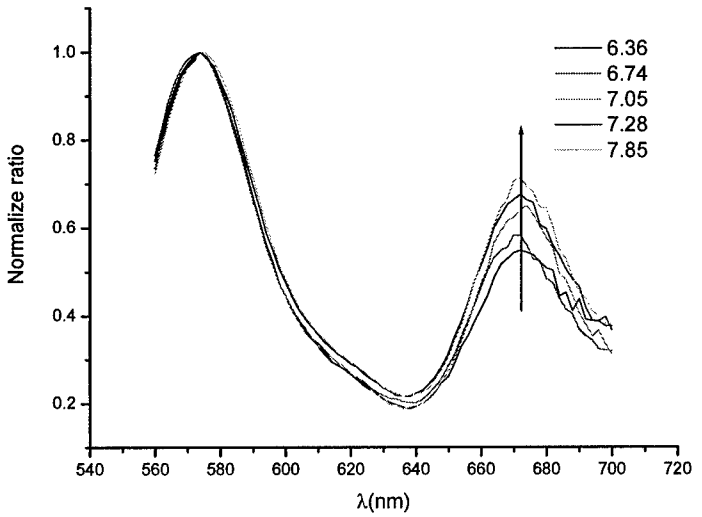

(a)

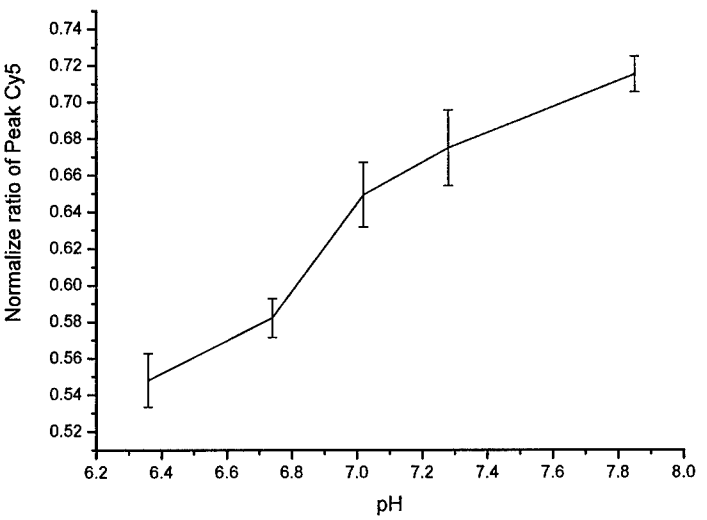

(b)

Figure 45 (a and b): The normalized fluorescent spectra of TRITC and CY5® labeled chitosan/gelatin microspheres in 0.01MPBS at different pH (a). The change in the CY5®/TRITC peak intensity ratio while the pH of the solution was changed (b). (Experiments were run in triplicate per sample. All data were expressed as means±standard deviation(SD) for n=3)

TRITC-Alexa Fluor 647™ Pair

Because of their relative pH-stability and anti-photo-bleaching property, TRITC and Alexa Fluor 647™ were used as the primary choice to test RET-based response caused by pH changes in this study.

Methods

All RET experiments involving TRITC and Alexa Fluor 647™ dual-labeled

chitosan/gelatin microspheres were performed in 0.01M PBS or DI water. Observations of RET-response caused by pH changes in solution were performed with a fluorescence spectrometer using 543nm excitation, with emission scans collected across the range of 555-700nm. The spectra were normalized to the TRITC peak at 572nm to accentuate the changes in the Alexa Fluor 647™ fluorescence.

Results and Discussion

The fluorescence spectra of TRITC and Alexa Fluor 647™ dual-labeled microspheres (Ex=543nm, Em=555-700nm) in DI water was normalized to the TRITC peak at 572nm. The change of normalized spectra as the function of DI-water pH is shown in Figure 46. It can be observed that the Alexa Fluor 647™ /TRITC peak intensity ratio increases as the pH of solution increases from pH 2 to 8.

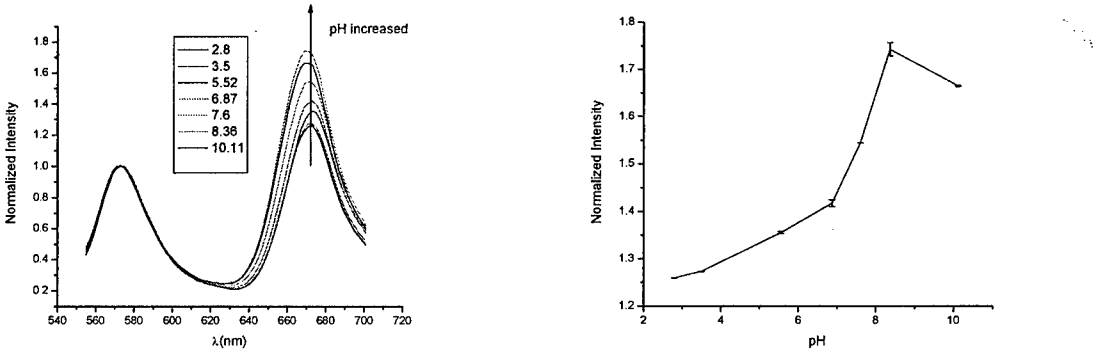

(a) (b)

Figure 46 (a and b): The fluorescent spectra of TRITC and Alexa Fluor 647™ dual-labeled microspheres (Ex=543nm, Em=555-700nm) after normalized to TRITC peak at 572nm in DI-water with different pH (a). Alexa Fluor 647™/TRITC peak intensity ratio vs. pH (b) (Experiments were run in triplicate per sample. All data were expressed as means±standard deviation(SD) for n=3)

As the chitosan/gelatin ionic-crosslinked hydrogel microspheres were exposed to lower pH solutions, the free amine group on the chitosan chain becomes protonated to form a NH_3^+ group. The microspheres swell because of increased electrostatic repulsion between the cationic chains; at the same time, the polymer chains become more hydrophilic, leading to increased hydration of the polymer chain. On the other hand, while the solution pH was increased, the NH_3^+ groups became neutralized by OH^-, to form NH_2, which decreased the repulsion force between the chitosan chains. In addition, the hydrophobicity of the gel also increased because of more NH_2 groups on the chitosan chains. The hydrophobic effect caused the molecular chains to aggregate and water molecules between the chains were pushed out of the structure. Therefore, the microspheres shrank when the external pH increases.

RET is the transfer of the excited state energy from a donor to an acceptor. The intervening solvent or macromolecule has little effect on the efficiency of energy transfer, which depends primarily on the donor-acceptor distance, as given by:

$$E = \frac{R_0^6}{R_0^6 + r_0^6} \qquad (25)$$

As mentioned above, the microspheres shrink when the external pH increases. Under these

conditions, the distance between the donor and acceptor (r_0) becomes smaller. Thus the energy transfer efficiency (E) is increased. Consequently, the fluorescent intensity of the acceptor dye compared to the donor dye, or the Alexa Fluor 647™/TRITC peak intensity ratio, increases.

Effect of Media Solution

The fluorescent spectra of TRITC and Alexa Fluor 647™ dual-labeled microspheres in 0.01M PBS solutions with different pH (Ex=543nm, Em=555-700nm) was normalized to TRITC the TRITC emission peak at 572nm. The change of normalized spectra as a function of the pH of 0.01M PBS is shown in Figure 47. The Alexa Fluor 647™/TRITC peak intensity ratio increases as the pH of PBS increased from 2 to 10.

The change in the Alexa Fluor 647™/TRITC peak intensity ratio as function of pH in water and 0.01M PBS is compared in Figure 48. In the pH range from 6 to 8, the Alexa Fluor 647™/TRITC peak intensity ratio in water increases more quickly then that in 0.01M PBS.

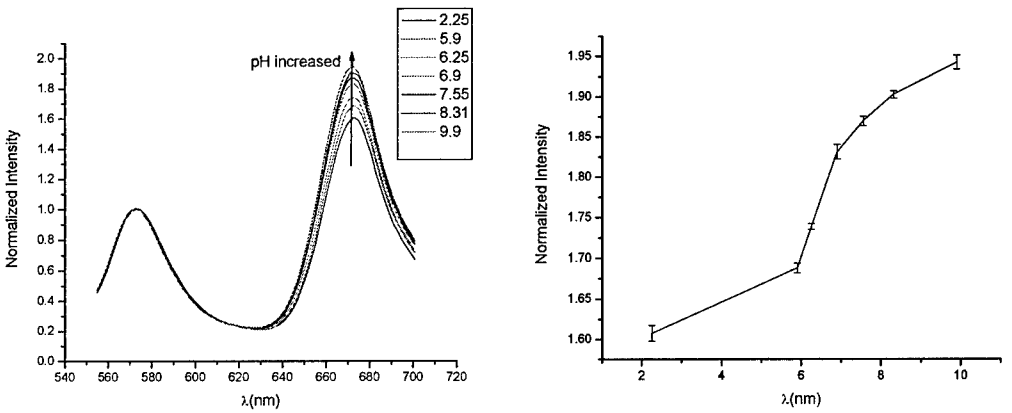

(a) (b)

Figure 47: The fluorescent spectra of TRITC and Alexa Fluor 647™ dual-labeled microspheres (Ex=543nm, Em=555-700nm) after normalized to TRITC peak at 572nm changed as the function of pH of 0.01M PBS solution. (a) The Alexa Fluor 647™/TRITC peak intensity ratio vs. pH (b) (Experiments were run in triplicate per sample. All data were expressed as means±standard deviation(SD) for n=3)

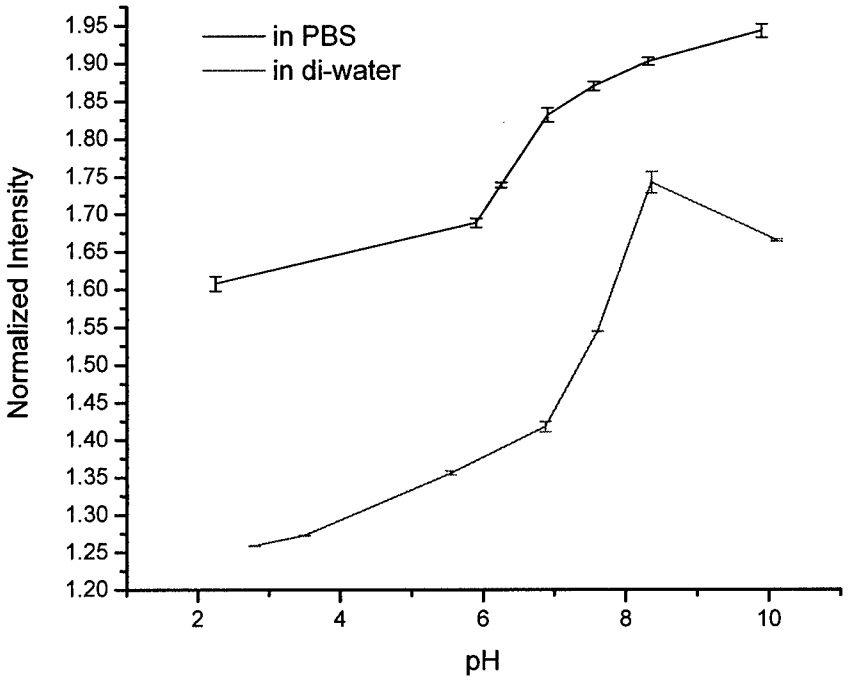

Figure 48: The comparison of the change in the Alexa Fluor 647™/TRITC peak intensity ratio as function of pH in water and 0.01M PBS. (Experiments were run in triplicate per sample. All data were expressed as means±standard deviation(SD) for n=3)

Conclusions:

The results from the pH-response of RET pair dyes labeled chitosan based microspheres experiments display that TRITC and Alexa Fluor 647™ were used as the primary choice to test RET-based response caused by pH changes in this study. Alexa Fluor 647™ /TRITC peak intensity ratio increases as the pH of solution increases from pH 2 to 8. In the pH range from 6 to 8, the Alexa Fluor 647™/TRITC peak intensity ratio in water increases more quickly then that in 0.01M PBS.

RET-based response of microspheres to glucose changes

Glucose oxidase(GOx) will be used to oxidize glucose to gluconic acid, which is capable of protonating the amine groups on the chitosan molecular chains, leading to increased electrostatic repulsion between polymer chains and a resulting expansion of the network. If this chitosan network is also labeled by the RET pair dyes, the expansion of the net work will be transduced to the decrease of RET efficiency.

Methods:

GOx was loaded into the TRITC and Alexa Fluor 647™ dual-labeled microspheres with the following procedure. 1ml of labeled microspheres was centrifuged and 50µl GOx (20mg/ml) was added; the microspheres were then kept overnight at 4°C. The GOx-RET-microspheres were centrifuged and washed with DI-water several times. The generation of acid by immobilized GOx in the presence of glucose was measured by RET based response. Alexa Fluor 647™ and

TRITC were used as the RET pair. All RET experiments were performed in 0.01M PBS or DI water. Observations of RET changes caused by glucose concentration were performed with a Photon Technology International fluorescence spectrometer using 543nm excitation, with emission scans collected across the range of 555-700nm. The spectra were normalized to the TRITC peak at 572nm to accentuate the changes in the Alexa Fluor 647™ fluorescence.

Results and Discussions

The change in the Alexa Fluor 647™/TRITC peak intensity ratio as function of time after 2000μg glucose was added in the DI water is illustrated in Figure 49. After addition of glucose into the water for 30min, the change in the Alexa Fluor 647™/TRITC peak intensity ratio was comparatively stable; therefore, spectra was taken 30 minutes after glucose addition. The change in the Alexa Fluor 647™/TRITC peak intensity ratio with the titration of glucose into DI water is shown in Figure 50. As the amount of glucose in the water increases, the Alexa Fluor 647™/TRITC peak intensity ratio decreases.

The change in the Alexa Fluor 647™/TRITC peak intensity ratio and the external pH with the titration of glucose into the DI water is illustrated in Figure 51. The external pH drops dramatically at the early state. While the pH drops to around 2.7, the external pH kept stable while the glucose was added into the solution. On the contrary, the Alexa Fluor 647™/TRITC peak intensity ratio still kept decreasing while the glucose was added into the solution in this state.

After glucose addition into the microsphere solution, it diffuses into the microspheres, and reacts with the GOx loaded into the microspheres and produces a proton. The produced protons could protonate the free amine group on the chitosan chain and increase the positive charge density of the chitosan chain. As mentioned above in the pH response section, microspheres swell while the free amine group on chitosan chain is protonated. Thus, the distance between donor and acceptor increases; therefore, the Alexa Fluor 647™/TRITC peak intensity ratio decreases. Meanwhile, there are an abundant amount of protons produced by the GOx-glucose reaction inside the microsphere, which causes the pH inside the microsphere to be lower than the eternal pH. In order to reach osmotic equilibrium, unreacted protons moved out of the microspheres into the surrounding solution, which leads to a decrease in external pH. While the external pH drops to 2.7, the pH inside and outside the microspheres is maintained. Therefore, the external pH does not change during addition of glucose to the microsphere solution.

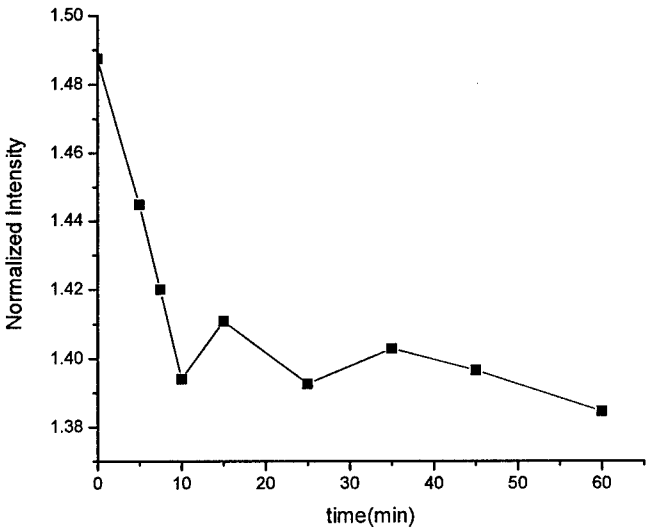

Figure 49: The change in the Alexa Fluor 647™/TRITC peak intensity ratio as function of time after 2000µg glucose added in deionized water.

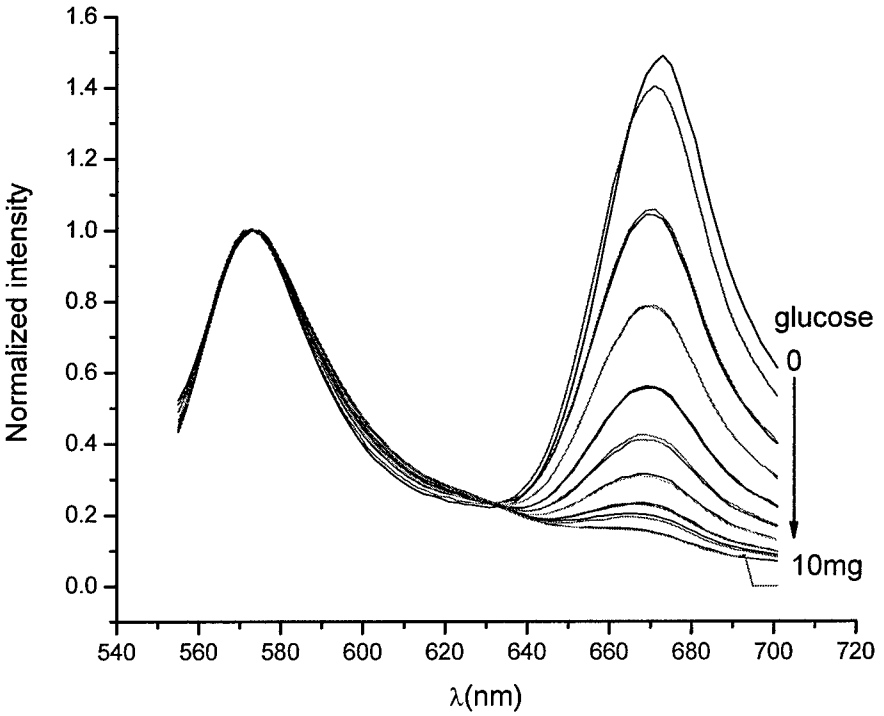

Figure 50: Change in the normalized fluorescent spectra of GOx loaded TRITC and Alexa Fluor 647™-labeled chitosan/gelatin microspheres with the titration of glucose into deionized water. (Ex=543nm, Em=555-700nm)

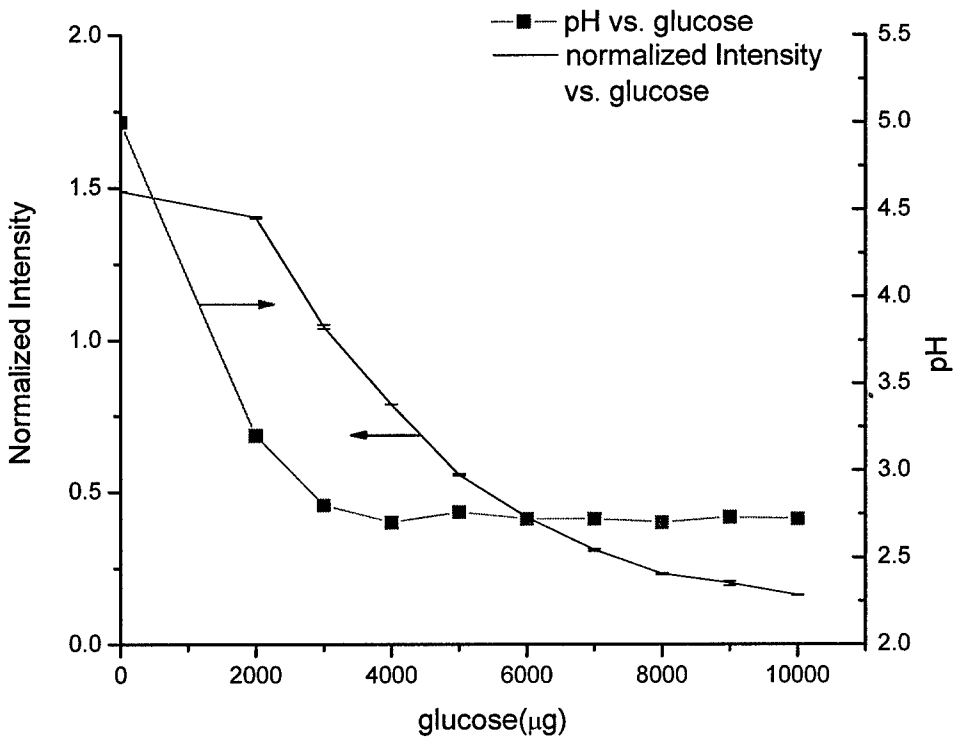

Figure 51: Change in the Alexa Fluor 647™/TRITC peak intensity ratio and external pH with the titration of glucose into deionized water. (Experiments were run in triplicate per sample. All data were expressed as means±standard deviation(SD) for n=3)

Effect of Media on Response

Changes in the Alexa Fluor 647™/TRITC peak intensity ratio with the titration of glucose into 0.01M PBS is shown in Figure 52. As the amount of glucose in the PBS increases, the Alexa Fluor 647™/TRITC peak intensity ratio decreases. The change in the Alexa Fluor 647™/TRITC peak intensity ratio and external pH with the titration of glucose into the 0.01M PBS is illustrated in Figure 53. The response of the microspheres in PBS is unlike to the change observed in DI water, the external pH decreases with the same trend as the change in the Alexa Fluor 647™/TRITC peak intensity ratio while glucose is added into the PBS solution.

As mentioned above, the proton produced by the GOx-glucose reaction could cause a decrease in the Alexa Fluor 647™/TRITC peak intensity ratio. The difference between these two experiments was the media solution. The 0.01M PBS buffer could diffuse into the microspheres, so some unreacted protons are consumed by the buffer inside the microspheres before they are allowed to diffuse into the PBS solution. The other protons, which could not be consumed before diffusion, enter the media solution. Because the effective pH range of PBS buffer is above 6, the decrease of external pH above 6 occurs slowly, whereas when the external pH drops below 6, the decrease becomes faster.

This can also be proven by comparing the change in the Alexa Fluor 647™/TRITC peak intensity ratio and external pH with the titration of glucose in DI water and 0.01M PBS, as

shown in Figure 54 and Figure 55. The decrease of Alexa Fluor 647™/TRITC peak intensity ratio in 0.01M PBS is slower than that in DI water, due to the PBS inside of the microspheres neutralizing more protons that are produced by the reaction between GOx and glucose than DI water. The same reason causes the difference between the two external pH change plots in Figure 52.

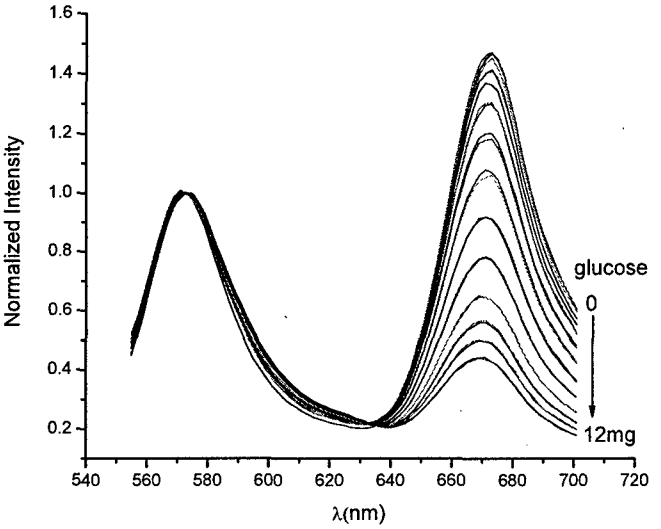

Figure 52: Change in the normalized fluorescent spectra of GOx loaded TRITC and Alexa Fluor 647™ labeled chitosan/gelatin microspheres with the titration of glucose into 0.01MPBS. (Ex=543nm, Em=555-700nm)

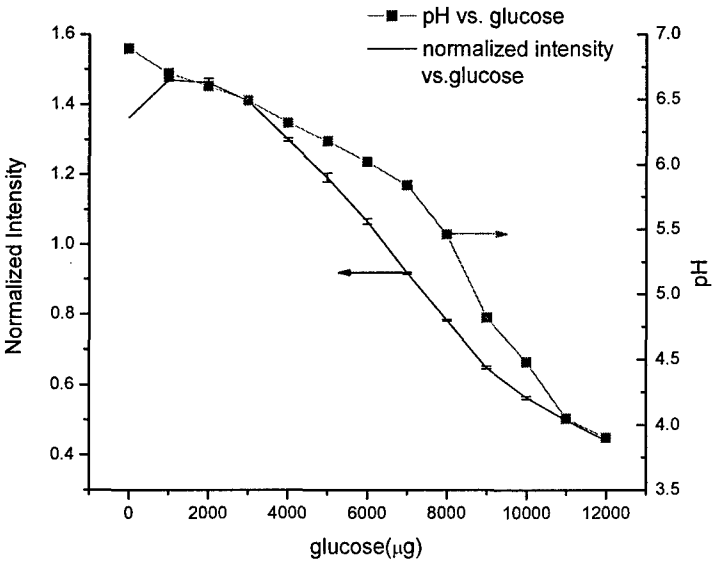

Figure 53: Change in the Alexa Fluor 647™/TRITC peak intensity ratio and external pH with the titration of glucose into 0.01MPBS. (Experiments were run in triplicate per sample. All data were expressed as means±standard deviation(SD) for n=3)

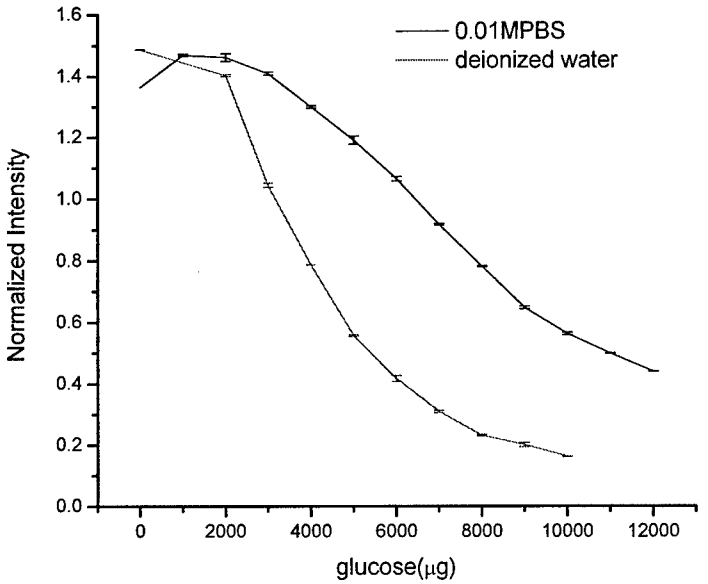

Figure 54: Comparison of the changes in the Alexa Fluor 647™/TRITC peak intensity ratio with the titration of glucose into deionized water and 0.01M PBS. (Experiments were run in triplicate per sample. All data were expressed as means±standard deviation(SD) for n=3)

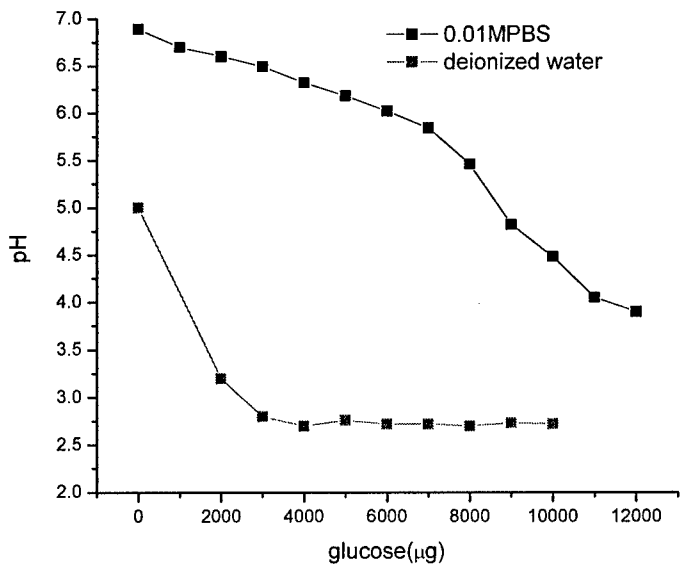

Figure 55: Comparison of the changes in external pH with the titration of glucose into deionized water and 0.01M PBS.

Compared with that of the GOx loaded microspheres, the normalized ratio of 673nm/572nm from microspheres without GOx did not change much while glucose was added into the solution, as shown in Figure 56. This result indicates that the normalized ratio change of the dual-labeled chitosan microspheres is caused by the reaction between GOx and glucose.

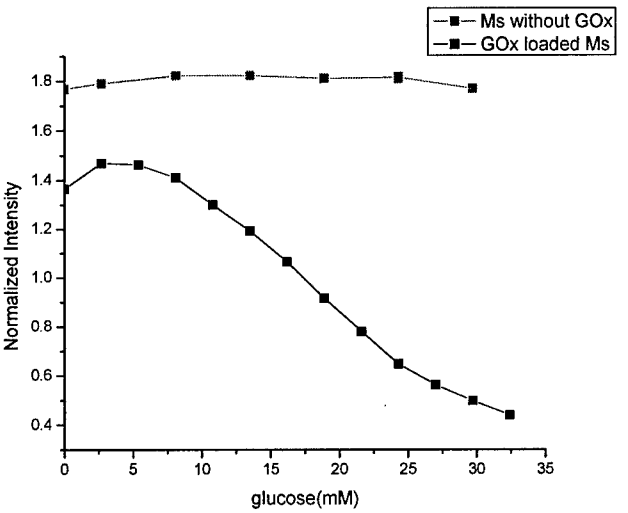

Figure 56: The normalized ratio of Em673/Em572 of TRITC and Alexa Fluor 647™ dual-labeled chitosan microspheres with or without GOx response to glucose concentration. (Experiments were run in triplicate per sample. All data were expressed as means±standard deviation(SD) for n=3)

Single dye-labeled microspheres loaded with GOx did not show much change in spectra, when compared to the RET-based fluorescent change in dual-labeled hydrogels, and this is shown in Figure 57. This result suggests that the normalized ratio change of the dual-labeled chitosan microspheres loaded with GOx is caused by the RET between the TRITC and Alexa Fluor 647™ in the microspheres.

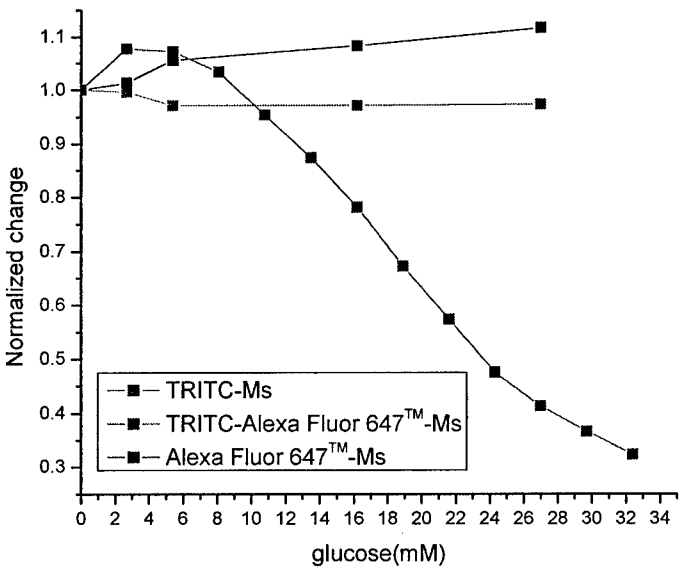

Figure 57: The normalized change of TRITC, or Alexa Fluor 647™ labeled microspheres, and TRITC and Alexa Fluor 647™ dual-labeled chitosan microspheres with loaded GOx response to glucose concentration. (Experiments were run in triplicate per sample. All data were expressed as means±standard deviation(SD) for n=3)

Conclusions

GOx can be stably loaded into the TRITC /Alexa Fluor 647 dual-labeled chitosan-based microspheres. These microspheres can be used as glucose biosensors, using the RET readout approach. As the glucose concentration increased, the Alexa Fluor 647™/TRITC peak intensity ratio was found to decrease substantially and approximately linearly. These findings are extremely promising, and form the basis of a series of planned studies using a customized flow-through apparatus that will allow control of glucose, oxygen, and pH in a special small volume reaction chamber designed for monitoring fluorescence from microsphere sensors (See Appendix).

d. Develop design models to predict spectral properties for swelling hydrogels with alternative donor-acceptor pairs, select primary choices for final system (Month 19)

This aim will be pursued in the current performance period (Grant-Year 2).

e. Optimize the labeling and crosslinking properties for new dyes, demonstrate and fully characterize sensor performance (Months 20-24)

This aim will be pursued in the current performance period (Grant-Year 2).

KEY RESEARCH ACCOMPLISHMENTS

1. In addition to the originally-proposed poly(acrylamide) system, ionically-crosslinked chitosan hydrogels have been shown as promising candidates for the purpose of pH-sensitive sensor.
2. Microcantilevers coated with the chitosan-based hydrogel show a sensitive and repeatable pH response to different pH.
3. Chitosan can be conjugated with amine-reactive dyes, such as succinimidyl esters (Alexa Fluor 647), isothiocyanates (FITC, TRITC), and sulfonyl chlorides (HPTS).
4. TRITC and Alexa Fluor 647™ were used as the primary choice to test RET-based response caused by pH changes, due to their relative environmental insensitivity
5. GOx can be loaded into the TRITC and Alex 647 dual-labeled chitosan-based microspheres using electrostatic absorption.
6. The TRITC and Alexa Fluor 647™ dual-labeled chitosan-based microspheres loaded with GOx show an extremely sensitive glucose response.
7. PAA/PAM hydrogels are also promising candidates for smart gels. These may provide a more sensitive pH response than chitosan hydrogels, are likely more durable than chitosan hydrogels, and demonstration of glucose sensing of this material will exhibit the generality of the RET optical sensing scheme.
8. The microcantilevers coated with PAA/PAM-based hydrogels with GOx inclusions showed a repeatable pH sensitive response and glucose sensitive response.
9. PAA can be conjugated with amine-containing dyes, such as D113 and amine-containing TRITC
10. GOx-containing hydrogels modified cantilever responded to glucose concentration linearly over 4-10 mM.
11. A model was successfully built to quantitatively describe the correlation between glucose concentration and cantilever deflection.

REPORTABLE OUTCOMES

1. Mao J.S., S. Kondu,H.F. Ji, M.J. McShane. Response of chitosan/gelatin hydrogel coated microcantilever to small pH change. Abstract of presentation at the 230th ACS National Meeting, in Washington, DC, Aug 28-Sept 1, 2005.(Accepted)
2. Mao J.S., S. Kondu, H.F. Ji, M.J. McShane. Study of the pH-sensitivity of chitosan/gelatin hydrogel in neutral pH range by microcantilever method. (manuscript of Biotechnology and Bioengineering)
3. Mao J.S., M.J. McShane. Novel RET based glucose-sensitive biosensor. (in preparation)
4. Mack, A. C., J. Mao , and M. J. McShane. "Transduction of pH- and Glucose-Sensitive Hydrogel Swelling Through Fluorescence Resonance Energy Transfer." IEEE Sensors 2005: The Fourth IEEE Conference on Sensors. October 31st-November 3rd 2005.
5. Mack, A. C., J., Mao and M. J. McShane.. "Transduction of pH- and Glucose-Sensitive Hydrogel Swelling Through Fluorescence Resonance Energy Transfer." 1st Annual BME Day, Louisiana Tech University. May 11th, 2005
6. H. –F. Ji, X. Yan, M. Mcshane "Glucose Measurement Using a Microcantilever Modified by Glucose-Oxidase-Containing polyacrylamide Hydrogel", to be submitted
7. X. Yan, Y. Lvov, M. McShane, H.-F. Ji "Modification of Microcantilever with LbL self-assembly film and hydrogel for Glucose Measurement" the fourth annual Diabetes Technology Meeting, Oct. 28-30, **2004**

CONCLUSIONS:

At the completion of one project year, successful demonstrations of glucose sensing have been accomplished in both areas, and interesting discoveries of hydrogel structure and properties have been uncovered using the novel measurement approaches. The methods developed with this grant are specifically relevant to glucose monitoring, as they offer unique properties and advantages over other techniques under consideration. In particular, the exquisite sensitivity of both the MEMS cantilever and RET approach that was proposed as a key feature of this project have already been demonstrated.

Year 2 efforts will be focused on more careful characterization and optimization of the performance characteristics of the prototype glucose sensors described in this report, with the goal of reaching a level of quality that will be useful for field studies that can be pursued in future studies or by other parties. The microcantilever system will require packaging and

microelectronics integration to make it suitable for *in vivo* or field use, while the RET microsphere system will require development of a dedicated optical reader device for *in vivo* transdermal interrogation. These tasks are beyond the scope of this work, but successful completion of the aims of this project will enable transfer of the technology for further development.

While the project is ahead of schedule according to the expected milestones for demonstrating sensing capabilities, optimization of sensitivity, range, and stability are key goals for the second project year. The project has generated three manuscripts to be submitted for peer review and four conference reports, with similar products expected for the second year.

References

1 Krajewska B. J. Chem Technol Biotechnol, 76(2001): 636-642

2 Agnihotri S.A., N. N. Mallikarjuna, T.M. Aminabhavi. J. Controlled Release, 100(2004): 5-28

3 Einerson, N. J., K. R. Stevens, W. J. Kao. "Synthesis and Physicochemical Analysis of Gelatin-Based Hydrogels for Cell/Drug Carrier Matrices." 2nd Annual International IEEE-EMBS Special Topic Conference on Microtechnologies in Medicine & Biology. May2-4, 394-399.(2002)

4 Berger, J., M. Reist, J. M. Mayer, O. Felt, R. Gurney. European Journal of Pharmaceutics and Biopharmaceutics. 57 (2004): 35-52.

5 Berger, J., M. Reist, J. M. Mayer, O. Felt, N. A. Peppas, R. Gurney. European Journal of Pharmaceutics and Biopharmaceutics. 57 (2004) 19-34.

6 Hoffman, A. S.Advanced Drug Delivery Reviews." 43(2002): 3-12.

7 Mi, F., S. Shyu, S. Lee, T. Wong. Journal of Polymer Science: Part B: Polymer Physics. 37 (1999): 1551–1564.

8 Wang, H., L. Wenjun, Y. Lu, Z. Wang. "Studies on Chitosan and Poly(acrylic acid) Interpolymer Complex. I. Preparation, Structure, pH-Sensitivity, and Salt Sensitivity of Complex-Forming Poly(acrylic acid): Chitosan Semi-Interpenetrating Polymer Network." Journal of Applied Polymer Science. Volume 65, Issue 8 (1998), Pages 1445 – 1450.

9 Pourjavadi, A., G. R. Mahdavinia, M. J. Zohuriaan-Mehr. Journal of Applied Polymer Science. 90(2003): 3115-3121.

10 Zhou, X. L. Weng, Q. Chen, J. Zhang, D. Shen, Z. Li, M. Shao, J. Xu. Polymer International. 52 (2003): 1153-1157.

11 Ji, H.-F., X. Yan, M. McShane. "Glucose Measurement Using a Microcantilever Modified by Glucose-Oxidase-Containing Polyacrylamide Hydrogel" (in preparation for Diabetes Technology and Therapeutics)

12 Isik, B. Jounal of Applied Polymer Science. 91 (2004): 1289-1293.

13 Nagashima, S., M. Koide, S. Ando, K. Makino, T. Tsukamoto, H. Ohshima. Colloids and Surfaces. 153 (1999): 221-227.

[14] Zhang, J., N. A. Peppas. "Synthesis and Characterization of pH- and Temperature Sensitive Poly(methacrylic acid)/Poly(N-isopropylacrylamide) Interpenetrating Polymer Networks." Macromolecules. 33, (2000): 102-107.

[15] Olpan, D., S. Duran, D. Saraydin, O. Guven. "Adsorbtion of methyl violet in aqueous solutions by poly(acrylamide-co-arylic acid) hydrogels." Radiation Physics and Chemistry. 66 (2003) 117-127.

16 Zhu, H., R. Srivastava, M.J McShane. "Spontaneous Loading of Positively-Charged Macromolecules into Alginate-Templated Polyelectrolyte Multilayer Capsules", Biomacromolecules, (accepted 5/4/05).

17 Cosnier, S., A. Le Pellec, R.S. Marks, K. Perie, J.-P. Lellouche. "A permselective biotinylated polydicarbazole film for the fabrication of amperometric enzyme electrodes." Electrochemistry Communications, Nov 2003: 507-520.

18 Goncalves, O., T. Dintinger, D. Blanchard, C. Tellier. "Functional mimicry between anti-Tendamistat antibodies

and a-amylase." Journal of Immunological Methods, Nov 2002: 29-37.

19 Kim B, N.A. Peppas. J. Biomater. Sci. Polymer Edn, 13(2002): 1271-1281

20 Sakiyama T, H. Takata, M. Kikuchi, K. Nakanishi.J. Appl. Poly. Sci. 73(1999): 2227-2233

21 Shu X.Z., K.J. Zhu, W.H. Song. Int. J. Pharm. 212(2001): 19-28

22 Mattison K.W., I.J. Brittain, P.L. Dubin. Biotechnol. Prog., 11(1995): 632-637

23 Veis A, C. Aranyi. J. Phy. Chem., 64(1960): 1203

24 Shu X.Z., K.J. Zhu. J Microencapsulation, 18(2001): 237-245

25 Fritz J., M.K. Baller, H.P. Lang, H. Rothuizen, P. Vettiger, E. Meyer, H.J. Güntherodt, C. Gerber, and J.K. Gimzewski. Science, 288 (2000): 316-318

26 Zhang Y, G.M. Brown, D. Snow, R. Sterling, H.F. Ji. Instrument Science & Technology, 32(2004): 361-369

27 Yan X, H. Ji, Y. Ivov. Chemical physics letters, 396 (2004): 34-37.

28 Xie, S. L., E. Wilkins, and P. Atanasov, Sensors and Actuators B, 17 (1994): 133-142,

29 Kim B, Peppas NA. 2002. Synthesis and characterization of pH-sensitive glycopolymers for oral drug delivery system. J. Biomater. Sci. Polymer Edn, 13(11): 1271-1281

30 Sakiyama T, H. Takata, M. Kikuchi, K. Nakanishi. J. Appl. Poly. Sci. 73(1999): 2227-2233

31 Shu XZ, Zhu KJ, Song WH. 2001. Norvel pH-sensitive citrate cross-linked chitosan film for drug controlled release. Int. J. Pharm. 212: 19-28

32 Mi F.L., S.S. Shyu, S.T. Lee, T.B. Wong. J Polym. Sci. B: Polym Phys, 37 (1999): 1551-1564

33 Russell R., M. Pishko, C. Gefrides, M. McShane, G. Coté. Anal. Chem., 71(1999): 3126-3132.

34 Erckens R. J., J. P. Wicksted, M. Motamedi, and W. F. March, Investigative Ophthalmology & Visual Science, 34 (1993): 936-936,.

35 Wang S. Y., C. E. Hasty, P. A. Watson, J. P. Wicksted, R. D. Stith, and W. F. March, Applied Optics, 32 (1993): 925-929

[36] Janas, V.F., F. Rodriguez, C. Cohen, Macromolecules, 13(1980): 977-983

37 Leypoldt, J. K., D.A. Gough, Anal. Chem. 56(1984): 2896-2904.

38 Wang, Y., A. Warshawsky, C. Wang, N. Kahana, C. Chevallard, V. Steinberg. Macromol. Chem. Phys. 203 (2002): 1833–1843

39 Shu, X. Z., K. J. Zhu. International Journal of Pharmaceutics 233 (2002): 217–225

40 Sukhorukov, G. B., E. Donath, S. Davis, H. Lichtenfield, F. Caruso, V.I. Popov, H. Möhwald, Poly. Adv. Technol. 9(1998): 759-767.

Appendices

Two significant aspects of the project have been left to the appendix, as these were pursued in parallel with the stated work plan. The following sections on fiber optic probes and flow-through testing apparatus describe methods developed for testing the optical RET sensors that will be used in continued assessment of the prototypes as refinement and optimization are investigated in project Year 2.

Fiber optic system

To assess the structural and spectral properties of crosslinked, fluorescently labeled hydrogels, optical fiber was used as a method of light delivery and collection. This architecture allows for direct measurement of photobleaching and observance of the transient response of the spectra from the material. This architecture also permits rapid replacement of the surrounding buffer, and it can be used to assess the response of individual dyes in the material, which is impossible with microsphere architectures that must be centrifuged for separation from solution.

Methods

The distal tip of a fiber with an exposed core was coated with a pre-hydrogel solution containing TRITC- and/or CY5®- labeled chitosan, along with unlabeled chitosan. The exposed core of the fiber was slightly etched and negatively charged with KOH cleaning solution (1% KOH, 39% EtOH, 60% DI water) prior to addition of the hydrogel material. The negative charge of the core is attracted to the positively-charged chitosan solution, and facilitates material deposition. The coated fiber was then moved to a 10% weight NaTPP solution for several minutes. This dip-coating/crosslinking procedure was repeated until a noticeable amount of labeled hydrogel was attached to the distal fiber tip. Once there was a visible amount of hydrogel on the tip, the tips were left in 10% weight NaTPP overnight to ensure full crosslinking. Prior to experimentation, the hydrogel-fibers were removed from the 10% weight NaTPP solution and moved to PBS 7.0 for 24 hours to remove excess crosslinker and to allow for the hydrogel to reach equilibrium at a neutral pH. Experimentation involved continuous monitoring of the spectra from hydrogel on the fiber while exposure to PBS with a known pH between pH 5 and 8. An Ocean Optics USB2000 spectrometer and an Ocean Optics tungsten-halogen source with a 540nm or 570nm bandpass filter was used for spectra collection. For hydrogels labeled with only one dye, the dye emission intensity was compared to the excitation source intensity returned from the fiber. For hydrogels labeled with a FRET pair of dyes, the emission intensity of the two dyes was compared to produce a ratio value, which was indicative of the amount of FRET from dyes in the hydrogel.

Results

The results from experiments with dual-labeled (TRITC and CY5®) hydrogels show a response to different pH solutions, and the ratio increased at higher pH or decreased at lower pH (**Error! Reference source not found.**). However, this response is usually slow and can be influenced by CY5®'s pH sensitivity and photobleaching rate, which returns skewed results. This described response can be seen in the graph below (Figure 1). Exposure to PBS 7.0 usually results in a slowly increasing ratio value, while

exposure to PBS at lower pH results in a slowly decreasing ratio value. The slope of the decreasing ratio value is directly related to the acidity of the PBS solution, with higher rates of change being displayed at lower pH values. This incidence can be seen in Figure 1.

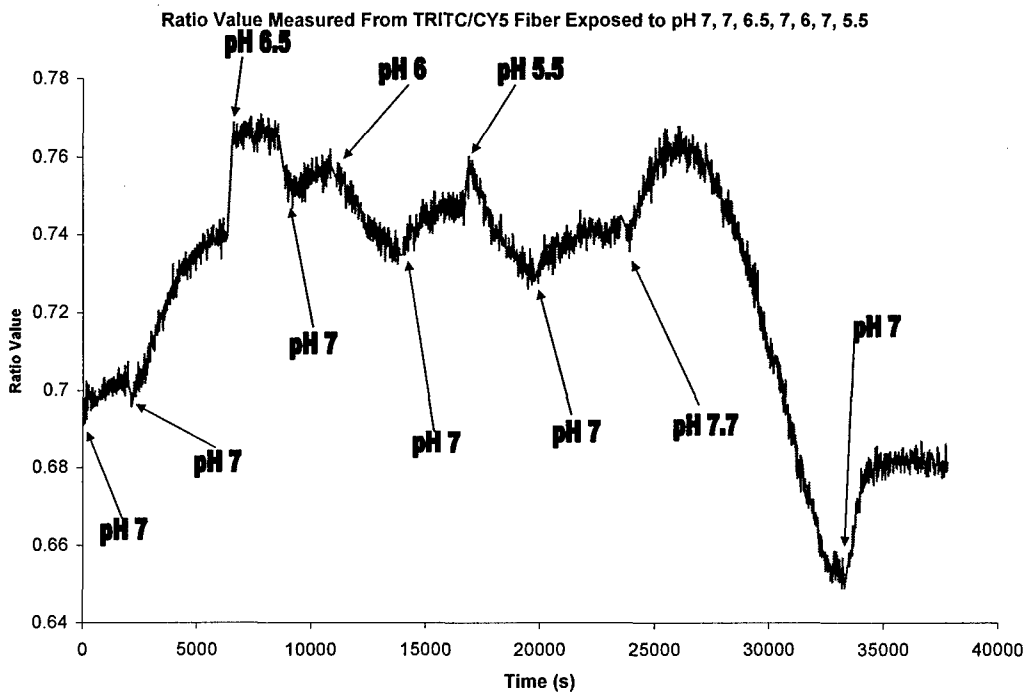

Figure 1: Results from pH-Sensitivity Experiment on Fibers Coated With TRITC and CY5® Labeled Chitosan Hydrogels

Throughout the preliminary experiments it was noted that above pH 7.4 and below pH 5.5, the spectra from the fiber changed in irregular ways. For example, during exposure to pH 7.7, the TRITC and CY5® peaks decreased for a long period, then increased for a long period. This odd reaction resulted in the parabolic shape of the ratio output in the above figure during exposure to pH 7.7, and could be a result of chitosan precipitation at higher pH. Also, during exposure to pH lower than 5.5, a distinct drop in the emission of both dyes was observed. This was attributed to the chitosan/gelatin hydrogel detaching from the fiber and falling into the solution, and this is due to the increased amount of hydrogel swelling at lower pH values. Graphs of these two occurrences can be seen below in Figure 2. A proposed solution to the hydrogel detachment problem is silanization. The fiber tips are composed of the glass core of the fiber optic wire, and the glass surface can be modified with APTES or GPTES, which would produce a covalent bond between the modified glass and the chitosan hydrogel. This bond should be more robust than the electrostatic bond currently used to attach the chitosan hydrogels to the optical fiber tips, and could potentially withstand a larger pH range.

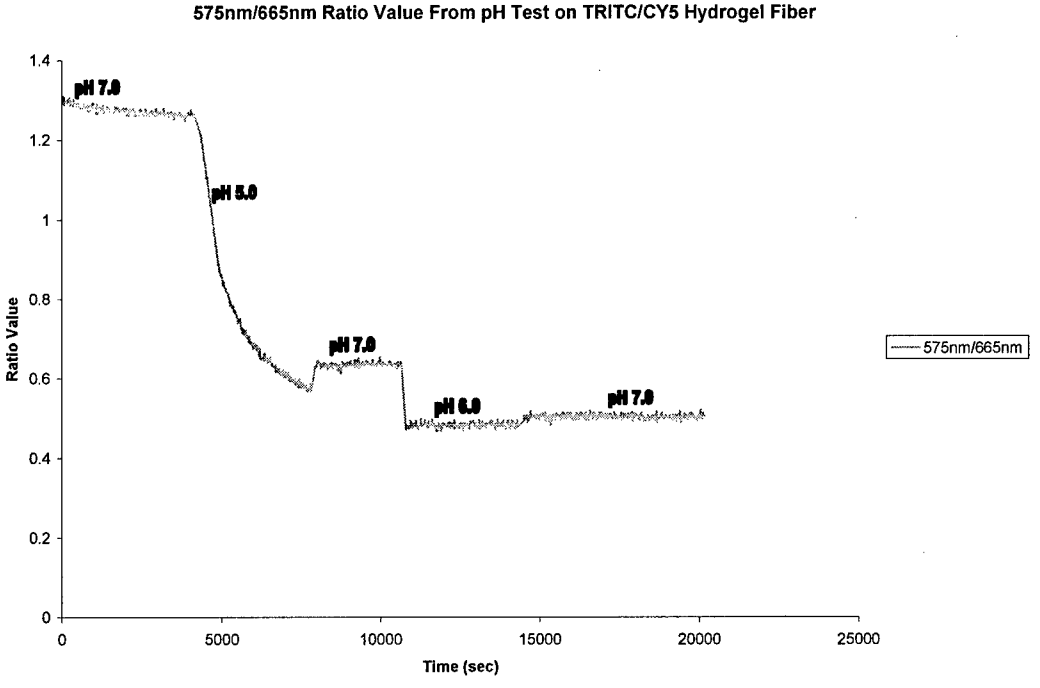

Figure 2: Example of Ratiometric Response of Fiber Coated with CY5®-Labeled Hydrogels and Exposed to Low pH

After observing the results from pH-sensitivity experiments with TRITC/ CY5® labeled hydrogels attached to optical fiber, the individual response of the dyes in the hydrogels to pH changes was determined. Pre-hydrogel solutions containing only TRITC or CY5® were made and pH-sensitivity spectra were taken. The results of these experiments are in Figure 3 and Figure 4. The hydrogels containing only TRITC responded to a decrease in pH with an increase in detected TRITC emission with respect to the amount of excitation light detected. TRITC is known to be insensitive to pH changes in solution, and for this reason, the increase in ratio value with decrease in pH is attributed to the increase in dye concentration at the fiber tip, due to hydrogel shrinking. The results also seem to show a linear response to decreasing pH below 7.0.

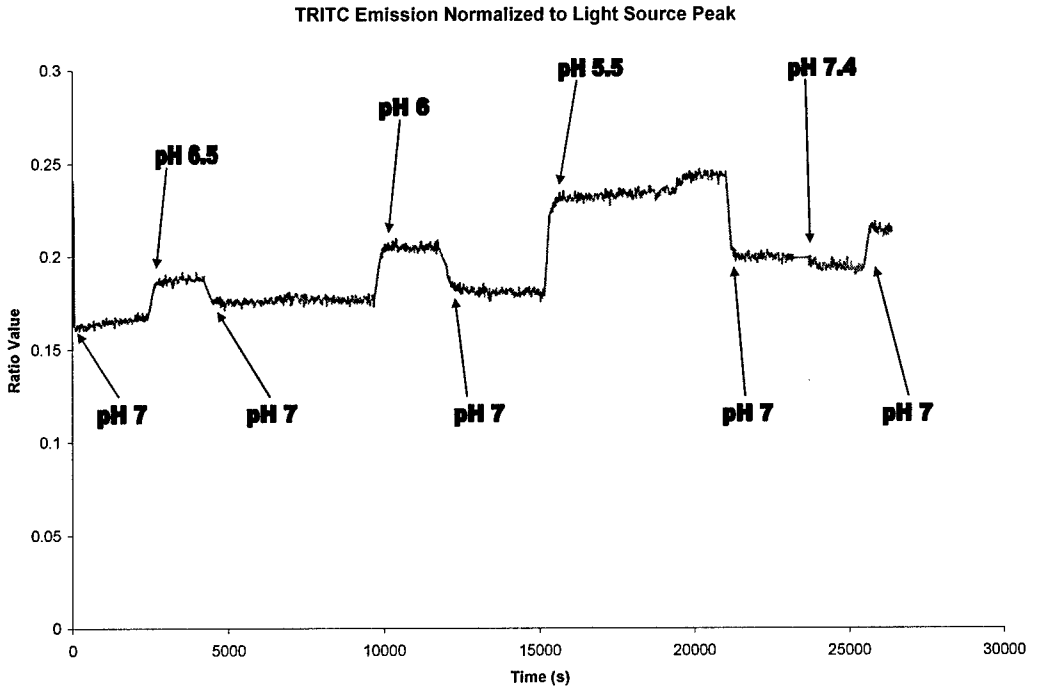

Figure 3: Response of TRITC-Labeled Chitosan Hydrogel to Changes in pH

The results from the pH-sensitivity experiment with CY5®-labeled hydrogels are displayed in Figure 4. As the pH drops, the CY5®-labeled chitosan hydrogels respond with a decrease in CY5® emission intensity. This response is the exact opposite of that seen in the TRITC hydrogels. Also, this response is the opposite of that seen in other pH sensitive CY5® dye experiments.[i] It is known that subtle alterations of the structure of the dye molecules could result in distinct changes in the pH sensitivity of the dye, and its resulting fluorescence at a given pH. However, it is unknown whether a structural change will result in CY5® reversing its fluorescence response to pH. It is also important to notice that the response of the spectra from the CY5® hydrogel takes quite a while to reach an equilibrium value, and this may be an artifact from photobleaching. The photobleaching rate of CY5® in several different pH PBS solutions has yet to be determined; however, if the photobleaching of CY5® is insensitive to pH, it should only be responsible for the overall downward trend of the ratio value in the graph. In this case, the change in dye emission intensity could be related to the amount of volume change in the hydrogel, and might indicate the permeability of the hydrogel. At a neutral pH, the hydrogel is swollen, and allows for more movement of solution throughout the hydrogel. As the pH drops, the hydrogel shrinks and becomes less permeable, restricting the movement of solution throughout the matrix, and forcing some material out of the matrix. The restriction of solution could result in an environmental change around the dye, which could reduce its fluorescence despite the drop in pH. A final explanation of the response of the CY5®-labeled chitosan hydrogel is that the local environment surrounding the dye molecules is experiencing a change in hydrophobicity. At low ph, chitosan is hydrophilic and is capable of dissolution into aqueous solutions; as the pH of the chitosan solution increases, so does the hydrophobicity of the material, and above pH 7.4, chitosan will

precipitate out of aqueous solutions. It is known that some fluorescent dyes respond to hydrophobic and hydrophilic environments differently; however, the response of CY5® to hydrophobic or hydrophilic interactions has yet to be determined.

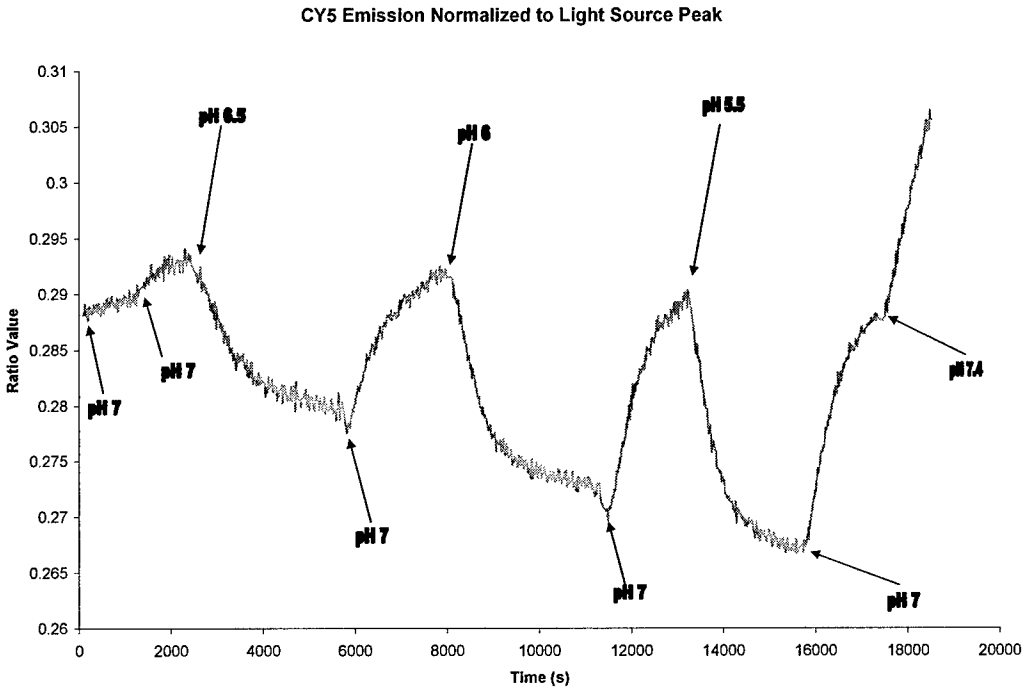

Figure 4: Response of CY5®-Labeled Chitosan Hydrogel to Changes in pH

Conclusions

The results from the optical fiber experiments highlight several variables to consider in each type of dye tested. TRITC dye seemed to show the least amount of environmental sensitivity, while the CY5® dye responded over several minutes of spectral data collection. CY5®'s sensitivity limits its use in the FRET-based measurement of hydrogel swelling because there are many different variables to account for in CY5®'s spectral response. For this reason, CY5® was replaced with Alexa Fluor 647™, which is less sensitive to pH and more photostable. Optical fiber photobleaching and pH-sensitivity testing will continue with Alexa Fluor 647™-labeled chitosan hydrogels, as well as chitosan hydrogels labeled with the TRITC/Alexa Fluor 647™ FRET-pair. As mentioned above, silanization will be used to covalently attach hydrogel materials to optical fibers so that a larger range of stimuli can be assessed.

Flow-through apparatus for dynamic testing

To assess the dynamic response of microsphere sensors to changing glucose levels, a custom apparatus has been designed and constructed for complete environmental control and continuous fluorescence monitoring. Figure.. is an illustration of the setup, which includes automated control of oxygen and glucose (glucose oxidase co-substrates) levels in the reaction chamber, which is designed to hold a glass microscope slide with an immobilized sensor gel. Using the LabVIEW control module, preprogrammed test

sequences can be used to evaluate sensors for response time, accuracy, drift, photobleaching, etc. The flow rate of fluid passed through the sample chamber can also be controlled as necessary. This system is just now being applied to test the hydrogel RET sensors developed with this grant. It is anticipated that positive results with further enable testing of glucose sensors in scattering skin tissue phantoms.

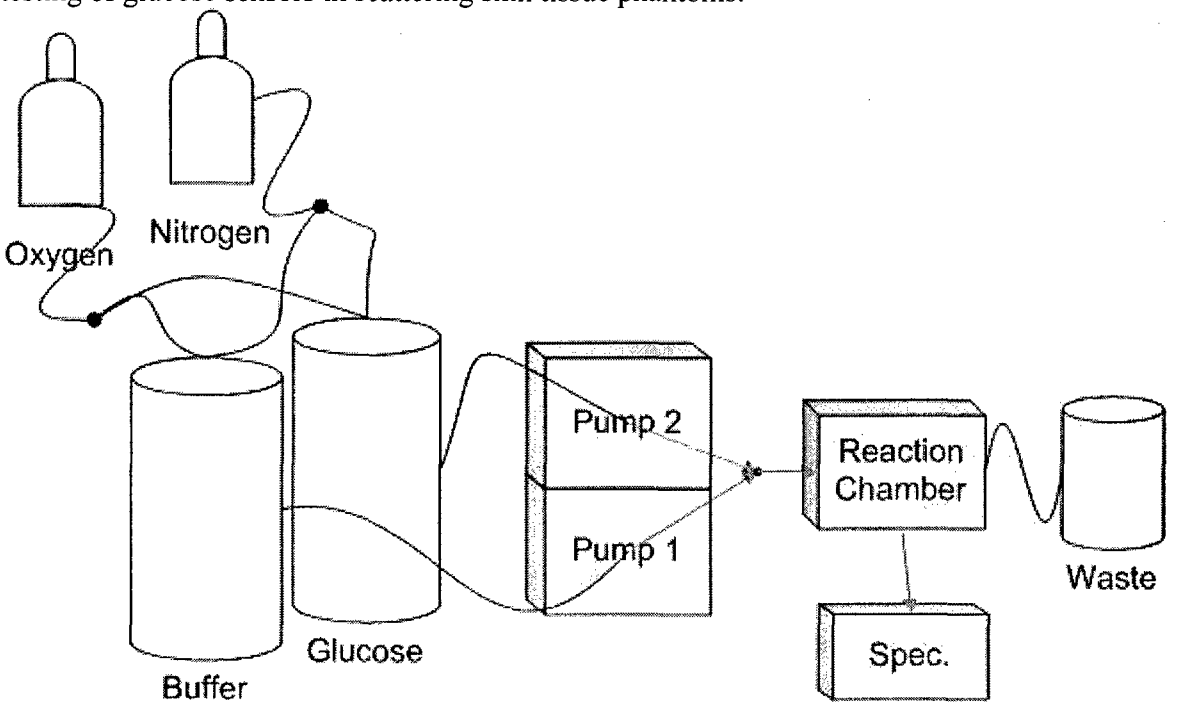

Figure 5. Dynamic testing apparatus (computer control workstation, oxygen sensors not shown).

---

i Cooper, M.E., S.J. Gregory, E. Adie, S. Kalinka, D.D. Burns. "pH Sensitive Cyanine Dyes for Biological Applications." Proceedings of the 7th Conference on Methods and Applications of Fluorescence. September 2001.